UNIVERSIDADE DE BRASÍLIA
Faculdade de Medicina
Programa de Pós-Graduação em Patologia Molecular

RESPOSTA IMUNE DO HOSPEDEIRO MURINO ÀS INFECÇÕES FÚNGICAS: UMA ABORDAGEM TRANSCRITÔMICA

Fabián Andrés Hurtado Erazo, MSc.

Brasília-DF
Dezembro de 2022

FABIÁN ANDRÉS HURTADO ERAZO, MSc.

Resposta imune do hospedeiro murino às infecções fúngicas: uma abordagem transcritômica

Tese de doutorado apresentada ao programa de Pós-Graduação em Patologia Molecular, da Faculdade de Medicina da Universidade de Brasília, como parte dos requisitos necessários para a obtenção do título de Doutor em Patologia Molecular.

Orientadora: Prof.ª Dr.ª Ildinete Silva Pereira
Coorientadora: Dr.ª Priscila Grynberg

Brasília-DF
Dezembro de 2022

FABIÁN ANDRÉS HURTADO ERAZO, MSc.

Resposta imune do hospedeiro murino às infecções fúngicas: uma abordagem transcritômica

BANCA EXAMINADORA

Prof.ª Dr.ª Ildinete Silva Pereira
Universidade de Brasília – UnB (Orientadora)

Dr.ª Priscila Grynberg
Embrapa Recursos Genéticos e Biotecnologia (Coorientadora)

Prof.ª Dr.ª Carolina Coelho
University of Exeter – EXON - UK (Avaliadora)

Prof.ª Dr.ª Karen Spadari Ferreira
Universidade Federal de São Paulo – UNIFESP (Avaliadora)

Prof. Dr. Georgios Joannis Pappas
Universidade de Brasília – UnB (Avaliador)

Prof. Dr. Gabriel Sergio Costa Alves
Universidade de Brasília – UnB (Avaliador - Suplente)

DEDICATÓRIA

A mi madre quien siempre me enseñó a valorar el

camino del sacrifico para alcanzar

los propósitos

AGRADECIMIENTOS

A conclusão desta tese não teria sido possível sem a colaboração e apoio de muitas pessoas...

Primeiramente, meus agradecimentos se destinam à minha família que nunca saiu do meu lado, mesmo quando eu mudei para o Brasil. Especialmente, agradeço à minha mãe, irmãos, sobrinhas(os) e avó por sempre terem acreditado em meus caminhos e por serem minha base nos momentos difíceis que passei longe deles. A custas da imensurável saudade que sentimos nasceu este trabalho, que hoje dedico a vocês. Foi mais um sonho realizado e agradeço por tanto amor e apoio. Um lugar especial é para minha esposa, amiga e parceira, *Marina quien fue mi soporte, mi compañía y estuvo a mi lado desde el inicio de este sueño. Me tendió su mano para levantarme siempre, con todo el amor y cariño, en cada momento que las sombras asechaban. En mi mundo es un ángel y siempre le estaré agradecido*.

Gostaria de estender meus mais sinceros agradecimentos à minha orientadora, Dra. Ildinete Silva-Pereira, por me brindar a oportunidade de estudar sob sua orientação e por sempre apoiar a independência em meu trabalho. Seu apoio, suporte e orientação contínuos, desde o mestrado, foram fundamentais para o desenvolvimento da minha carreira científica.

À Dra. Priscila Grynberg, agradeço pela coorientação e por ter me ajudado a direcionar e delinear as análises bioinformáticas da minha pesquisa.

Agradeço às pessoas do meu laboratório, em especial ao Jhones, Lara, Stefânia, pela amizade, companhia e colaboração em minha pesquisa. Foi muito especial compartilhar com vocês tanto tempo no laboratório em meio a risadas, momentos de preocupação e de felicidade quando um experimento atingia seu objetivo. A Calliandra, por todo o aprendizado na sala de cultura celular, nos experimentos e na bioinformática.

Agradeço aos professores do meu grupo de pesquisa: Lorena, Patrícia, André e Hugo pelos momentos em que pude contar com vocês e por todos os aprendizados decorrentes desses encontros. Especialmente a Lorena, quem me orientou no mestrado e me ensinou muitas das metodologias sem as quais este trabalho não teria sido possível. A Patrícia, quem sempre compartilha com muita dedicação todo o conhecimento que ela tem.

Agradeço aos grupos de pesquisa e aos coautores dos trabalhos científicos publicados durante o Doutorado. Especialmente aos líderes de cada grupo, Dra. Anamélia Bocca, Dr.

Aldo Henrique Tavares, Dr. André Nicola, Dra. Maria Emília Machado e Dr. Arturo Casadevall.

Dedico um agradecimento especial ao professor Márcio Poças pela confiança que teve em mim e que sem me conhecer, abriu as portas para poder chegar ao Brasil. Ademais, pelas inúmeras orientações que sempre está disposto a me conceder.

Agradeço, com especial carinho, à família que me permiti formar no Brasil. À Beatriz, que abriu suas portas para mim no momento de minha chegada; a Osmel, César e Harry tanto pelos momentos de descontração e confidencialidade quanto pelas trocas e aprendizados que compartilhamos.

Agradeço àqueles amigos que a UnB me presenteou, João Heitor, Otávio e Jhones, que ajudaram a me sentir um pouco mais "em casa" no Brasil, que se propuseram a me ajudar em muitos momentos, não só com relação aos meus experimentos, mas com as dificuldades que enfrentei aqui. Ao Rafael pela grande ajuda nos experimentos e pelas trocas e discussões científicas que sempre tivemos.

Por fim, agradeço à Universidade de Brasília e ao Programa de Pós-Graduação em Patologia Molecular, por me receber com tanto acolhimento e tornar possível a subida de mais um degrau em minha vida.

Pelo apoio financeiro, sem o qual eu não teria estado aqui, agradeço ao CNPq, a FAP-DF e ao Decanato de Pesquisa e Pós-Graduação (DPP).

SUMÁRIO

Lista de figuras

Capítulo I

Capítulo II

Capítulo III

Lista de tabelas

Lista de abreviaturas

AIDS - Síndrome da imunodeficiência adquirida

ANOVA - Análise de variância

APCs - Células apresentadoras de antígenos

BMDMs – Macrófagos derivados da medula óssea

BMDCs – Células dendríticas derivadas da medula óssea

C3 – Componente 3 do complemento

CFU – Unidade formadora de colônia

CLR – Receptores de lecitina tipo C

CR – Receptores do complemento

cDNA – DNA complementar

Ct – *Threshold cycle*

DEG - Genes diferencialmente expressos

dNTP – Deoxirribonucleotídeos fosfato

ELISA - Ensaio de ligação imunoenzimático

g – Unidade gravitacional

GO – Ontologia gênica

GXM – Glucoronoxilomanana

GalXM/GXMgal – Glucuronoxilomanogalactana

Fc-γR - Receptores Fc-γ

h – Hora(s)

HIV - Vírus da Imunodeficiência Humana

IFNγ – Interferon gama

IL – Interleucina

iNOS – Óxido nítrico-sintase induzida

IRAK4 - *Interleukin-1 receptor-associated kinase 4*

LPS – Lipopolissacarídeo

MFI – Mediana da intensidade de fluorescência

MHCII - Complexo Maior de Histocompatibilidade II

min – Minuto(s)

mM – Milimolar

mL – Mililitro

MOI – Multiplicidade de infecção

miRNA/miR – MicroRNA

miRISC – Complexo de silenciamento induzido por microRNAs

mRNA – RNA mensageiro

MR – Receptores de manose

NADPH – Nicotinamida adeninadinucleotídeo fosfato oxidases

ncRNA - RNAs não-codificadores

NFκB - *Nuclear Factor kappa-B*

ηg – Nanograma

NLRP – Receptor do tipo NOD que contêm pirin

NO – Óxido nítrico

Nts – Nucleotídeos

PAMPs - Padrões moleculares associados a patógenos

PBS – Tampão fosfato-salino

PCM - Paracoccidioidomicose

pH – Potencial hidrogeniônico

pre-miRNA - miRNA precursor

pri-miRNA - miRNA primário

PRR – Receptores de reconhecimento de padrões

RNA-seq - Sequenciamento em larga escala

ROS – Espécies reativas de oxigênio

RPMI – Meio Roswell Park Memorial Institute

RT-qPCR – Transcrição reversa seguida de PCR quantitativa

RT-qPCR *array* – Transcrição reversa seguida análise de microarranjo por qPCR

rpm – Rotações por min

s – Segundo(s)

SDS – Dodecil Sulfato de Sódio

SFB – Soro fetal bovino

SNC – Sistema Nervoso Central

snRNA – Pequenos RNAs nucleares

Th – Resposta/Linfócito T auxiliar

THP-1 – Linhagem celular de monócito humano

TLR – Receptores do tipo *Toll*

TNF-α – Fator de necrose tumoral alfa

U – Unidade de ação enzimática

u.a. – Unidades arbitrarias

UV – Ultravioleta

YPD – Meio Extrato de levedura, peptona e dextrose

5'/ 3' UTR - 5'/ 3' *Untranslated region*

µL – Microlitro

µg – Micrograma

µm – Micrometro

µM – Micromolar

°C – Grau Celsius

% - Porcentagem

Resumo

O aumento das infecções fúngicas sistêmicas associadas à emergente necessidade de novas alternativas terapêuticas impõem a necessidade de conhecimento dos mecanismos de controle da expressão gênica relacionados à regulação da resposta imune. Dados da literatura demonstram que as infecções fúngicas representam uma impactante causa de morbidade e mortalidade, especialmente no que tange ao universo crescente de imunocomprometidos. Compreender as bases da resposta imune protetora do hospedeiro às infecções fúngicas pode ajudar a prever a progressão da doença e influenciar diretamente o tratamento e o prognóstico do paciente. Há grande diversidade de espécies de fungos que afetam os seres humanos e que causam estas infecções. Fungos como *Paracoccidioides brasiliensis* e *Cryptococcus neoformans*, entre outros, são os agentes etiológicos da paracoccidioidomicose e criptococose, respectivamente. As primeiras células a detectar a infecção são os macrófagos e as células dendríticas, que reconhecem e fagocitam o fungo desencadeando a resposta imune inata necessária à erradicação da infecção. A resposta do hospedeiro à interação com patógenos microbianos envolve ampla reprogramação gênica, que é finamente regulada tanto para conter ou eliminar efetivamente o patógeno, bem como para orquestrar uma resposta imune adaptativa efetiva e protetora. Esse estudo visou a caracterização do perfil transcritômico de fagócitos em resposta aos modelos de infecção por *P. brasiliensis* e *C. neoformans*, a fim de contribuir a um melhor entendimento das bases moleculares da interação patógeno-hospedeiro. O primeiro trabalho, foi focado na análise do transcritoma de células dendríticas derivadas da medula óssea (BMDCs) de camundongos resistentes (A/J) e suscetíveis (B10.A) em resposta à infecção por *P. brasiliensis*. O segundo trabalho, foi direcionado à análise transcritômica de macrófagos derivados da medula óssea (BMDMs) de camundongos em resposta à infecção pelas linhagens capsulares (B3501) e acapsulares (Cap67) de *C. neoformans*. Neste sentido, empregamos o sequenciamento de RNA para fornecer uma imagem global da expressão gênica do hospedeiro em resposta aos dois modelos de infecção. Os principais resultados mostraram que as BMDCs do camundongo suscetível apresentaram uma resposta mais intensa à infecção por *P. brasiliensis*, sugerindo que uma precoce reação imunológica exagerada ao fungo pode estar ligada à suscetibilidade do hospedeiro. Adicionalmente, as BMDCs reprimem processos/genes envolvidos na apresentação de antígenos, como na atividade lisossômica e na autofagia. Os resultados sugerem que a deficiência nesses processos é parcialmente responsável pela ativação ineficiente da resposta imune adaptativa no modelo susceptível da paracoccidioidomicose.

Por outro lado, os resultados do modelo de infecção por *C. neoformans* mostraram um atraso na ativação de uma resposta imune inata e adaptativa adequada em macrófagos infectados pela linhagem encapsulada, afetando a apresentação de antígenos e a ativação dos macrófagos. Adicionalmente, houve um aumento da modulação de vários microRNAs nos macrófagos infectados com a linhagem encapsulada. Esses resultados contribuíram para a compreensão dos mecanismos celulares e moleculares da interação patógeno-hospedeiro entre fagócitos e fungos patogênicos.

Palavras-chave: paracoccidioidomicose, criptococose, resposta imune, susceptibilidade, resistência, análise transcritômica, células dendríticas, macrófagos.

Abstract

The increase in systemic fungal infections associated with the emerging need for new therapeutic alternatives imposes the need for knowledge of the gene expression mechanisms underlying the regulation of immune response. Literature data demonstrate that fungal infections represent an impacting cause of morbidity and mortality, especially with regard to the growing universe of immunocompromised people. Understanding host´s protective immune responses to fungal infections can help predict disease progression and directly influence patient treatment and prognosis. There is a great diversity of fungal species that affect humans and cause these infections. Fungi such as *Paracoccidioides brasiliensis* and *Cryptococcus neoformans*, among others, are the etiologic agents of paracoccidioidomycosis and cryptococcosis, respectively. The main cells detecting the infection are the macrophages and dendritic cells, which recognize and phagocytose the fungus, mounting an innate immune response necessary to eradicate the infection. The host's response to interaction with microbial pathogens involves extensive gene reprogramming, which is finely regulated both to effectively contain or eliminate the pathogen, as well as to orchestrate an effective and protective adaptive immune response. This study aimed to characterize the transcriptomic profile of phagocytes in response to infection models by *P. brasiliensis* and *C. neoformans*, in order to contribute to a better understanding of the molecular bases of the host-pathogen interaction. The first work was focused on the analysis of the transcriptome of bone marrow-derived dendritic cells (BMDCs) from resistant (A/J) and susceptible (B10.A) mice in response to infection by *P. brasiliensis*. The second work was directed to the transcriptomic analysis of mouse bone marrow-derived macrophages (BMDMs) in response to capsular (B3501) and acapsular (Cap67) strains of *C. neoformans*. In this regard, we employed RNA sequencing to provide a global landscape of host gene expression in response to the two infection models. The main results showed that BMDCs from the susceptible mouse showed a stronger response to *P. brasiliensis* infection, suggesting that an early exaggerated immune reaction to the fungus may be linked to host susceptibility. Additionally, BMDCs also repress genes/processes involved in antigen processing and presentation, such as lysosomal activity and autophagy. These results suggest that impairment at these processes is partially responsible for the inefficient activation of the adaptive immune response in the susceptible model of paracoccidioidomycosis. On the other hand, results from the *C. neoformans* infection model showed a delay in the activation of an adequate innate and adaptive immune response in macrophages infected by the encapsulated

strain, affecting antigen presentation and macrophage activation. Additionally, there was an increase in the modulation of several microRNAs in macrophages infected with the encapsulated strain. These results contributed to the understanding of cellular and molecular mechanisms of host-pathogen interaction between phagocytes and pathogenic fungi.

Keywords: paracoccidioidomycosis, cryptococcosis, immune response, susceptibility, resistance, transcriptomic analysis, dendritic cells, macrophages.

Capítulo I:

Revisão da literatura

1. Introdução

Desvendar as alterações na expressão gênica usando metodologias de alto rendimento é uma questão central para entender as redes reguladoras envolvidas na resposta imune do hospedeiro às infecções fúngicas. Neste contexto, a principal temática abordada neste trabalho consiste na análise da expressão gênica do hospedeiro na interface da interação hospedeiro murino - fungo patogênico, empregando os modelos de infecção por *Paracoccidioides brasiliensis* e *Cryptococcus neoformans*.

Este trabalho está organizado em capítulos que abordam os itens descritos a continuação:

No Capítulo I, são introduzidos conceitos fundamentais requeridos para o desenvolvimento desse trabalho. São revisados conceitos a respeito da resposta imune às infecções fúngicas, principalmente, relacionados aos fungos patogênicos *C. neoformans* e *P. brasiliensis*. Adicionalmente, é realizada uma descrição dos miRNAs e sua importância na regulação da expressão gênica relacionada à resposta imune das infecções por patógenos microbianos.

Nos capítulos II e III são apresentados os resultados da caracterização do transcritoma de células dendríticas e macrófagos em resposta às infecções por *P. brasiliensis* e *C. neoformans*, respectivamente. Cada capítulo apresenta um *background* introdutório, métodos aplicados, resultados, discussão e referências bibliográficas. Finalmente, são levantadas as principais considerações e perspectivas, assim como também são apresentados os trabalhos científicos publicados durante o percurso do doutorado.

1.1. Relevância das infecções fúngicas

A importância das infecções fúngicas invasivas aumentou nas últimas duas décadas, representando relevante causa de morbidade e mortalidade, especialmente no que tange ao universo crescente de imunocomprometidos (pacientes de HIV/AIDS, com doenças autoimunes, em quimioterapia contra o câncer e recipientes de transplantes de órgãos) (1–3). Há grande diversidade de espécies de fungos que afetam os seres humanos e que causam estas infecções. Fungos como *Candida albicans*, *Cryptococcus neoformans*, *Histoplasma capsulatum*, *Paracoccidioides brasiliensis* e espécies de *Aspergillus* e *Pneumocystis* representam importantes agentes patogênicos (4–8). O controle dessas infecções depende tanto da ação de antifúngicos eficazes como do restabelecimento funcional da resposta imune (6).

Os fungos *P. brasiliensis* e *C. neoformans* são considerados os principais agentes etiológicos da paracoccidioidomicose (PCM) e a criptococose, respectivamente (9,10). Essas micoses apresentam uma variedade de manifestações clínicas, desde uma infecção focalizada até uma infecção sistêmica, afetando indivíduos imunocomprometidos e imunocompetentes (10–12). Dados para o Brasil indicam que: i) a PCM é a micose sistêmica mais prevalente, onde são notificados 80% dos casos totais da doença; ii) a criptococose é destacada como a mais frequente dentre as micoses sistêmicas associadas à HIV/AIDS, atingindo cerca de 4.316 mortes entre os anos 2000 e 2012; e iii) as estatísticas em relação às infecções fúngicas podem ser ainda maiores, dado que a notificação não é mandatória (10,13,14). Estas estimativas demonstram a relevância desses fungos no panorama das micoses no Brasil.

Tais dados incentivam as investigações de mecanismos envolvidos na imunopatogênese das infecções microbianas, que dependem da espécie do patógeno, do local da infecção e do estado imunológico do hospedeiro (15–17). Nessa perspectiva, a pesquisa científica é essencial ao entendimento das bases moleculares da interação hospedeiro-patógeno, ao conhecimento dos mecanismos envolvidos na resistência/suscetibilidade às micoses, à descoberta de novos fármacos mais eficazes, assim como de terapias imunológicas que melhorem a resposta do hospedeiro, e ao desenvolvimento de novas abordagens de intervenção terapêutica para controlar as infecções fúngicas invasivas que ainda são um importante desafio (17,18).

1.2. Paracoccidioidomicose

A paracoccidioidomicose é uma micose sistêmica geograficamente confinada às regiões tropicais e subtropicais da América Latina, sendo uma das micoses profundas mais prevalentes

(9,19). Os principais agentes etiológicos desta infecção são os fungos dimórficos *P. brasiliensis* e *P. lutzii* (20). Além disso, a doença pode ser causada por pelo menos quatro espécies filogenéticas do complexo *P. brasiliensis* (21,22).

As manifestações clínicas apresentam um grande espectro, desde uma lesão focalizada até uma micose disseminada, afetando tanto indivíduos imunocompetentes e imunocomprometidos (19,23). Os pulmões são os órgãos mais frequentemente afetados, embora a infecção possa se disseminar para outras áreas do organismo, incluindo o sistema nervoso central (24,25).

Esta infecção fúngica é prevalente no Brasil, Colômbia e Venezuela, no entanto, casos têm sido relatados desde o norte da Argentina até o sul de México (26). Alguns casos de PCM têm sido reportados na Europa, África e Ásia, estando associados à migração ou viagens (27). Na América Latina, o maior número de casos da PCM é reportado no Brasil, com 80% do total, seguido por Colômbia, Venezuela, Equador e Argentina (26). A taxa de prevalência da infecção em áreas rurais endêmicas foi estimada em 45,8% para o Brasil, seguido da Colômbia (45%), e do Equador (41%). No Brasil, a incidência estabelecida em áreas endêmicas atinge cerca de 4/100.000 habitantes (28). Nas últimas décadas, foram observadas mudanças na distribuição geográfica da incidência da PCM. Na região norte (Amazônia), as taxas de incidência aumentaram (entre 9 - 40 casos/100.000) (25,28). É a décima causa de morte entre as doenças infecto-parasitárias; e entre 1998 e 2006, foi a principal causa de morte por micoses sistêmicas em pacientes imunocomprometidos (29). A mortalidade associada a PCM em indivíduos imunocompetentes é menor do 5%, mas as sequelas são permanentemente documentadas, o que inclui a insuficiência respiratória crônica (12).

O principal fator de risco para adquirir a infecção é o trabalho ou atividades relacionadas com a exposição ao solo, um reservatório do fungo. Os agricultores das zonas rurais são os mais afetados, por contato com aerossóis contendo partículas do solo contaminadas, sendo infectados pela fase saprofítica do fungo (30,31).

1.3. *Paracoccidioides brasiliensis*

O fungo dimórfico *P. brasiliensis* encontra-se naturalmente como micélio no ambiente (multicelular), onde produze os propágulos infeciosos (ex. conídios ou fragmentos de hifas), e apresenta forma de levedura (unicelular) quando cresce dentro dos hospedeiros (20,32). O fungo tem sido associado com outras espécies de hospedeiros mamíferos, sendo principalmente

isolado das espécies de tatus *Dasypus novemcinctus* e *Cabassus centralis*, configurando o reservatório natural do patógeno (9,20,32).

A variação na temperatura induz a transição dimórfica do *P. brasiliensis* (9). Em culturas do fungo e no solo, a temperaturas inferiores a 26 °C, apresenta morfologia de micélio, caracterizada por longos filamentos septados. Em quanto que, nos hospedeiros e em culturas a 37 °C, apresenta morfologia de levedura com brotamentos periféricos e tamanho variável (10 - 40 µm) (9,19). Essa característica morfológica facilita a identificação da infecção e, consequentemente, o diagnóstico da PCM (25,33). O atributo do dimorfismo tem sido estreitamente relacionado com a capacidade patogênica do fungo, dado que linhagens sem capacidade de transitar para levedura são avirulentas (34–36).

A parede celular do fungo é uma estrutura complexa composta por glicoproteínas, peptídeos, lipídios e polissacáridos. O conteúdo de quitina na parede celular de *P. brasiliensis* na fase de micélio é menor em comparação com a fase de levedura, com α-1,3-glicana na forma de levedura e β-1,3-glicana na fase de micélio (19,37). Concentrações altas de α-1,3-glicana e baixas de galactomanana foram relacionadas à virulência do fungo na fase unicelular (19).

Estudos realizados no transcritôma de *P. brasiliensis* demonstraram ampla reprogramação gênica na transformação morfológica de conídio para levedura (34). Essa transição dimórfica leva a mudanças na composição, estrutura e organização da parede celular mediada pela expressão de vários genes. Alguns exemplos são: o gene Pbfks1 que codifica uma β-1,3-glicana sintase envolvida na alteração da composição; Pbchs4, que codifica uma quitina sintase essencial na formação da parede celular e que desempenha um papel importante na virulência de P. brasiliensis. Tais alterações podem representar um importante mecanismo adaptativo ao reduzir a resposta imune do hospedeiro (19,38).

Além disso, demonstrou-se que o fungo é capaz de sobreviver e replicar dentro do fagossomo dos macrófagos, tendo desenvolvido mecanismos para controlar as limitações metabólicas impostas pelas células fagocíticas (39). Um destes mecanismos é a adaptação do ciclo do glioxilato, que permite a utilização de compostos de dois carbonos como fonte de carbono pela levedura (38,40). Desse ciclo participam os genes, *icl*1 e *mls*1 que codificam as enzimas isocitrato liase e malato sintase, respectivamente (40). Outro atributo de virulência do fungo é produção de melanina, que diminui a internalização das leveduras pelos fagócitos e aumenta a capacidade de resistência às espécies reativas de oxigênio (ROS) dentro do hospedeiro (41).

1.4. Resposta imune a *Paracoccidioides* spp.

A infecção ocorre principalmente pela inalação de propágulos infeciosos ou conídios produzidos pela forma saprofítica do fungo no ambiente. Uma vez dentro dos pulmões, o conídio germina na forma patogênica de levedura que é capaz de se espalhar para outros tecidos, como os linfonodos. A infecção inicialmente pode ser assintomática e não progredir para a doença, tornar-se latente ou crônica, ou ainda ser erradicada pela resposta imune do hospedeiro (19,25,26).

Numerosos estudos sugerem que a susceptibilidade ao fungo depende de fatores tais como a resposta imune associada ao perfil genético, sexo, estado de saúde, às características sociodemográficas e ao estilo de vida do indivíduo. Assim como de fatores associados com o fungo como a virulência, fenótipo celular e carga fúngica (26,28). A adesão de *P. brasiliensis* às células do hospedeiro é o passo crucial para a posterior invasão, colonização e crescimento (42).

A infecção pulmonar pode levar ao desenvolvimento de granulomas, que são essenciais para contenção e destruição do fungo, a fim de evitar sua disseminação pelo organismo (43). Entretanto, o padrão do granuloma formado varia em virtude do isolado de *P. brasiliensis* e da resposta do hospedeiro. Hospedeiros resistentes à infecção por *P. brasiliensis*, por exemplo, são aptos a formar um granuloma epitelióide compacto e a desenvolver uma resposta imunológica efetiva (26).

Estudos têm demonstrado que durante a infecção por *P. brasiliensis*, a resposta inicial envolve o reconhecimento do fungo pelos macrófagos alveolares, células dendríticas (DCs), e células epiteliais alveolares (44). Em termos gerais, as células fagocíticas, expressam receptores de reconhecimento de padrões (PRRs) na superfície celular ou no compartimento endossômico, como os receptores tipo *Toll* (TLRs), receptores de lecitina tipo C (CLRs), receptores do complemento (CR) e receptores de manose (MRs), dentre outros. Esses receptores medeiam o reconhecimento de um grupo de padrões moleculares associados a patógenos (PAMPs), presentes na parede celular do fungo (45).

A participação dos PRRs no reconhecimento do fungo pelos fagócitos tem sido abordada em diversos trabalhos. Em neutrófilos humanos a interação com *P. brasiliensis* levou a um incremento na expressão do TLR2 e uma diminuição no TLR4 (46). Outro estudo aponta que os TLR1, 2, e 4 apresentaram um aumento da sua expressão em neutrófilos, embora tenha sido observada uma diminuição em monócitos (47). O receptor Dectina-1 em macrófagos foi

associado com a fagocitose e eliminação do fungo pela ativação do inflamassoma NLRP3 (48–50). Outro trabalho com neutrófilos, relaciona os receptores TLR4 e Dectina-1 com uma resposta protetora, enquanto o TLR2 é associado à susceptibilidade (51). Em DCs foi avaliada a expressão do TLR2, indicando que esse receptor poderia estar relacionado com a susceptibilidade à infecção (52). No mesmo tipo celular, os receptores TLR4, Dectina-1 e o MR foram associados a proteção contra a infecção (53). O receptor TLR9 demostrou um papel protetor contra infecção pelo fungo (49).

O tipo de resposta celular determina a natureza da resistência ou susceptibilidade ao desenvolvimento da doença. A resposta imune protetora está relacionada com um perfil *T helper 1* (Th1) predominante, incluindo citocinas como interferon-gama (IFN-γ), interleucina 12 (IL12) e IL2 (26,54). A produção de IFN-γ é particularmente importante na PCM, por ativar macrófagos e aumentar produção de óxido nítrico (NO), que atua como o principal agente microbicida. Similarmente, estimula os macrófagos infectados a secretar fator de necrose tumoral-alfa (TNF-α), necessário para a persistência do granuloma (55). A participação neutrófilo e de DCs com eficientes mecanismos de apresentação de antígenos também são relevantes na proteção contra a infecção (26). Por outro lado, em indivíduos com PCM a resposta imunitária primária mostra-se incapaz de suprimir o foco da infecção (56). Relacionando-se ao incremento de citocinas do perfil Th2/Th9, em particular IL4, IL10 e TFG-β; a presença de macrófagos ativados alternativamente (M2); eosinofilia e alta produção de imunoglobulinas; levando para uma progressiva proliferação do fungo e posterior disseminação para outros tecidos (**Figura 1**).

Diversos estudos demonstram um papel crucial das células dendríticas na resposta imune contra fungos patogênicos, pelo reconhecimento e fagocitose dos patógenos, formação do fagossomo, que idealmente, fusiona-se com o lisossomo e leva à eliminação do fungo, e a apresentação de antígenos às células T (57,58). O papel central das DCs na imunidade antifúngica, incluída a PCM, é devida a interação necessária entre a imunidade inata, que reconhece o patógeno, e a imunidade adaptativa, que é essencial para eliminar a infecção (57,58). No estado imaturo, as DCs apresentam uma maior capacidade fagocítica, e são especializadas na captação e processamento de antígenos, e na produção de citocinas inflamatórias como TNF-α, IFN-γ, IL12. Por outra parte, as DCs maturas são mais efetivas na apresentação de antígenos, migrando aos linfonodos para apresentação de antígenos no complexo de histocompatibilidade (MHC-I e MHC-II), para as células T (57,59).

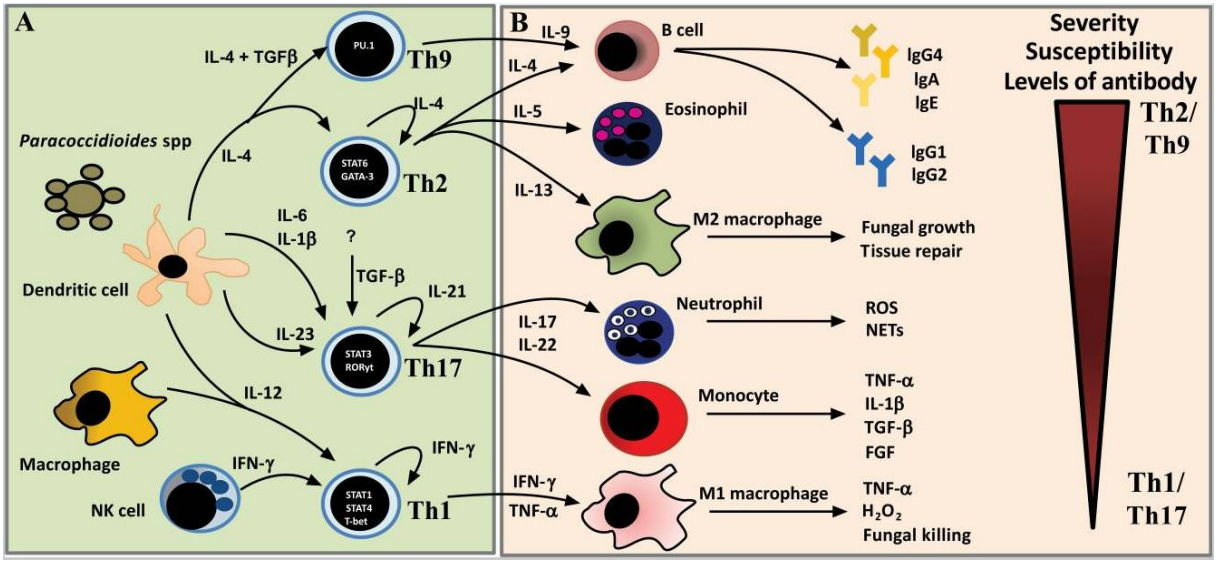

Figura 1. Polarização da resposta imune na paracoccidioidomicose.
A) Ativação dos linfócitos T *helper*. **B)** Fase efetora da resposta das células-T. **Fonte:** Martinez (2017).

A significativa contribuição por Calich *et al*. (1985) com o estabelecimento do modelo murino isogênico resistente e suscetível à PCM, tem permitido um maior entendimento da resposta protetora para essa micose. Camundongos isogênicos da linhagem B10.A apresentam alta mortalidade e desenvolvem uma resposta imune análoga aos hospedeiros susceptíveis. Os modelos murinos da linhagem A/Sn ou A/J apresentam uma resposta imune equivalente aos hospedeiros resistentes (61,62). Em camundongos resistentes, a resposta é associada com a imunidade celular eficiente, caracterizada por uma polarização em direção ao fenótipo de ativação clássica (Th1) dos fagócitos, com produção de citocinas pro-inflamatórias como IFN-γ, IL12 e IL2; baixos níveis de anticorpos específicos para *P. brasiliensis* e poucos granulomas compactos com número reduzido de fungos (62). Por outro lado, em camundongos suscetíveis a resposta imune é associada a uma diminuída resposta celular, com propensão de ativação de células B, grande quantidade de anticorpos, granulomas difusos com alto número de fungos, e secreção precoce de IL5, IL10 e TGF-β (61,62).

1.5. Criptococose

A criptococose é uma infecção fúngica invasiva com diversas manifestações clínicas e que ocorre no mundo todo. Pode representar desde uma infecção cutânea simples até uma infecção sistêmica que atinge o sistema nervoso central (SNC), causando meningite (10,63).

Estima-se que no mundo ocorram aproximadamente 112.000 mortes anuais por criptococose associada à infecção por HIV (64). Em regiões subdesenvolvidas do mundo, a incidência e a mortalidade são mais altas, como consequência do acesso limitado às terapias antirretrovirais e antifúngicas. Na África subsaariana acontece o 63% das mortes por criptococose associadas a HIV/AIDS (64).

Embora a maioria dos casos de criptococose, assim como dos óbitos, ocorra na África (64), há uma incidência significativa na América Latina, especialmente no Brasil e Colômbia (1001 a 2500 casos/ano), que registram cerca de 4,5 casos por milhão de habitantes (65). No Brasil, embora não seja doença de notificação obrigatória, estudos locais sugerem que a criptococose seja a principal doença oportunista em pacientes HIV/AIDS em 6% dos casos, representando a maior causa de meningoencefalite (66). No Norte e Nordeste do país, estudos indicam 40% de letalidade por criptococose provocada por *C. gattii* em crianças imunocompetentes (67). Ainda no Brasil, a letalidade em indivíduos soropositivos varia entre 50% e 77% (65).

1.6. *Cryptococcus neoformans*

Cryptococcus neoformans é um patógeno oportunista que acomete principalmente indivíduos imunodeprimidos. É um dos agentes etiológicos da criptococose, e a causa mais importante de meningoencefalite fúngica no mundo (10,68). A importância médica desse fungo aumentou drasticamente após a década de 1980 em consequência da pandemia HIV/AIDS (3,69). Há outros fatores de risco para o desenvolvimento da criptococose, como transplantes de órgãos e uso de drogas imunossupressoras, diabetes e quimioterapia contra o câncer (5,70).

O fungo é comumente encontrado em forma de levedura haploide, no entanto, pode exibir um crescimento filamentoso no ambiente (71). As leveduras apresentam uma cápsula composta por polissacarídeos que envolve o fungo e é descrita como seu principal fator de virulência (72,73). No ambiente a capsula confere proteção contra a dessecação, também da fagocitose e eliminação por predadores unicelulares como amebas (74). No hospedeiro mamífero, a cápsula confere proteção contra a fagocitose, o estresse oxidativo e eliminação por macrófagos e outros fagócitos (75,76). Além disso, a capsula contribui com o 25% do total da virulência do fungo (77).

A formação da capsula é um processo estimulado por vários fatores e condições similares ao ambiente dentro do hospedeiro como como níveis elevados de CO_2, pH

neutro/alcalino, e privação de ferro (72). A estrutura capsular é composta principalmente por glucuronoxilomanana (GXM), que compõe ~90% da massa total da capsula, e componentes em menor proporção como glucuronoxilomananagalactana (GXMGal ou GalXM) e manoproteínas (78). Os polissacarídeos capsulares possuem propriedades imunomodulatórias podendo atuar na evasão do sistema imune e, facilitando a sobrevivência do patógeno no interior do hospedeiro (79,80).

Diversos estudos mostraram a correlação da capsula e a virulência. Isso é reforçado pelo fato que mutantes acapsulares de *C. neoformans*, são considerados avirulentos em modelos murinos imunocompetentes sem desenvolvimento da doença (81,82). No trabalho realizado por Fromtling *et al* (1982) foram gerados seis mutantes acapsulares (Cap-55, -59, -64, -66, -67, -70) pelo emprego de mutagênese química derivados da linhagem capsular B-3501. A linhagem B3501 é um isolado clinico com capacidade de desenvolver a infecção em camundongos. Após 3 semanas de inoculação intramuscular em camundongos, as linhagens mutantes não sintetizaram a capsula. As linhagens Cap-64, -66, -67 e -70 foram incapazes de disseminar-se a outros tecidos; após 21 dias após infecção foram eliminadas dos locais de inoculação (82,83). Adicionalmente, nenhum mutante acapsular recuperou a capacidade de sintetizar capsula após um ano de cultura, demostrando que as linhagens foram geneticamente estáveis. No entanto, outros estudos reportam que linhagens acapsulares podem causar uma infecção persistente de baixo grado inclusive atingindo o cérebro, ou aumentar a virulência quando comparado às linhagens parentais (84,85).

Uma ampla gama de outros fatores de virulência têm sido descrita para *C. neoformans*, entre esses pode-se destacar a produção de melanina e secreção de enzimas extracelulares que contribuem com a patogênese e a modulação da resposta do hospedeiro. A melanina protege o fungo contra diferentes condições como: radiação ultravioleta, temperatura extrema, antifúngicos e espécies reativas de oxigênio e nitrogênio (86). As fosfolipases são enzimas secretadas pelo fungo que degradam os fosfolipídios das membranas celulares. Essas enzimas são essenciais na disseminação extrapulmonar e inibem a eliminação do fungo dentro dos fagossomos dos macrófagos (63).

1.7. Resposta imune a *Cryptococcus* spp.

A infecção naturalmente ocorre pela inalação de leveduras dessecadas ou esporos do ambiente que se alojam nos pulmões e, em condições normais, são eliminados pelo sistema

imune do hospedeiro (87). No entanto, em indivíduos imunocomprometidos, se a infecção não é erradicada ou quando é reativada, o fungo pode invadir o SNC causando meningoencefalite (63,88). A infecção nos pulmões desencadeia uma resposta imune inflamatória, que envolve a participação de macrófagos, células dendríticas, linfócitos e a produção de citocinas como TNF-α, IFN-γ e IL-12, associadas à resposta Th1, visando à erradicação da infecção. Contrariamente, uma resposta não protetora envolve um recrutamento insuficiente de macrófagos e células dendríticas, com a produção de citocinas do tipo Th2, como a IL4 (**Figura 2**) (89,90). Na maioria dos casos, o fungo não erradicado pode entrar em um estado de latência nos pulmões, formando granulomas, sem levar à evolução da doença (91).

Uma vez nos pulmões do hospedeiro, *C. neoformans* é fagocitado principalmente por macrófagos alveolares e células dendríticas. Nesse processo, é indispensável a participação das proteínas do sistema complemento, levando à deposição do componente 3 do complemento (C3) na cápsula do fungo, como um importante mediador da fagocitose (91). As leveduras opsonizadas são reconhecidas pelos receptores de complemento (CR) CR1, CR3 e CR4, presentes na superfície dos fagócitos, induzindo a internalização das leveduras (**Figura 2**) (92). A fagocitose pode ainda ser mediada pelos receptores Fc-γ (Fc-γR) dos macrófagos e de células dendríticas e por meio da interação com leveduras opsonizadas por anticorpos (93,94). Neste caso, a região Fc dos anticorpos é reconhecida e ligada aos receptores Fc das células fagocíticas, induzindo a fagocitose (92,94). Observou-se ainda que a opsonização com anticorpos produz mudanças na estrutura da cápsula do fungo, que levam à exposição de domínios de união à subunidade CD18 dos receptores CR3 e CR4, otimizando a fagocitose (94).

Há evidências de que os MRs participem no reconhecimento de resíduos de manose da parede celular de *C. neoformans*. Os receptores TLR2 e Dectina-2 (CLR) reconhecem, respectivamente, moléculas de mananas e α-mananas presentes na cápsula do fungo, enquanto TLR9, presente no lisossomo, reconhece o DNA e parece ser o receptor essencial para a ativação da resposta anti-criptococose (45,91).

Um mecanismo de evasão da fagocitose, selecionado ao longo da evolução do fungo, foi a secreção da proteína antifagocítica 1 (App1), que interage com os receptores do complemento CR2 e CR3, diminuindo a fagocitose mediada por esses receptores (95).

Após o reconhecimento do fungo pelos PRRs, os macrófagos e células dendríticas o fagocitam e, em seguida, a fusão dos endossomos com o lisossomo, promove a degradação do patógeno e processamento de antígenos para a apresentação às células T, associados ao

complexo principal de histocompatibilidade de classe II (MHC-II). Nesse processo, também ocorre a liberação de citocinas, como INF-γ, TNF-α, IL12 e IL23, em conjunto, levam à indução de uma resposta imune adaptativa do tipo Th1, necessária à eliminação do patógeno (**Figura 2**) (91).

Embora o ambiente no interior de fagócitos seja extremamente hostil, *C. neoformans* é capaz de sobreviver e se replicar no interior dessas células (96,97). A persistência no interior de células fagocíticas pode facilitar a disseminação do fungo, uma vez que macrófagos alveolares contendo leveduras em seu interior podem se deslocar do pulmão para outros órgãos (98), servindo assim como carreadores (hipótese do *Cavalo de Tróia*). A disseminação pode levar à forma mais grave da infecção, que ocorre quando as leveduras atingem o SNC, causando meningite criptocócica (63).

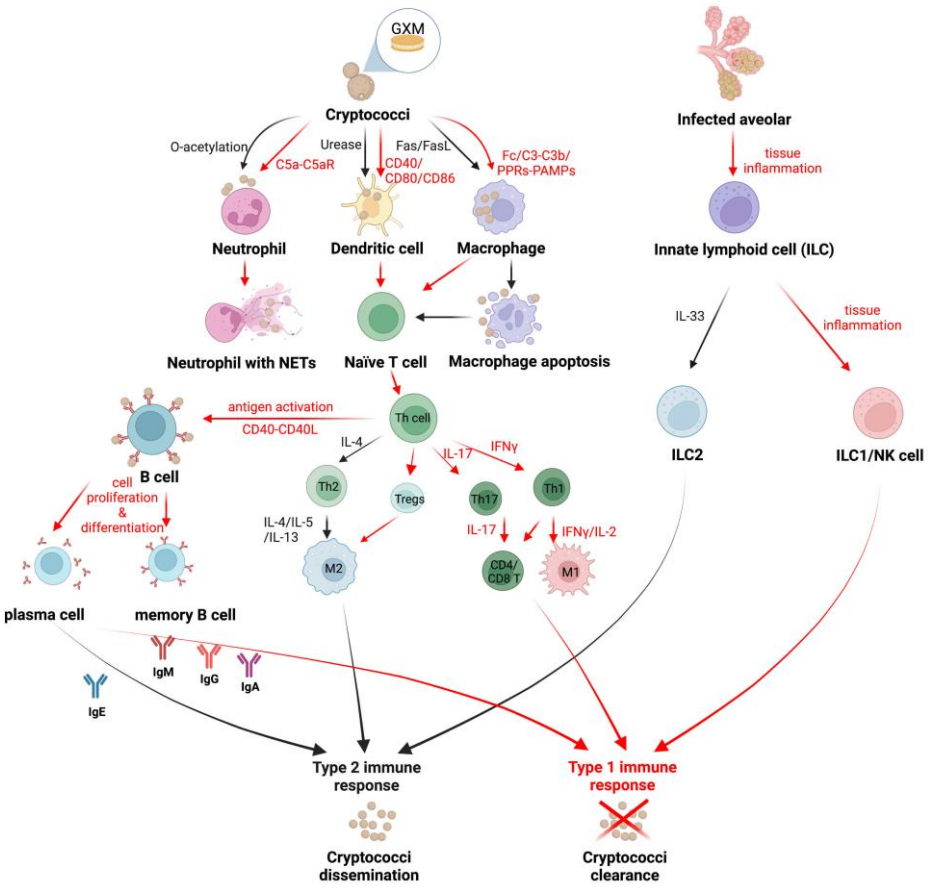

Figura 2. Estratégia de escape de *Cryptococcus* do sistema imune.

As setas vermelhas indicam os mecanismos da resposta do hospedeiro para a eliminação do fungo. As setas pretas indicam a via de escape do fungo ao sistema imune do hospedeiro. **Fonte:** Yang *et al.* (2022).

1.8. Participação de miRNAs na resposta imune

MicroRNAs (miRNAs ou miRs) são pequenos RNAs não-codificadores (ncRNAs) endógenos, de cerca de 22 nucleotídeos (nts), que promovem a repressão pós-transcricional em organismos eucarióticos (100). São produzidos de forma rápida através de vias canônicas e não canônicas, envolvendo diversas etapas e proteínas no processo. A maioria dos miRNAs são transcritos pela RNA polimerase II, a partir de regiões de éxons ou íntrons de genes codificadores, de longos RNAs não codificadores ou de regiões intergênicas (**Figura 3**) (101). O processo de biogênese inicia com a transcrição do gene originando um miRNA primário (pri-miRNA), com uma estrutura de *stem-loop*. Esse precursor é clivado pela enzima Drosha e o cofator DGCR8, o qual produz uma molécula de ~70 nt que apresenta estrutura em forma de grampo (pre-miRNA). Posteriormente, o pre-miRNA é transportado para o citoplasma pela Exportina-5, onde um complexo microprocessador conformado por Dicer e o cofator TRBP (do inglês *TAR RNA-binding protein*) cliva o pre-miRNA gerando um duplex de RNA constituído pelas fitas 5p e 3p do miRNA maduro. Na **Figura 3** é apresentada uma visão geral do processo de biogênese dos miRNAs tanto da via canônica, quanto da via não canônica.

O duplex de miRNA é integrado no complexo de silenciamento induzido por miRNA (miRISC), conformado pela enzima Argonauta-2 com atividade de endonuclease, e o complexo TNRC6 (*trinucleotide repeat containing 6 protein*). Para induzir a repressão do mRNA alvo, uma das fitas é degradada dependendo da estabilidade termodinâmica. O complexo miRISC, identifica um mRNA alvo através da complementariedade da sequência do miRNA (100,102). O mecanismo regulatório envolve o reconhecimento específico por meio do pareamento de bases da região *seed* do miRNA (uma sequência de 2-8 nts do extremo 5') com uma região do mRNA, geralmente em uma sequência na região 3' não traduzida (3'UTR), causando sua degradação e/ou repressão da tradução (**Figura 3**). Sabe-se que um único miRNA pode regular vários mRNAs diferentes e que um mesmo mRNA pode ser regulado por um grande número de miRNAs. Vários relatos da literatura descrevem a diversidade de processos biológicos regulados por estes pequenos RNAs regulatórios: proliferação celular, diferenciação, e apoptoses, entre outros (100,102,103).

Os miRNAs representam uma das principais classes de ncRNAs com papel central na regulação da resposta imune inata e adaptativa (100). Esses pequenos RNAs também participam no controle da resposta inflamatória (104). Sabe-se que após o contato com o patógeno, ocorre uma reprogramação da expressão de centenas de genes tanto na célula hospedeira quanto no

patógeno. Entretanto, esse processo deve ser extremamente controlado para eliminar rapidamente o patógeno sem causar danos excessivos ao hospedeiro (100).

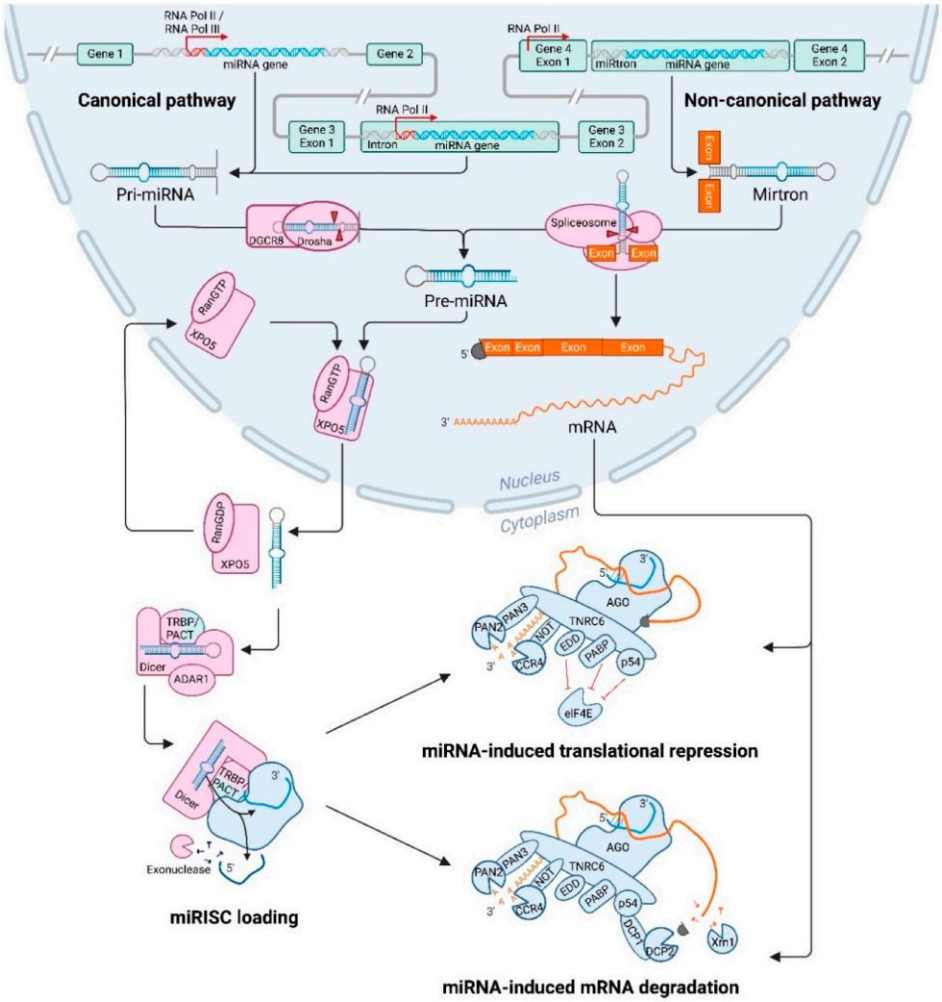

Figura 3. Processo de biogênese dos microRNAs.

Visão geral das etapas das vias canônica e não canônica do processo de biogênese desde a transcrição do miRNA até a regulação do mRNA alvo. **Fonte:** Rooij *et al*. (2022).

Vários estudos demonstram um importante papel de diversos miRNAs controlando processos relacionados à eliminação de patógenos, enquanto assegura um rápido retorno à homeostase (100,101). Após o reconhecimento de patógenos pelos fagócitos, se inicia um processo de ativação coordenada de vários sinais que modula a expressão de genes reguladores das respostas pro-inflamatória e anti-inflamatória. Como, por exemplo, a via de ativação do fator de transcrição NF-κB, que induz a expressão de genes pro-inflamatórios, como citocinas

e quimiocinas (100). Além disso, NF-κB também regula a transcrição de diversos miRNAs, incluindo miR-21, miR-146a e miR-155, que subsequentemente regulam a resposta inflamatória como um *feedback* adicional para proteger o hospedeiro de uma ativação exacerbada (105–107). No entanto, a capacidade dos miRNAs na modulação funcional de vias geralmente depende da convergência de seu efeito em vários níveis da determinada via (100). Por exemplo, a regulação do miR-146 que é direcionado para várias moléculas da via de sinalização e ativação TLR/Myd88/NF-κB (**Figura 4**). Adicionalmente, diferentes miRNAs podem cooperar na regulação alvos chaves da resposta imune em diversos de tipos de células (100).

Outros estudos demonstraram que TNF-α é capaz de levar à indução da expressão de miR-155 por meio das vias de sinalização TRAF ou MyD88, ativando o fator de transcrição NF-κB, que por sua vez se liga ao promotor do gene *MIR155HG* (107). miR-155 também atua como regulador negativo de SHIP1, proteína multifuncional importante em células hematopoiéticas (108), alguns supressores de sinalização de citocinas como SOCS1 (109) e SOCS3 (110), igualmente de TAB2 (111), molécula adaptadora em diferentes vias de transdução de sinal (**Figura 4**). Tal regulação está envolvida na ativação/inativação de células mielóides. SHIP1 e SOCS1 regulam negativamente as vias de sinalização ativadas por ligantes de TLRs, enquanto TAB2 é componente essencial da via de sinalização TLR/IL-1, necessária para produção de citocinas pro-inflamatórias como IL-1β (111).

Outro miRNA potencialmente importante na resposta imune é miR-132, que regula negativamente a produção de citocinas pró-inflamatórias como IL-1β e IL-6, por meio da regulação negativa de IRAK4 (*interleukin 1 receptor associated kinase 4*) (112).

Além do envolvimento de miR-146 na resposta de monócitos humanos ao LPS (105), demostrou-se posteriormente que o aumento da expressão desse miRNA é uma resposta geral de células mielóides ativadas pelas vias TLR2, TLR4 e TLR5 por componentes de superfície de bactérias e fungos, ou após exposição às citocinas pro-inflamatórias TNF-α ou IL-1β (113). A análise da sequência promotora do gene de miR-146a revelou potenciais motivos de ligação a fatores de transcrição, incluindo NF-κB, que se mostrou responsável pela ativação do gene de miR-146a em resposta a LPS.

Entre os mRNAs alvos de miR-146 estão TRAF6 e IRAK1, dois componentes chaves da via de sinalização derivada dos receptores *Toll*, o que indica que o aumento na expressão de miR-146a e miR-146b pode ocorrer por retroalimentação negativa (105). O aumento da

expressão de miR-146 também resulta na diminuição da produção de várias quimiocinas e citocinas pro-inflamatórias, incluindo CXCL8, CCL5 (114), IL-6, CXCL8 (115), e IL-1β (116). Isso sugere que esse miRNA atue impedindo uma resposta imune exacerbada e reestabelecendo a homeostase do sistema (117).

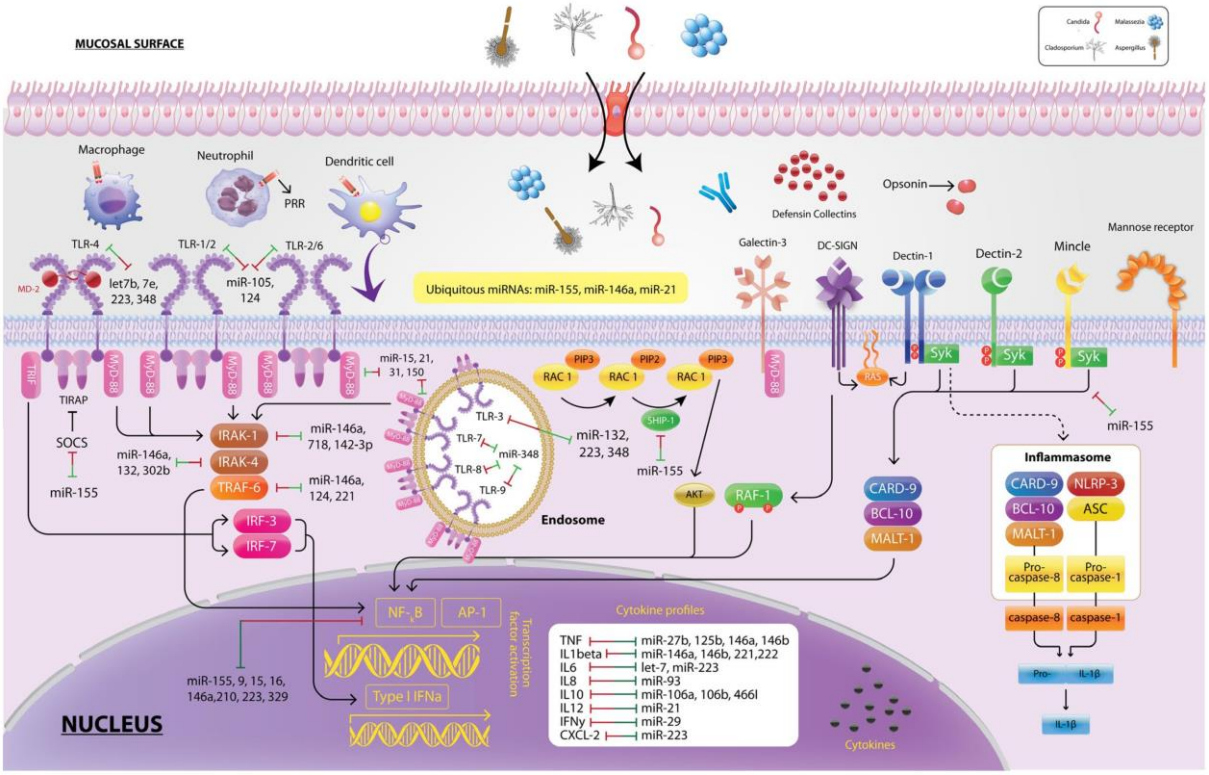

Figura 4. Participação de miRNAs na resposta imune contra fungos patogênicos.
A interação entre PAMPs e PRRs leva à ativação de diferentes vias de sinalização (MyD88, CARD9, IRAK, TRAF) que finalmente estimula fatores de transcrição (NF-κB, AP-1) que permitem a produção e secreção de mediadores inflamatórios como citocinas (TNF-α, IL6, IL1). Vários miRNAs (Mir-155, miR146, miR-21) atuam nesse processo, regulando os níveis de diferentes moléculas que participam das vias de sinalização modulando a intensidade da resposta. **Fonte:** Pakshir *et al*. (2020).

Enquanto um esforço considerável tem sido feito na identificação de miRNAs regulatórios importantes na resposta imune a infecções causadas por bactérias e vírus, pouco se sabe a respeito da regulação mediada por esses pequenos RNAs em resposta a fungos patogênicos. Previamente, foi levantada a hipótese de que os fungos patogênicos podem manipular a rede de sinalização de miRNAs alterando os perfis de expressão durante a evolução da infecção (101).

Anteriormente, Monk e colaboradores (2010) mostraram que miR-146 e miR-155 tiveram a expressão aumentada em macrófagos murinos em resposta à inoculação de células de *C. albicans* mortas pelo calor (118).

Muhammad e colaboradores (2015) investigaram o perfil de expressão de miRNAs em células epiteliais respiratórias de humanos infectados por diferentes espécies de *Candida* spp; os autores demonstraram elevação substancial nos níveis de miR-16-1 e diminuição na expressão do miR-17-3p (119). Mais recentemente, Agustinho *et al*. (2017) reportaram que o receptor Dectina-1 é o principal PRR que participa no aumento da expressão de miR-155, sugerindo que os eventos de sinalização mediados pelos PRRs são fatores importantes na regulação gênica mediada por miRNAs durante as infecções por *Candida* (120).

Em outros estudos, empregando diversas linhagens celulares, observou-se regulação positiva de miRNAs associados à resposta imune contra fungos patogênicos, mais especificamente miR-155, miR-146a, miR-132 e miR-125b em resposta à infecção por *C. albicans* e *P. brasilienses* (121,122). miR-155, além de descrito como regulador negativo de alguns fatores da resposta mediada pela sinalização de TLRs, está associado à ativação de macrófagos e promove uma resposta imune do tipo Th2 durante infecção por *C. albicans*. Já miR-146a é descrito como regulador negativo da resposta mediada pela sinalização dos TLRs de macrófagos em resposta a infecção por *C. albicans* (123). miR-146a, miR-155, miR-30b foram também regulados positivamente na infecção de células THP-1 com a linhagem WN148 de *C. neoformans* (124). Um incremento na expressão do miR-30b foi observado em camundongos e pacientes humanos em resposta à infecção por *P. brasiliensis* (121,125). Mais recentemente, Wei *et al.* (126) demostraram que miR-155 inibe a resposta inflamatória induzida pela infecção de *C. albicans* em células dendríticas humanas, regulando o NF-κB p65.

O aumento das infecções fúngicas sistêmicas associadas à emergente necessidade de novas alternativas terapêuticas impõem a necessidade de conhecimento dos mecanismos de controle da expressão gênica relacionados à regulação da resposta imune. Dados da literatura indicam que a paracoccidioidomicose e criptococose são importantes infecções no mundo, sendo consideradas um grave problema de saúde pública, particularmente em regiões que carecem de recursos médicos necessários ao seu controle efetivo, convertendo-se em um desafio para as agências de saúde mundiais (1,15).

Tendo em vista a crescente importância das infecções fúngicas invasivas, dos poucos dados referentes à reprogramação gênica na susceptibilidade/resistência do hospedeiro, e da

participação de miRNAs na regulação da resposta imunológica a fungos patogênicos, este trabalho teve como objetivo investigar à reprogramação transcritômica de fagócitos murinos, como células dendríticas e macrófagos, em reposta a infecção por *P. brasiliensis* e *C. neoformans*.

2. Referências

1. Dhandapani K, Sivarajan K, Ravindhiran R, Sekar JN. Fungal Infections as an Uprising Threat to Human Health: Chemosensitization of Fungal Pathogens With AFP From Aspergillus giganteus. Front Cell Infect Microbiol [Internet]. 2022 May 25 [cited 2022 Dec 15];12. Available from: https://pubmed.ncbi.nlm.nih.gov/35694549/

2. Dangarembizi R, Wasserman S, Hoving JC. Emerging and re-emerging fungal threats in Africa. Parasite Immunol [Internet]. 2022 [cited 2022 Dec 15]; Available from: https://pubmed.ncbi.nlm.nih.gov/36175380/

3. Ibe C, Okoye CA. Integrated healthcare approach can curb the increasing cases of cryptococcosis in Africa. PLoS Negl Trop Dis [Internet]. 2022 Aug 1 [cited 2022 Dec 15];16(8):e0010625. Available from: /pmc/articles/PMC9409514/

4. Sifuentes-Osornio J, Corzo-León DE, Ponce-De-León LA. Epidemiology of invasive fungal infections in Latin America. Curr Fungal Infect Rep. 2012;6(1):23–34.

5. Datta K, Hamad M. Immunotherapy of Fungal Infections. Immunol Invest. 2015;44(8):738–76.

6. Armstrong-James D, Harrison TS. Immunotherapy for fungal infections [Internet]. Vol. 15, Current Opinion in Microbiology. 2012 [cited 2019 Sep 2]. p. 434–9. Available from: https://linkinghub.elsevier.com/retrieve/pii/S1369527412000835

7. McCarthy MW, Navarro EE, Walsh TJ, Hay RJ. Histoplasmosis. In: Hunter's Tropical Medicine and Emerging Infectious Diseases [Internet]. Elsevier; 2020 [cited 2022 Dec 23]. p. 662–5. Available from: https://linkinghub.elsevier.com/retrieve/pii/B9780323555128000855

8. Kazanjian P. Pneumocystis Pneumonia. In: Hunter's Tropical Medicine and Emerging Infectious Diseases [Internet]. Elsevier; 2020 [cited 2022 Dec 23]. p. 686–8. Available from: https://linkinghub.elsevier.com/retrieve/pii/B9780323555128000910

9. Negroni R. Paracoccidioidomycosis. In: Hunter's Tropical Medicine and Emerging Infectious Diseases. 10th ed. Elsevier; 2020. p. 674–7.

10. Chammard TB, Lanternier F, Lortholary O. Cryptococcosis. In: Hunter's Tropical Medicine and Emerging Infectious Diseases [Internet]. Elsevier; 2020 [cited 2022 Dec 16]. p. 678–81. Available from: https://linkinghub.elsevier.com/retrieve/pii/B9780323555128000892

11. Mada P, Nowack B, Cady B, Joel Chandranesan AS. Disseminated cryptococcosis in an immunocompetent patient. BMJ Case Rep [Internet]. 2017 [cited 2022 Dec 23];2017. Available from: /pmc/articles/PMC5534820/

12. de Almeida JN, Peçanha PM, Colombo AL. Paracoccidioidomycosis in immunocompromised patients: A literature review. J Fungi [Internet]. 2019 Mar 1 [cited 2020 Jul 31];5(1). Available

from: https://pubmed.ncbi.nlm.nih.gov/30587784/

13. Alves Soares E, Lazera M dos S, Wanke B, Faria Ferreira M de, Carvalhaes de Oliveira RV, Oliveira AG, et al. Mortality by cryptococcosis in Brazil from 2000 to 2012 A descriptive epidemiological study. PLoS Negl Trop Dis [Internet]. 2019 Jul 1 [cited 2022 Dec 23];13(7). Available from: /pmc/articles/PMC6687200/

14. dos Reis DST, de Brito MTFM, Guimarães RJ de PS, Quaresma JAS. Cryptococcosis: Identification of Risk Areas in the Brazilian Amazon. Microorganisms [Internet]. 2022 Jul 1 [cited 2022 Dec 23];10(7). Available from: /pmc/articles/PMC9324227/

15. Perfect JR, Dismukes WE, Dromer F, Goldman DL, Graybill JR, Hamill RJ, et al. Clinical Practice Guidelines for the Management of Cryptococcal Disease: 2010 Update by the Infectious Diseases Society of America. Clin Infect Dis [Internet]. 2010;50(3):291–322. Available from: https://academic.oup.com/cid/article-lookup/doi/10.1086/649858

16. Trzeciak-Ryczek A, Tokarz-Deptuła B, Deptuła W. Antifungal immunity in selected fungal infections [Internet]. Vol. 69, Postepy Higieny i Medycyny Doswiadczalnej. 2015 [cited 2019 Sep 3]. p. 469–74. Available from: http://www.ncbi.nlm.nih.gov/pubmed/25897108

17. Jiang S. Immunity against fungal infections. Immunol Immunogenet Insights [Internet]. 2016 Jan 10 [cited 2019 Sep 2];8:3–6. Available from: http://journals.sagepub.com/doi/10.4137/III.S38707

18. Armstrong-James D, Meintjes G, Brown GD. A neglected epidemic: Fungal infections in HIV/AIDS [Internet]. Vol. 22, Trends in Microbiology. 2014 [cited 2019 Sep 3]. p. 120–7. Available from: http://www.ncbi.nlm.nih.gov/pubmed/24530175

19. Mendes RP, Cavalcante R de S, Marques SA, Marques MEA, Venturini J, Sylvestre TF, et al. Paracoccidioidomycosis: Current Perspectives from Brazil. Open Microbiol J [Internet]. 2017 Nov 2 [cited 2020 Aug 31];11(1):224–82. Available from: https://pubmed.ncbi.nlm.nih.gov/29204222/

20. De Melo Teixeira M, Theodoro RC, De Oliveira FFM, MacHado GC, Hahn RC, Bagagli E, et al. Paracoccidioides lutzii sp. nov.: Biological and clinical implications. Med Mycol [Internet]. 2014 [cited 2022 Dec 23];52(1):19–28. Available from: https://pubmed.ncbi.nlm.nih.gov/23768243/

21. Turissini DA, Gomez OM, Teixeira MM, McEwen JG, Matute DR. Species boundaries in the human pathogen Paracoccidioides. Fungal Genet Biol [Internet]. 2017 Sep 1 [cited 2022 Dec 23];106:9–25. Available from: https://pubmed.ncbi.nlm.nih.gov/28602831/

22. De Macedo PM, De Melo Teixeira M, Barker BM, Zancopé-Oliveira RM, Almeida-Paes R, Do Valle ACF. Clinical features and genetic background of the sympatric species Paracoccidioides brasiliensis and Paracoccidioides americana. PLoS Negl Trop Dis [Internet]. 2019 [cited 2020 Jul 31];13(4). Available from: https://pubmed.ncbi.nlm.nih.gov/30986220/

23. Romani L. Immunity to fungal infections. Nat Rev Immunol [Internet]. 2011 Apr [cited 2020 Sep 9];11(4):275–88. Available from: https://pubmed.ncbi.nlm.nih.gov/21394104/

24. Dantas KC, Mauad T, de André CDS, Bierrenbach AL, Saldiva PHN. A single-centre, retrospective study of the incidence of invasive fungal infections during 85 years of autopsy service in Brazil. Sci Rep [Internet]. 2021 Dec 1 [cited 2022 Dec 23];11(1):3943. Available from: /pmc/articles/PMC7889920/

25. Shikanai-Yasuda MA, Mendes RP, Colombo AL, de Queiroz-Telles F, Kono ASG, Paniago AMM, et al. Brazilian guidelines for the clinical management of paracoccidioidomycosis. Rev Soc Bras Med Trop [Internet]. 2017 Sep 1 [cited 2020 Jul 31];50(5):715–40. Available from: https://pubmed.ncbi.nlm.nih.gov/28746570/

26. Martinez R. New trends in paracoccidioidomycosis epidemiology. J Fungi [Internet]. 2017 Mar 1 [cited 2020 Jul 14];3(1). Available from: /pmc/articles/PMC5715958/?report=abstract

27. Wagner G, Moertl D, Glechner A, Mayr V, Klerings I, Zachariah C, et al. Paracoccidioidomycosis diagnosed in europe—a systematic literature review. J Fungi [Internet]. 2021 Feb 1 [cited 2022 Dec 23];7(2):1–25. Available from: /pmc/articles/PMC7926554/

28. Peçanha PM, Peçanha-Pietrobom PM, Grão-Velloso TR, Rosa Júnior M, Falqueto A, Gonçalves SS. Paracoccidioidomycosis: What We Know and What Is New in Epidemiology, Diagnosis, and Treatment. J Fungi [Internet]. 2022 Oct 1 [cited 2022 Dec 23];8(10). Available from: /pmc/articles/PMC9605487/

29. Coutinho ZF, Wanke B, Travassos C, Oliveira RM, Xavier DR, Coimbra CEA. Hospital morbidity due to paracoccidioidomycosis in Brazil (1998-2006). Trop Med Int Heal [Internet]. 2015 May 1 [cited 2020 Jul 14];20(5):673–80. Available from: https://pubmed.ncbi.nlm.nih.gov/25645820/

30. Bellissimo-Rodrigues F, Machado AA, Martinez R. Paracoccidioidomycosis epidemiological features of a 1,000-cases series from a hyperendemic area on the southeast of Brazil. Am J Trop Med Hyg [Internet]. 2011 Sep 9 [cited 2022 Dec 23];85(3):546–50. Available from: /pmc/articles/PMC3163882/

31. Arantes TD, Theodoro RC, Teixeira M de M, Bosco S de MG, Bagagli E. Environmental Mapping of Paracoccidioides spp. in Brazil Reveals New Clues into Genetic Diversity, Biogeography and Wild Host Association. PLoS Negl Trop Dis [Internet]. 2016 Apr 5 [cited 2022 Dec 23];10(4). Available from: https://pubmed.ncbi.nlm.nih.gov/27045486/

32. Hrycyk MF, Garcia Garces H, Bosco S de MG, de Oliveira SL, Marques SA, Bagagli E. Ecology of Paracoccidioides brasiliensis, P. lutzii and related species: infection in armadillos, soil occurrence and mycological aspects. Med Mycol [Internet]. 2018 Nov 1 [cited 2022 Dec 23];56(8):950–62. Available from: https://pubmed.ncbi.nlm.nih.gov/29325170/

33. Poplin V, Smith C, Milsap D, Zabel L, Bahr NC. Diagnosis of pulmonary infections due to endemic fungi. Diagnostics [Internet]. 2021 [cited 2022 Dec 23];11(5). Available from: /pmc/articles/PMC8151383/

34. Felipe MSS, Andrade R V., Arraes FBM, Nicola AM, Maranhão AQ, Torres FAG, et al. Transcriptional profiles of the human pathogenic fungus Paracoccidioides brasiliensis in mycelium and yeast cells. J Biol Chem [Internet]. 2005 Jul 1 [cited 2022 Dec 23];280(26):24706–14. Available from: https://pubmed.ncbi.nlm.nih.gov/15849188/

35. Rezende TCV, Borges CL, Magalhães AD, de Sousa MV, Ricart CAO, Bailão AM, et al. A quantitative view of the morphological phases of Paracoccidioides brasiliensis using proteomics. J Proteomics [Internet]. 2011 Dec 21 [cited 2022 Dec 23];75(2):572–87. Available from: https://pubmed.ncbi.nlm.nih.gov/21920475/

36. Rooney PJ, Klein BS. Linking fungal morphogenesis with virulence. Cell Microbiol [Internet]. 2002 [cited 2022 Dec 23];4(3):127–37. Available from: https://pubmed.ncbi.nlm.nih.gov/11906450/

37. San-Blas G, San-Blas F. Paracoccidioides brasileensis: Cell wall structure and virulence - A review. Mycopathologia [Internet]. 1977 Dec [cited 2022 Dec 23];62(2):77–86. Available from: https://pubmed.ncbi.nlm.nih.gov/340954/

38. Tavares AHFP, Silva SS, Dantas A, Campos ÉG, Andrade R V., Maranhão AQ, et al. Early transcriptional response of Paracoccidioides brasiliensis upon internalization by murine macrophages. Microbes Infect [Internet]. 2007 Apr [cited 2020 Aug 3];9(5):583–90. Available from: https://pubmed.ncbi.nlm.nih.gov/17387029/

39. Gonzalez A, De Gregori W, Velez D, Restrepo A, Cano LE. Nitric oxide participation in the fungicidal mechanism of gamma interferon-activated murine macrophages against Paracoccidioides brasiliensis conidia. Infect Immun [Internet]. 2000 May [cited 2020 Sep 1];68(5):2546–52. Available from: https://pubmed.ncbi.nlm.nih.gov/10768942/

40. Derengowski LS, Tavares AH, Silva S, Procópio LS, Felipe MSS, Silva-Pereira I. Upregulation of glyoxylate cycle genes upon Paracoccidioides brasiliensis internalization by murine macrophages and in vitro nutritional stress condition. Med Mycol [Internet]. 2008 Mar [cited 2022 Dec 23];46(2):125–34. Available from: https://pubmed.ncbi.nlm.nih.gov/18324491/

41. da Silva MB, Thomaz L, Marques AF, Svidzinski AE, Nosanchuk JD, Casadevall A, et al. Resistance of melanized yeast cells of Paracoccidioides brasiliensis to antimicrobial oxidants and inhibition of phagocytosis using carbohydrates and monoclonal antibody to CD18. Mem Inst Oswaldo Cruz [Internet]. 2009 [cited 2022 Dec 23];104(4):644–8. Available from: https://pubmed.ncbi.nlm.nih.gov/19722091/

42. de Oliveira HC, da Silva J de F, Scorzoni L, Marcos CM, Rossi SA, de Paula e Silva ACA, et al. Importance of adhesins in virulence of Paracoccidioides spp. Front Microbiol [Internet]. 2015 [cited 2022 Dec 23];6(MAR). Available from: https://pubmed.ncbi.nlm.nih.gov/25914695/

43. de Oliveira SAM, Reis JN, Catão E, Amaral AC, Souza ACO, Ribeiro AM, et al. β2 Integrin-Mediated Susceptibility to Paracoccidioides brasiliensis Experimental Infection in Mice. Front Cell Infect Microbiol [Internet]. 2021 Mar 16 [cited 2022 Dec 23];11. Available from: /pmc/articles/PMC8007971/

44. Mendes-Giannini MJS, Monteiro Da Silva JL, De Fátima Da Silva J, Donofrio FC, Miranda ET, Andreotti PF, et al. Interactions of Paracoccidioides brasiliensis with host cells: Recent advances. Mycopathologia [Internet]. 2008 Apr [cited 2022 Dec 23];165(4–5):237–48. Available from: https://pubmed.ncbi.nlm.nih.gov/17940851/

45. Ramirez-Ortiz ZG, Means TK. The role of dendritic cells in the innate recognition of pathogenic fungi (A. fumigatus, C. neoformans and C. albicans). Virulence. 2012;3(7):635–46.

46. Acorci-Valério MJ, Bordon-Graciani AP, Dias-Melicio LA, De Assis Golim M, Nakaira-Takahagi E, De Campos Soares ÂMV. Role of TLR2 and TLR4 in human neutrophil functions against paracoccidioides brasiliensis. Scand J Immunol [Internet]. 2010 Feb [cited 2020 Aug 31];71(2):99–108. Available from: https://pubmed.ncbi.nlm.nih.gov/20384861/

47. Bonfim CV, Mamoni RL, Lima Blotta MHS. TLR-2, TLR-4 and dectin-1 expression in human monocytes and neutrophils stimulated by Paracoccidioides brasiliensis. Med Mycol [Internet]. 2009 [cited 2022 Dec 23];47(7):722–33. Available from: https://pubmed.ncbi.nlm.nih.gov/19888805/

48. Diniz SN, Nomizo R, Cisalpino PS, Teixeira MM, Brown GD, Mantovani A, et al. PTX3 function as an opsonin for the dectin-1-dependent internalization of zymosan by macrophages. J Leukoc Biol [Internet]. 2004 Apr [cited 2022 Dec 23];75(4):649–56. Available from: https://pubmed.ncbi.nlm.nih.gov/14726497/

49. Menino JF, Saraiva M, Gomes-Alves AG, Lobo-Silva D, Sturme M, Gomes-Rezende J, et al. TLR9 Activation Dampens the Early Inflammatory Response to Paracoccidioides brasiliensis, Impacting Host Survival. PLoS Negl Trop Dis [Internet]. 2013 [cited 2022 Dec 23];7(7). Available from: https://pubmed.ncbi.nlm.nih.gov/23936560/

50. Feriotti C, Bazan SB, Loures F V., Araújo EF, Costa TA, Calich VLG. Expression of dectin-1 and enhanced activation of NALP3 inflammasome are associated with resistance to paracoccidioidomycosis. Front Microbiol [Internet]. 2015 [cited 2022 Dec 23];6(SEP). Available from: /pmc/articles/PMC4558525/

51. Rodrigues DR, Fernandes RK, Balderramas H de A, Penitenti M, Bachiega TF, Calvi SA, et al.

Interferon-gamma production by human neutrophils upon stimulation by IL-12, IL-15 and IL-18 and challenge with Paracoccidioides brasiliensis. Cytokine [Internet]. 2014 [cited 2022 Dec 23];69(1):102–9. Available from: https://pubmed.ncbi.nlm.nih.gov/25022968/

52. Ferreira KS, Bastos KR, Russo M, Almeida SR. Interaction between Paracoccidioides brasiliensis and Pulmonary Dendritic Cells Induces Interleukin-10 Production and Toll-Like Receptor–2 Expression: Possible Mechanisms of Susceptibility. J Infect Dis [Internet]. 2007 Oct [cited 2020 Jul 14];196(7):1108–15. Available from: https://pubmed.ncbi.nlm.nih.gov/17763336/

53. Loures F V., Araújo EF, Feriotti C, Bazan SB, Calich VLG. TLR-4 cooperates with Dectin-1 and mannose receptor to expand Th17 and Tc17 cells induced by Paracoccidioides brasiliensis stimulated dendritic cells. Front Microbiol [Internet]. 2015 [cited 2020 Jul 14];6(MAR). Available from: https://pubmed.ncbi.nlm.nih.gov/25873917/

54. Calvi SA, Peraçoli MTS, Mendes RP, Marcondes-Machado J, Fecchio D, Marques SA, et al. Effect of cytokines on the in vitro fungicidal activity of monocytes from paracoccidioidomycosis patients. Microbes Infect [Internet]. 2003 Feb 1 [cited 2022 Dec 23];5(2):107–13. Available from: https://pubmed.ncbi.nlm.nih.gov/12650768/

55. Souto JT, Figueiredo F, Furlanetto A, Pfeffer K, Rossi MA, Silva JS. Interferon-γ and tumor necrosis factor-α determine resistance to Paracoccidioides brasiliensis infection in mice. Am J Pathol [Internet]. 2000 [cited 2022 Dec 23];156(5):1811–20. Available from: /pmc/articles/PMC1876914/

56. Mamoni RL, Blotta MHSL. Flow-cytometric analysis of cytokine production in human paracoccidioidomycosis. Cytokine [Internet]. 2006 Aug [cited 2022 Dec 23];35(3–4):207–16. Available from: https://pubmed.ncbi.nlm.nih.gov/17045486/

57. Thind SK, Taborda CP, Nosanchuk JD. Dendritic cell interactions with Histoplasma and Paracoccidioides. Virulence [Internet]. 2015 Jan 1 [cited 2020 Jul 14];6(5):424–32. Available from: https://pubmed.ncbi.nlm.nih.gov/25933034/

58. Eastman AJ, Osterholzer JJ, Olszewski MA. Role of dendritic cell-pathogen interactions in the immune response to pulmonary cryptococcal infection. Future Microbiol [Internet]. 2015 Nov 1 [cited 2022 Jul 5];10(11):1837–57. Available from: https://pubmed.ncbi.nlm.nih.gov/26597428/

59. Tavares AH, Derengowski LS, Ferreira KS, Silva SS, Macedo C, Bocca AL, et al. Murine dendritic cells transcriptional modulation upon Paracoccidioides brasiliensis infection. PLoS Negl Trop Dis [Internet]. 2012 Jan [cited 2020 Jul 17];6(1). Available from: https://pubmed.ncbi.nlm.nih.gov/22235359/

60. Garcia Calich VL, Singer-Vermes LM, Siqueira AM, Burger E. Susceptibility and resistance of inbred mice to Paracoccidioides brasiliensis. Br J Exp Pathol [Internet]. 1985 [cited 2020 Jul

14];66(5):585–94. Available from: /pmc/articles/PMC2042050/?report=abstract

61. Calich VLG, Da Costa TA, Felonato M, Arruda C, Bernardino S, Loures FV, et al. Innate immunity to Paracoccidioides brasiliensis infection. Mycopathologia [Internet]. 2008 Apr [cited 2020 Jul 14];165(4–5):223–36. Available from: https://pubmed.ncbi.nlm.nih.gov/18777631/

62. De Souza Silva C, Tavares AH, Sousa Jeronimo M, Soares De Lima Y, Da Silveira Derengowski L, Lorenzetti Bocca A, et al. The Effects of Paracoccidioides brasiliensis Infection on GM-CSF- and M-CSF-Induced Mouse Bone Marrow-Derived Macrophage from Resistant and Susceptible Mice Strains. Mediators Inflamm [Internet]. 2015 [cited 2020 Jul 14];2015. Available from: http://dx.doi.org/10.1155/2015/605450

63. Chen Y, Shi ZW, Strickland AB, Shi M. Cryptococcus neoformans Infection in the Central Nervous System: The Battle between Host and Pathogen. J fungi (Basel, Switzerland) [Internet]. 2022 Oct 1 [cited 2022 Dec 15];8(10). Available from: https://pubmed.ncbi.nlm.nih.gov/36294634/

64. Rajasingham R, Govender NP, Jordan A, Loyse A, Shroufi A, Denning DW, et al. The global burden of HIV-associated cryptococcal infection in adults in 2020: a modelling analysis. Lancet Infect Dis [Internet]. 2022 Dec [cited 2022 Dec 15];22(12). Available from: https://pubmed.ncbi.nlm.nih.gov/36049486/

65. Firacative C, Lizarazo J, Illnait-Zaragozí MT, Castañeda E. The status of cryptococcosis in Latin America. Mem Inst Oswaldo Cruz [Internet]. 2018;113(7):1–23. Available from: http://www.scielo.br/scielo.php?script=sci_arttext&pid=S0074-02762018000700203&lng=en&tlng=en

66. Corrêa Pinheiro M, dos Reis DST, de Brito MTFM, Simões Quaresma JA. Cryptococcosis in the Amazon: A current overview and future perspectives. Acta Trop [Internet]. 2019 Sep 1 [cited 2022 Dec 23];197. Available from: https://pubmed.ncbi.nlm.nih.gov/31181189/

67. Kon AS, Grumach AS, Colombo AL, Penalva ACO, Wanke B, Telles FDQ, et al. Consenso em criptococose - 2008. Rev Soc Bras Med Trop. 2008;41(5):524–44.

68. Maziarz EK, Perfect JR. Cryptococcosis. Infect Dis Clin North Am. 2016;30(1):179–206.

69. Perfect JR, Casadevall A. The History of Cryptococcus and Cryptococcosis. In: Cryptococcus [Internet]. American Society of Microbiology; 2011 [cited 2019 Sep 18]. p. 17–26. Available from: http://www.asmscience.org/content/book/10.1128/9781555816858.ch02

70. Enoch DA, Yang H, Aliyu SH, Micallef C. The changing epidemiology of invasive fungal infections. In: Methods in Molecular Biology [Internet]. 2017 [cited 2019 Sep 11]. p. 17–65. Available from: http://www.ncbi.nlm.nih.gov/pubmed/27837497

71. Lin X, Heitman J. Chlamydospore formation during hyphal growth in Cryptococcus neoformans.

Eukaryot Cell [Internet]. 2005 Oct [cited 2022 Dec 23];4(10):1746–54. Available from: /pmc/articles/PMC1265899/

72. Alspaugh JA. Virulence mechanisms and Cryptococcus neoformans pathogenesis. Fungal Genet Biol [Internet]. 2015 May 1 [cited 2022 Dec 23];78:55–8. Available from: https://pubmed.ncbi.nlm.nih.gov/25256589/

73. Freitas GJC, Gouveia-Eufrasio L, Emidio ECP, Carneiro HCS, de Matos Baltazar L, Costa MC, et al. The Dynamics of Cryptococcus neoformans Cell and Transcriptional Remodeling during Infection. Cells [Internet]. 2022 Dec 1 [cited 2022 Dec 23];11(23). Available from: /pmc/articles/PMC9740611/

74. Casadevall A, Fu MS, Guimaraes A, Albuquerque P. The 'amoeboid predator-fungal animal virulence' hypothesis. J Fungi [Internet]. 2019 Mar 1 [cited 2022 Dec 23];5(1). Available from: /pmc/articles/PMC6463022/

75. Kozel TR, Pfrommer GST, Guerlain AS, Highison BA, Highison GJ. Role of the Capsule in Phagocytosis of Cryptococcus neoformans. Clin Infect Dis [Internet]. 1988 [cited 2018 May 23];10(Supplement 2):S436–9. Available from: http://www.ncbi.nlm.nih.gov/pubmed/3055212

76. Kozel TR. Opsonization and phagocytosis of Cryptococcus neoformans. Arch Med Res [Internet]. 1993 [cited 2018 May 23];24(3):211–8. Available from: http://www.ncbi.nlm.nih.gov/pubmed/8298269

77. McClelland EE, Bernhardt P, Casadevall A. Estimating the relative contributions of virulence factors for pathogenic microbes. Infect Immun [Internet]. 2006 Mar [cited 2022 Dec 23];74(3):1500–4. Available from: /pmc/articles/PMC1418678/

78. Doering TL. How sweet it is! Cell wall biogenesis and polysaccharide capsule formation in Cryptococcus neoformans. Annu Rev Microbiol [Internet]. 2009 Oct [cited 2022 Dec 23];63:223–47. Available from: /pmc/articles/PMC2880894/

79. Monari C, Bistoni F, Vecchiarelli A. Glucuronoxylomannan exhibits potent immunosuppressive properties. FEMS Yeast Res. 2006;6(4):537–42.

80. Vecchiarelli A, Monari C. Capsular Material of Cryptococcus neoformans: Virulence and Much More. Mycopathologia. 2012;173(5–6):375–86.

81. Chang YC, Kwon-Chung KJ. Complementation of a capsule-deficient mutation of Cryptococcus neoformans restores its virulence. Mol Cell Biol [Internet]. 1994 Jul [cited 2022 Dec 15];14(7):4912–9. Available from: https://pubmed.ncbi.nlm.nih.gov/8007987/

82. Fromtling RA, Shadomy HJ, Jacobson ES. Decreased virulence in stable, acapsular mutants of Cryptococcus neoformans. Mycopathologia [Internet]. 1982 [cited 2019 Sep 11];79(1):23–9.

Available from: http://link.springer.com/10.1007/BF00636177

83. Jacobson ES, Ayers DJ, Harrell AC, Nicholas CC. Genetic and phenotypic characterization of capsule mutants of Cryptococcus neoformans. J Bacteriol [Internet]. 1982 Jun [cited 2019 Aug 11];150(3):1292–6. Available from: http://www.ncbi.nlm.nih.gov/pubmed/7042689

84. O'Meara TR, Norton D, Price MS, Hay C, Clements MF, Nichols CB, et al. Interaction of Cryptococcus neoformans Rim101 and protein kinase a regulates capsule. PLoS Pathog [Internet]. 2010 Feb [cited 2022 Dec 15];6(2). Available from: https://pubmed.ncbi.nlm.nih.gov/20174553/

85. Salkowski CA, Balish E. Susceptibility of congenitally immunodeficient mice to a nonencapsulated strain of Cryptococcus neoformans. Can J Microbiol [Internet]. 1991 [cited 2022 Dec 23];37(11):834–9. Available from: https://pubmed.ncbi.nlm.nih.gov/1777860/

86. Almeida F, Wolf JM, Casadevall A. Virulence-Associated Enzymes of Cryptococcus neoformans. Eukaryot Cell [Internet]. 2015 [cited 2022 Dec 23];14(12):1173. Available from: /pmc/articles/PMC4664877/

87. Velagapudi R, Hsueh YP, Geunes-Boyer S, Wright JR, Heitman J. Spores as infectious propagules of Cryptococcus neoformans. Infect Immun [Internet]. 2009 Oct [cited 2022 Dec 23];77(10):4345–55. Available from: https://pubmed.ncbi.nlm.nih.gov/19620339/

88. Leopold Wager CM, Hole CR, Wozniak KL, Wormley FL. Cryptococcus and phagocytes: Complex interactions that influence disease outcome. Front Microbiol. 2016;7(FEB):1–16.

89. Guillot L, Carroll SF, Homer R, Qureshi ST. Enhanced innate immune responsiveness to pulmonary Cryptococcus neoformans infection is associated with resistance to progressive infection. Infect Immun. 2008;76(10):4745–56.

90. Cheng PY, Sham A, Kronstad JW. Cryptococcus gattii isolates from the British Columbia cryptococcosis outbreak induce less protective inflammation in a murine model of infection than Cryptococcus neoformans. Infect Immun. 2009;77(10):4284–94.

91. Rohatgi S, Pirofski L-A. Host immunity to Cryptococcus neoformans. Future Microbiol [Internet]. 2015;10(4):565–81. Available from: http://www.scopus.com/inward/record.url?eid=2-s2.0-84927725574&partnerID=tZOtx3y1

92. Zaragoza O, Taborda CP, Casadevall A. The efficacy of complement-mediated phagocytosis of Cryptococcus neoformans is dependent on the location of C3 in the polysaccharide capsule and involves both direct and indirect C3-mediated interactions. Eur J Immunol. 2003;33(7):1957–67.

93. Netski D, Kozel TR. Fc-dependent and Fc-independent opsonization of Cryptococcus neoformans by anticapsular monoclonal antibodies: Importance of epitope specificity. Infect Immun. 2002;70(6):2812–9.

94. Taborda CP, Casadevall A. CR3 (CD11b/CD18) and CR4 (CD11c/CD18) are involved in complement-independent antibody-mediated phagocytosis of Cryptococcus neoformans. Immunity. 2002;16(6):791–802.

95. Stano P, Williams V, Villani M, Cymbalyuk ES, Qureshi A, Huang Y, et al. App1: an antiphagocytic protein that binds to complement receptors 3 and 2. J Immunol [Internet]. 2009;182(1):84–91. Available from: http://www.ncbi.nlm.nih.gov/pubmed/19109138

96. Tucker SC, Casadevall A. Replication of Cryptococcus neoformans in macrophages is accompanied by phagosomal permeabilization and accumulation of vesicles containing polysaccharide in the cytoplasm. Proc Natl Acad Sci U S A [Internet]. 2002 Mar 5 [cited 2019 Sep 4];99(5):3165–70. Available from: http://www.pnas.org/cgi/doi/10.1073/pnas.052702799

97. Voelz K, Lammas DA, May RC. Cytokine signaling regulates the outcome of intracellular macrophage parasitism by Cryptococcus neoformans. Infect Immun [Internet]. 2009 Aug 1 [cited 2019 Sep 4];77(8):3450–7. Available from: http://www.ncbi.nlm.nih.gov/pubmed/19487474

98. Charlier C, Nielsen K, Daou S, Brigitte M, Chretien F, Dromer F. Evidence of a role for monocytes in dissemination and brain invasion by Cryptococcus neoformans. Infect Immun [Internet]. 2009 Jan 1 [cited 2019 Sep 10];77(1):120–7. Available from: http://www.ncbi.nlm.nih.gov/pubmed/18936186

99. Yang C, Huang Y, Zhou Y, Zang X, Deng H, Liu Y, et al. Cryptococcus escapes host immunity: What do we know? Front Cell Infect Microbiol [Internet]. 2022 Oct 13 [cited 2022 Dec 23];12. Available from: /pmc/articles/PMC9606624/

100. Nejad C, Stunden HJ, Gantier MP. A guide to miRNAs in inflammation and innate immune responses. FEBS J [Internet]. 2018 Oct 1 [cited 2022 Dec 23];285(20):3695–716. Available from: https://pubmed.ncbi.nlm.nih.gov/29688631/

101. Pakshir K, Badali H, Nami S, Mirzaei H, Ebrahimzadeh V, Morovati H. Interactions between immune response to fungal infection and microRNAs: The pioneer tuners. Mycoses [Internet]. 2020 Jan 1 [cited 2022 Dec 23];63(1):4–20. Available from: https://pubmed.ncbi.nlm.nih.gov/31597205/

102. de Rooij LA, Mastebroek DJ, ten Voorde N, van der Wall E, van Diest PJ, Moelans CB. The microRNA Lifecycle in Health and Cancer. Cancers (Basel) [Internet]. 2022 Dec 1 [cited 2022 Dec 23];14(23). Available from: /pmc/articles/PMC9736740/

103. Croston TL, Lemons AR, Beezhold DH, Green BJ. MicroRNA regulation of host immune responses following fungal exposure. Front Immunol. 2018;9(FEB).

104. Zhang S, Meng Y, Zhou L, Qiu L, Wang H, Su D, et al. Targeting epigenetic regulators for inflammation: Mechanisms and intervention therapy. MedComm [Internet]. 2022 Dec [cited 2022

Dec 23];3(4). Available from: /pmc/articles/PMC9477794/

105. Taganov KD, Boldin MP, Chang K-J, Baltimore D. NF- B-dependent induction of microRNA miR-146, an inhibitor targeted to signaling proteins of innate immune responses. Proc Natl Acad Sci [Internet]. 2006;103(33):12481–6. Available from: http://www.pnas.org/cgi/doi/10.1073/pnas.0605298103

106. Ma X, Becker Buscaglia LE, Barker JR, Li Y. MicroRNAs in NF-κB signaling. J Mol Cell Biol [Internet]. 2011 Jun [cited 2022 Dec 23];3(3):159–66. Available from: /pmc/articles/PMC3104013/

107. Xiaoyan W, Pais EMA, Lan L, Jingrui C, Lin M, Fordjour PA, et al. MicroRNA-155: a Novel Armamentarium Against Inflammatory Diseases. Inflammation [Internet]. 2017;40(2):708–16. Available from: http://dx.doi.org/10.1007/s10753-016-0488-y

108. O'Connell RM, Chaudhuri AA, Rao DS, Baltimore D. Inositol phosphatase SHIP1 is a primary target of miR-155. Proc Natl Acad Sci [Internet]. 2009;106(17):7113–8. Available from: http://www.pnas.org/cgi/doi/10.1073/pnas.0902636106

109. Lu LF, Thai TH, Calado DP, Chaudhry A, Kubo M, Tanaka K, et al. Foxp3-Dependent MicroRNA155 Confers Competitive Fitness to Regulatory T Cells by Targeting SOCS1 Protein. Immunity [Internet]. 2009;30(1):80–91. Available from: http://dx.doi.org/10.1016/j.immuni.2008.11.010

110. Zhai A, Qian J, Kao W, Li A, Li Y, He J, et al. Borna disease virus encoded phosphoprotein inhibits host innate immunity by regulating miR-155. Antiviral Res [Internet]. 2013;98(1):66–75. Available from: http://dx.doi.org/10.1016/j.antiviral.2013.02.009

111. Ceppi M, Pereira PM, Dunand-Sauthier I, Barras E, Reith W, Santos MA, et al. MicroRNA-155 modulates the interleukin-1 signaling pathway in activated human monocyte-derived dendritic cells. Proc Natl Acad Sci [Internet]. 2009 Feb 24 [cited 2018 May 30];106(8):2735–40. Available from: http://www.pnas.org/lookup/doi/10.1073/pnas.0811073106

112. Kong H, Yin F, He F, Omran A, Li L, Wu T, et al. The Effect of miR-132, miR-146a, and miR-155 on MRP8/TLR4-Induced Astrocyte-Related Inflammation. J Mol Neurosci. 2015;57(1):28–37.

113. Lindsay MA, Fire A, al. et, Williams AE, Stefani G, Slack FJ, et al. microRNAs and the immune response. Trends Immunol [Internet]. 2008;29(7):343–51. Available from: http://www.ncbi.nlm.nih.gov/pubmed/18515182

114. Perry MM, Moschos SA, Williams AE, Shepherd NJ, Larner-Svensson HM, Lindsay MA. Rapid changes in microRNA-146a expression negatively regulate the IL-1beta-induced inflammatory response in human lung alveolar epithelial cells. J Immunol [Internet]. 2008 Apr 15 [cited 2018 May 30];180(8):5689–98. Available from:

http://www.ncbi.nlm.nih.gov/pubmed/18390754

115. Jones MR, Quinton LJ, Blahna MT, Neilson JR, Fu S, Ivanov AR, et al. Zcchc11-dependent uridylation of microRNA directs cytokine expression. Nat Cell Biol [Internet]. 2009;11(9):1157–63. Available from: http://dx.doi.org/10.1038/ncb1931

116. Nahid MA, Pauley KM, Satoh M, Chan EKL. miR-146a is critical for endotoxin-induced tolerance: Implication in innate immunity. J Biol Chem. 2009;284(50):34590–9.

117. Alam MM, O'Neill LA. MicroRNAs and the resolution phase of inflammation in macrophages. Eur J Immunol. 2011;41(9):2482–5.

118. Monk CE, Hutvagner G, Arthur JSC. Regulation of miRNA transcription in macrophages in response to candida albicans. PLoS One. 2010;5(10).

119. Muhammad SA, Fatima N, Syed N-H, Wu X, Yang XF, Chen JY. MicroRNA Expression Profiling of Human Respiratory Epithelium Affected by Invasive Candida Infection. PLoS One [Internet]. 2015;10(8):e0136454. Available from: http://dx.plos.org/10.1371/journal.pone.0136454

120. Agustinho DP, de Oliveira MA, Tavares AH, Derengowski L, Stolz V, Guilhelmelli F, et al. Dectin-1 is required for miR155 upregulation in murine macrophages in response to Candida albicans. Virulence. 2017;8(1):41–52.

121. De Lacorte Singulani J, De Fátima Da Silva J, Gullo FP, Costa MC, Fusco-Almeida AM, Enguita FJ, et al. Preliminary evaluation of circulating microRNAs as potential biomarkers in paracoccidioidomycosis. Biomed Reports [Internet]. 2017 Mar 1 [cited 2022 Dec 23];6(3):353–7. Available from: /pmc/articles/PMC5403430/

122. Cezar-dos-Santos F, Assolini JP, Okuyama NCM, Viana KF, de Oliveira KB, Itano EN. Unraveling the susceptibility of paracoccidioidomycosis: Insights towards the pathogen-immune interplay and immunogenetics. Infect Genet Evol [Internet]. 2020 Dec 1 [cited 2022 Dec 23];86. Available from: https://pubmed.ncbi.nlm.nih.gov/33039601/

123. Du L, Chen X, Duan Z, Liu C, Zeng R, Chen Q, et al. MiR-146a negatively regulates dectin-1-induced inflammatory responses. Oncotarget [Internet]. 2017 Jun 6 [cited 2019 Sep 15];8(23):37355–66. Available from: http://www.oncotarget.com/fulltext/16958

124. Chen H, Jin Y, Chen H, Liao I, Yan W, Chen J. MicroRNA-mediated inflammatory responses induced by Cryptococcus neoformans are dependent on the NF-κB pathway in human monocytes. Int J Mol Med [Internet]. 2017 Jun [cited 2018 May 30];39(6):1525–32. Available from: http://www.ncbi.nlm.nih.gov/pubmed/28440395

125. Marioto DTG, Dos Santos Ferraro ACN, De Andrade FG, Oliveira MB, Itano EN, Petrofeza S, et al. Study of differential expression of miRNAs in lung tissue of mice submitted to experimental

infection by Paracoccidioides brasiliensis. Med Mycol [Internet]. 2017 Oct 1 [cited 2022 Dec 23];55(7):774–84. Available from: https://pubmed.ncbi.nlm.nih.gov/28053145/

126. Wei T-T, Cheng Z, Hu Z-D, Zhou L, Zhong R-Q. Upregulated miR-155 inhibits inflammatory response induced by C. albicans in human monocytes derived dendritic cells via targeting p65 and BCL-10. Ann Transl Med [Internet]. 2019 Dec [cited 2022 Dec 15];7(23):758–758. Available from: /pmc/articles/PMC6989962/

Capítulo II:

Análise do transcritoma de células dendríticas em resposta à infecção por *Paracoccidioides brasiliensis*

Este capítulo II refere-se ao trabalho cujo manuscrito foi publicado na revista *Journal of Fungi*. O material suplementar encontra-se depositado no seguinte site:

https://doi.org/10.3390/jof6040311

Transcriptional remodeling patterns in murine dendritic cells infected with *Paracoccidioides brasiliensis*: more is not necessarily better

Calliandra M. de-Souza-Silva [#1], Fabián Andrés Hurtado [#1, 2], Aldo Henrique Tavares [3], Getúlio P. de Oliveira-Jr [4], Taina Raiol [5], Christiane Nishibe [6], Daniel Paiva Agustinho [7], Nalvo Franco Almeida [6], Maria Emília Machado Telles Walter [8], André Moraes Nicola [9], Anamélia Lorenzetti Bocca [§10], Patrícia Albuquerque [§1, 3, *], Ildinete Silva-Pereira [§1,2]

[1] Laboratory of Molecular Biology of Pathogenic Fungi. Department of Cell Biology, Institute of Biological Sciences, University of Brasília, Brasília, Brazil.
[2] Molecular Pathology Post-Graduation Program, University of Brasília Medical School, Brasília, Brazil
[3] Faculty of Ceilândia, University of Brasília, Brasília, Brazil.
[4] Division of Allergy and Inflammation, Department of Medicine, Beth Israel Deaconess Medical Center, Harvard Medical School, Boston, MA, USA.
[5] Fiocruz Brasília, Oswaldo Cruz Foundation, Brazil.
[6] Faculty of Computing, Federal University of Mato Grosso do Sul, Campo Grande, Brazil.
[7] Department of Molecular Microbiology, Washington University School of Medicine, St. Louis, Missouri, USA.
[8] Department of Computer Science, University of Brasília, Brasília, Brazil.
[9] Faculty of Medicine, University of Brasília, Brasília, Brazil.
[10] Laboratory of Applied Immunology, Department of Cell Biology, Institute of Biological Sciences, University of Brasília, Brasília, Brazil.

[#] These authors have contributed equally to the work and share first authorship.

[§] These authors have contributed equally to the work and share senior authorship.

***** Correspondence: palbuquerque@unb.br; Tel.: (+55) 61 985830129 (P.A.)

Received: date; Accepted: date; Published: date

Abstract: Most people infected with the fungus *Paracoccidioides* spp. do not get sick, but approximately 5% develop paracoccidioidomycosis. Understanding how host immunity determinants influence disease development could lead to novel preventative or therapeutic strategies; hence, we used two mouse strains that are resistant (A/J) or susceptible (B10.A) to *P. brasiliensis* to study how dendritic cells (DCs) respond to the infection. RNA sequencing analysis showed that the susceptible strain DCs remodeled their transcriptomes much more intensely than those from the resistant strain, agreeing with a previous model of more intense innate immunity response in the susceptible strain. Contrastingly, these cells also repress genes/processes involved in antigen processing and presentation, such as lysosomal activity and autophagy. After the interaction with *P. brasiliensis*, both DCs and macrophages from the susceptible mouse reduced the autophagy marker LC3-II recruitment to the fungal phagosome compared to the resistant strain cells, confirming this pathway's repression. These results suggest that impairment in antigen processing and presentation processes might be partially responsible for the inefficient activation of the adaptive immune response in this model.

Keywords: *Paracoccidioides brasiliensis*; fungal innate immunity; Dendritic cells; Resistance; Susceptibility; A/J and B10.A mouse strains; autophagy

1. Introduction

Paracoccidioidomycosis (PCM) is an endemic disease caused by the thermally dimorphic fungi *Paracoccidioides* spp. The disease is mainly found in humid tropical and subtropical areas

of several Latin American countries, especially in Brazil, Colombia, Venezuela, Argentina, and Ecuador [1–3]. Although the incidence and prevalence are not fully known due to the non-compulsory nature of its notification, it is deemed the most prevalent systemic mycosis in Brazil, where 80% of all PCM cases are reported [3]. In immunocompetent hosts, PCM case fatality rates are usually less than 5%, but it is associated with high morbidity due to frequent chronic sequelae [4,5]. These morbidity rates are even higher in immunocompromised patients [5,6]. In Brazil, PCM accounted for approximately 51.2% (1,853) of the total deaths attributed to the upper respiratory systemic fungal diseases between 1996-2006 [1,6].

Understanding the protective responses of the host's immune system to fungal infections can help predict disease progression and might directly influence the patient's treatment and prognosis. Resistance or susceptibility to *P. brasiliensis* infection is influenced by several factors, including fungal inoculum size and genetic background, as well as the host's age, genetic background, gender, overall health, the efficiency of antigen-presenting cells (APCs), such as dendritic cells (DCs), B-cells and differentiated macrophages, the infected site co-stimulatory microenvironment, and the type of $CD4^+$ T helper cell (Th) induced [7–10]. The overall result of these differences and the immune response's polarization pattern determine the PCM clinical form. A protective host defense mechanism is believed to be based on cell-mediated immunity with a predominant Th1 cytokine (INF-γ, IL12, IL2, TNF-α) production resulting in classical macrophage activation that will kill or inhibit fungal growth [3,11–14]. Though, an increased regulatory T cell activity with excessive immune suppression (high levels of IL10 and TGF-β, soluble or membrane-associated with LAP-1, and high expression of CTLA-4/CD152) leads to the severe forms of the disease [14,15]. In general, a Th2 and Th9 response usually leads to an uncontrolled inflammatory process (acute form), whereas a deficient Th1 mixed with a Th17 immune response leads to the chronic form [11–13]. In this sense, the comparative analysis of the early immune response to a fungal pathogen employing animal models with different immune response profiles could bring new clues about host-pathogen interaction, the stabilization of immunological patterns, and disease progression.

Different PCM mammalian (e.g., murine, rat, guinea pigs, hamsters, rabbits) and non-mammalian models (e.g., amoebas, nematode *Caenorhabditis elegans*, insect *Galleria mellonella*) have been used to investigate distinct aspects of fungal infection and host–fungal interaction in a complex organism, such as fungal virulence, pathogenesis, immunological response, test pharmacological therapies and find novel antimycotic compounds [13,16–18]. Albeit, the gold standard for *in vivo* studies still is the murine model of infection, and there are well-established models of PCM resistance (e.g., A/Sn or A/J murine strains) and susceptibility (e.g., B10.A, BIOD2/nSn, and BIOD2/oSn murine strains), both sharing high similarity to most common host responses observed in humans [19–25]. The B10.A, BIOD2/nSn, and BIOD2/oSn isogenic strains mimic the chronic, progressive, and disseminated forms of human PCM, whereas the A/Sn or A/J strains have similarities to the regressive or localized forms of infection [15,19,22]. The preeminent hypothesis in the resistance/susceptibility PCM model is that susceptibility to *P. brasiliensis* is associated with a stronger and more efficient initial innate immune response, which is later heavily repressed [26]. In contrast, resistance is associated with an initially milder/deficient response that later develops to a resistance pattern in the course of infection [26]. In the results previously reported by our group, this dichotomy was also found at the molecular level on GM-CSF- and M-CSF-Induced Bone Marrow-Derived Macrophage from resistant (A/J) and susceptible (B10.A) mouse strains infected by *P. brasiliensis* [25].

Dendritic cells (DCs) play a pivotal role in the immune system as the most effective antigen-presenting cells and a mediator between innate and adaptive immune responses. Their potential for fine-tuning the host's responses leading to the control or the eradication of the infection and its role in PCM has been highlighted in the literature [27–31]. Furthermore, although most *in vivo* studies focus on the late immune response presented by both resistant and susceptible mice, these studies suggested essential differences in the profile of Pattern Recognition Receptors (PRRs) used by these hosts in their initial interaction with *P. brasiliensis* [19,22,26,27,32]. As the activation of different PRRs would result in

different signaling pathways and immune responses, we decided to invest in a broader analysis of gene expression of Bone Marrow-Derived DCs (BMDCs) from resistant and susceptible mice in response to *P. brasiliensis* infection. To achieve this, we have employed RNA sequencing (RNA-seq) to provide a global picture of early phase host gene expression in response to *P. brasiliensis* interaction. We found that BMDCs from the susceptible mouse presented a more intense response to infection, suggesting that an early immunological overreaction to this fungus might be linked to host susceptibility.

2. Materials and Methods

2.1. Fungal cells and growth conditions

The virulent strain Pb18 of *P. brasiliensis* was maintained by weekly sub-cultivation in semisolid Fava-Netto's medium at 37 °C and used in the experiments after seven days of growth. Yeast cells were re-suspended in PBS and adjusted to the desired concentration based on hemocytometer counts using the Janus Green B vital dye to determine viability [33]. Only cultures with viability greater than 90% were used in our experiments. The virulence of the strain was maintained by *in vivo* passages in mice every three months.

2.2. Mouse strains and bone marrow-derived cells differentiation

P. brasiliensis resistant (A/J) and susceptible (B10.A) male mice [19,22,26,34], between 6 and 12 weeks old, were obtained from the Immunology Department of the University of São Paulo Biomedical Sciences Institute, Brazil. The animals were housed with food and water ad libitum at the Animal Care Center of the Biological Institute of the University of Brasília, Brazil. The mice were euthanized, and their bone marrows collected. All procedures involving animals were performed following the animal use guidelines according to Brazilian laws and approved by the Committee on Ethical Use of Animals (Proc. UnB Doc 52657/2011).

Bone marrow-derived macrophages (BMMs) and dendritic cells (BMDCs) were generated from bone marrow cells, as previously described [35]. Briefly, 2 x 10^6 bone marrow cells were plated on non-treated 100 mm culture dishes in complete RPMI-1640 medium (Sigma-Aldrich, MO, USA) supplemented with 10% heat-inactivated fetal bovine serum (FBS; Thermo Fisher Scientific), 50 μg/mL of gentamicin, 50 μM 2-mercaptoethanol (Sigma-Aldrich) and 20 ng/mL recombinant GM-CSF (PeproTech, SP, Brazil). The cultures were incubated for 8 days at 37 °C in a humidified 5% CO_2 atmosphere. On the third day, 10 mL of fresh completed medium was added to the culture. Half of the plated medium was removed on the sixth day and supplemented with fresh complete medium. Cells were collected on the eighth day, non-adherent BMDCs in the culture supernatant and loosely adherent cells harvested by gentle washing. We typically obtain around 80% of these cells expressing MHC class II and CD11c, which characterize bone marrow-derived DCs [36,37]. The attached BMMs were detached from plates with TrypLE™ Express (Thermo Fisher Scientific) and were separately collected.

2.3. Ex-vivo infection of dendritic cells from P. brasiliensis *resistant and susceptible mouse strains*

BMDCs uninfected (control) and infected with *P. brasiliensis* at a multiplicity of infection (MOI) of 5:1 were incubated in RPMI 10% fetal bovine serum for six hours in a humidified atmosphere of 5% CO_2 at 37 °C. This MOI has been previously shown to be non-deleterious to macrophage cultures [38,39]. After the incubation time, the culture supernatants were collected for cytokine and chemokine measurements, and the BMDCs lysed for total RNA extraction.

2.4. Cytokine and Chemokine Measurements

The levels of the cytokines TNF-α, IL6, IL10, and the chemokine MCP-1 in the co-culture supernatants were quantified by a capture enzyme-linked immunosorbent assay (ELISA) using specific kits from ELISA Ready-SET-Go!® (eBioscience, CA, U.S.A), according to the manufacturer's instructions. The absorbance values were measured in a spectrophotometer (SpectraMax M5 - Molecular Devices, CA, USA) and analyzed with the SoftMax 5.2 software. Cytokine and chemokine concentrations were determined using a standard curve, following the kit recommendations.

2.5. Resistant and susceptible BMMs and BMDCs ex-vivo infection with P. brasiliensis *for LC3 immunofluorescence*

Eight hundred thousand (8×10^5) BMMs or BMDCs were plated onto Mattek® glass-bottom dishes for 24 h (Mattek, MA, USA). On the day of the interaction, cells from five-day-old cultures of *P. brasiliensis* were collected, vortexed in PBS, and then passed through a 40 μm cell strainer before counting in hematocytometer. Following that, fungal cells were inoculated on the Mattek® Petri dishes containing BMMs or BMDCs at a MOI of 1:1. The dishes were incubated for 12 h at 37 °C in the presence of 5% CO_2 to allow infection. After infection, Mattek® dishes were used in immunofluorescence experiments to locate the microtubule-associated protein 1A/1B-light chain 3 (LC3), widely used to monitor autophagy [40].

2.6. Immunolocalization of LC3 in infected BMMs and BMDCs

After 12 hours of infection, the cells were fixed with ice-cold methanol for 10 minutes and washed with PBS. Afterward, they were incubated with primary antibody (rabbit polyclonal IgG against human LC3, 1:1000 dilution (Santa Cruz Biotechnology) for one hour at 37 °C. Subsequently, the cells were washed three times with PBS and incubated with a secondary antibody (goat IgG against rabbit IGG conjugated with AlexaFluors® 488, dilution 1: 2000, Thermo Fisher Scientific (MA, USA) for one hour at 37 °C. Following secondary antibody incubation, the cells were washed three times with PBS, and Mattek® dishes were mounted with ProLong Gold Antifade Mountant (Thermo Fisher Scientific, MA, USA) and a microscope coverslip. Mattek® dishes were then observed by epifluorescence microscopy on a Zeiss Axio Observer Z1 equipped with a 63x NA 1.4 objective (Zeiss, Germany). Micrographs were recorded with a cooled CCD camera and the Zeiss ZEN software. Image stacks were deconvolved with a constrained iterative algorithm on Zeiss Zen and manipulated on Adobe Photoshop. No non-linear modifications were made to the images, and when brightness adjustments were made, they were applied uniformly to the entire image. To quantify LAP. the phagocytosed fungal cells in each field were counted as well as the number of phagocytosed fungal cells positive for LC3. The analysts who performed the counting were blinded to the identity of the samples. The percentage of LC3-associated phagocytosis (LAP) was measured by the number of phagocytosed fungal cells positive for LC3 divided by the total number of phagocytosed fungal cells. As positive control, we made in parallel similar experiments using BALB/c BMMs infected with *C. neoformans* or *C. albicans* (Figure S3), a condition in which LAP has been previously detected [40].

2.7. RNA isolation

After six hours of interaction, the total RNA of *P. brasiliensis* infected dendritic cells or uninfected control cells was isolated using RNeasy® Plus Mini Kit (QIAGEN, Hilden,

Germany), following the manufacturer's protocol. After the quality analysis (Bioanalyser 2100 – Agilent, CA, USA) and quantification (Qubit® 2.0 Fluorometer - Life Technologies, CA, USA), 3.5-6.0 μg of total RNA from BMDCs of the different experimental conditions were prepared for transport at room temperature employing the RNA stable kit (Biomatrica, CA, USA), according to the manufacturer's recommendations.

2.8. Sequencing Parameters

Twelve barcoded libraries after poly (A) + RNA selection, according to the Illumina TruSeq RNA-seq methodology, were sequenced from total BMDC RNA samples obtained from resistant (A/J) and susceptible (B10.A) strains, infected or not by Pb18. Three noninfected and three Pb18-infected BMDC samples were used from each mouse strain. High-throughput RNA sequencing (RNA-seq) was subsequently performed using the Illumina HiSeq 2000 Analyzer platform at the Scripps DNA Sequencing Facility, generating paired-end reads of 100 base pairs (bp).

2.9. RNA-seq data analysis

The high throughput pipeline analysis of both transcriptomes of BMDCs from these two mice strains infected or not with the virulent Pb18 isolate of *P. brasiliensis* was analyzed as described below. FASTQ files obtained from Illumina sequencing [41] were evaluated using the FastQC software [42]. The adapters identified by FastQC were removed using the Cutadapt software [43], while the low-quality sequences were filtered using PRINSEQ [44]. Qualified reads were mapped onto the mouse reference genome (mouse build mm10) using TopHat2 [45]. The final BAM mapping files were ordered and indexed using Samtools [46], followed by a read count using HTSeq-count [47]. Transcripts with low counts (CPM<1) and not present in at least two libraries were removed from the analysis.

The differentially expressed genes (DEG) were estimated using the edgeR library, applying TMM library size normalization and likelihood ratio test, implemented in software R version 3.6.1 [48]. The false discovery rate (FDR) was controlled by the Benjamini-Hochberg algorithm [49]. A fold change ≥ ±1.4 and an FDR-adjusted p-value < 0.05 were used as cutoff criteria for differential gene expression.

Genes considered differentially expressed were used for the Gene Ontology (GO) and KEGG enrichment analysis by ClusterProfiler [50]. Only nodes with FDR-adjusted p-values < 0.01 and p-values < 0.05 were considered statistically significant for GO and KEGG analysis, respectively. Simplify method was used to reduce the enriched GO terms redundancy. Plots were produced in R using ggplot2. Heatmaps were generated using the ComplexHeatmap library and the Gene Ontology database [51].

2.10. Data access

All sequencing data were deposited in NCBI's Gene Expression Omnibus (GEO) database under accession number GSE158289.

2.11. RNA-seq Validation by Quantitative PCR (RT-qPCR)

We performed RT-qPCR of nine genes (Table S1) related to innate immunity using the same samples of total BMDC RNA used in the RNA-seq. After DNase I treatment (included in the RNeasy® Mini Kit Plus), first-strand cDNAs were synthesized from 500 ng of total RNA for each sample following the instructions for SuperScript III (Invitrogen). The RT-qPCR was

performed using SyBr Green Master Mix (Applied Biosystems) with this dye's standard cycling condition. Gene expression changes relative to control were estimated using the $2^{-\Delta\Delta Ct}$ method [52].

The internal control used was the 40S ribosomal protein S9 (RPS9) gene (Table S1), as described previously by our group [36,39]. Specific oligonucleotides for the genes encoding MyD88, NF-κB, TNF-α, and IL1β were designed as described before [39] and based on sequences obtained from the mouse transcriptome database (http://www.informatics.jax.org). The oligonucleotide sequences for the genes encoding IL6, IL10, IL12αp35, CXCL10, and CCL22 were obtained from the PrimerBank database http://pga.mgh.harvard.edu/primerbank/ [53]. All primer sequences are listed in Table S1.

2.12. Statistical Analysis

Three independent experiments were performed for every outcome measured. The differences between the groups, for all experiments except RNA-seq, were analyzed by Student's t-test, two-way ANOVA with Tukey's multiple comparisons post-test or by Fisher's exact test. The statistical analysis was performed using GraphPad Prism 7 (GraphPad Software). A p-value < 0.05 was considered significant.

3. Results

3.1. P. brasiliensis *infection triggers widespread transcriptional remodeling in a PCM-susceptible mouse strain*

We characterized the early transcriptional response of BMDCs derived from well-established murine models of resistance (A/J) and susceptibility (B10.A) to PCM after their interaction with *P. brasiliensis* [15,22,23]. For that, BMDCs were co-incubated with or without *P. brasiliensis* cells at a MOI of 5:1 for 6 hours; afterward, these cells were collected for RNA extraction and sequencing.

For all the samples, each replicate yielded an average of 16 million reads after the sequencing of both transcriptomes, and all the analyzed samples had more than 97% of their reads mapped to the mouse reference genome (Table S2). To generate a set of differentially expressed genes in *P. brasiliensis*-infected BMDCs relative to uninfected control, for both mouse strains, we adopted statistical and biological significance thresholds of adjusted p-value < 0.05 and FC ≥ ±1.4, respectively.

We observed a significant disparity in the number of differentially expressed genes upon infection (red dots) between cells derived from both mouse strains, as presented in Figure 1A. BMDCs from the susceptible strain modulated a much higher number of genes (2278) upon infection with *P. brasiliensis* than BMDCs from the resistant strain (221), and both sets have few genes in common (189) (Figure 1B). In fact, the resistant BMDCs seem to hardly alter their noninfected transcript landscape following *P. brasiliensis* infection. This difference was also reflected in the general immune response of both mouse strains upon infection with *P. brasiliensis* and could be more clearly discerned by analyzing the number of Differentially Expressed Genes (DEGs) clustered in the Gene Ontology (GO) terms: Immune Response, Immune System Process, Inflammatory Response, Innate Immune Response, and Metabolic Process genes. As presented in Figure 1B and 1C, BMDCs from the resistant A/J strain had only 213 up-regulated genes and eight down-regulated. In contrast, BMDCs from the susceptible B10.A strain not only presented a significantly higher overall number of up-regulated DEGs (1,128) but also displayed 1,150 down-regulated DEGs and a higher number of DEGs clustered in those GO terms than in the resistant strain. It was also interesting to note that the susceptible mouse strain seems to down-regulate its metabolic processes in response to infection. The complete list of genes is presented in Tables S3 and S4.

The RNA-seq results were validated using RT-qPCR to assess transcript levels of several genes related to the innate immune response; namely, those encoding the cytokines TNF-α, IL1β, IL6, IL10, and IL12, the chemokines CCL22 and CXCL10, the molecular adapter MyD88, and the transcription

factor NF-κB (Figure S1). Comparing infected to non-infected cells, a similar increase in TNF-α, IL6, and IL10 transcripts accumulation and cytokines release was observed for both strains (Figure S1 and S2). However, the susceptible mice produced significantly higher levels of those cytokines in comparison to the resistant strain. The MCP-1 (CCL2) release was also stimulated after infection in both mouse strain, in a similar fashion (Figure S2). Nevertheless, the MCP1-transcript was not differentially expressed after infection in either mouse strain, which could be explained by the post-transcriptional regulation of MCP-1 mRNA stability [54,55]. Depending on the stimulus, MCP1-transcript accumulation peak tends to occur at 2 h returning to normal levels at 4 h [56,57]; in our analyses, both RNA and cytokine/chemokine samples were collected after 6 h of infection with *P. brasiliensis*.

3.2. PCM-resistant mouse strain reveals a precise and coordinated immune response upon P. brasiliensis *infection*

A selected global GO analysis profile for the DEGs in BMDCs from resistant and susceptible strains upon infection with *P. brasiliensis* is represented in Figure 2. Genes modulated by BMDCs from the susceptible strain significantly clustered in 98 GO terms, of which 12 were down-regulated (Table S5). Meanwhile, modulated genes from BMDCs of the resistant strain were significantly grouped in 81 GO terms, all up-regulated (Table S6). Most of the GO biological processes, in both mouse strains, were involved in innate immunity, its regulation, or in immunity against internalized pathogens (Figure 2).

Further analysis focusing on GO biological processes revealed enrichment of up-regulated genes in GO immunological processes categories ($p < 0.01$) in both resistant and susceptible strains (Tables S3 and S4). The resistant BMDCs display fewer DEGs, grouped in a smaller number of categories but displaying a higher number of up-regulated genes, in an apparent higher interconnected organization (Figure 3), which might reflect a more precise and coordinated response to infection than the susceptible BMDCs (Figure 4). Both models shared six up-regulated biological process categories: response to interferon-beta, cytokine secretion, chemotaxis, regulation of cell killing, positive regulation of phagocytosis, and production of molecular mediators of the immune response (Figures 2 and 3). However, they markedly differed in the modulation of some categories. For example, BMDCs from the resistant strain up-regulated genes related to inflammatory response, positive regulation of cytokine production, neutrophil chemotaxis, and positive regulation of the apoptotic process (Figure 2). In contrast, BMDCs from the susceptible strain up-regulated genes involved in macrophage migration, negative regulation of catalytic activity, innate immunity, and antigen processing and presentation (Figure 2).

GO analysis performed for the down-regulated genes of BMDCs from the susceptible strain revealed enrichment for categories related to catabolic processes, mainly involving lipid and small molecule metabolism, and lyase activity, as well as coenzyme binding, which are in agreement with the previously observed upregulation of genes involved in negative regulation of catalytic activity (Figure 2; Table S5). We did not observe any significant enrichment (adjusted $p < 0.01$) of the immunological process among the repressed genes from the resistant strain BMDCs (Figure 2; Table S6).

In terms of Kyoto Encyclopedia of Genes and Genomes (KEGG) pathway analysis, a total of 69 up-regulated pathways clustered in the susceptible strain and 47 in the resistant strain (Tables S7 and S8), with both strains similarly clustering up-regulated genes in 14 pathways related to immune system processes, but differing only in their enrichment levels and genes counts (Figure 5).

Among the differences in gene modulation upon infection between the two strains, we noticed a positive regulation of apoptotic and the leukocyte apoptotic processes only in the resistant model (Figure 2). In contrast, the susceptible strain presented an up-regulation of several signal transduction pathways, including pathways involved in DC maturation, adaptive immune response polarization, apoptosis, and autophagy such as the MAPK, HIF-1, and PI3K-Akt (Figure 5) [58–61].

Similarly to the GO terms, only BMDCs of B10.A strain displayed down-regulation of KEGG pathways, most related to catabolism. The peroxisome proliferator-activated receptor (PPAR) signaling pathway, an essential modulator of the immune response, was also down-regulated in this mouse model (Figure 5).

.3.3. Resistant and susceptible strains had significant differences in the modulation of genes related to antigen presentation, autophagy, and lysosome function

Comparing the transcriptomes of *P. brasiliensis*-infected resistant and susceptible BMDCs, we noticed some critical differences in the GO and KEGG pathway analysis between the two mouse strains. The modulation of genes involved in autophagy (GO:0006914), lysosome (GO:0005764), and antigen processing and presentation (GO:0019882) are highly interconnected and have critical elements repressed in the susceptible strain, as seen in Figure 6, indicating a decreased functionality of these pathways (Figures 2 and 5). It is interesting to note that some genes from autophagy, lysosome, and antigen processing and presentation ontologies are similarly upregulated in both strains (Figure 6). However, different from the resistant mice, in which the down-regulated genes did not reach the cutoff limit, the susceptible mice modulated key genes leading to a repression of those pathways; for example, the upregulation of the transcription factor Hif1α (Hypoxia-inducible factor 1α), and the repression of catabolic enzymes, related to different exocytosis and endocytosis processes, regulatory enzymes, and pH altering enzymes, such as SGSH (N-Sulfoglucosamine Sulfohydrolase), SMPD1 (Sphingomyelin Phosphodiesterase 1), ACP5 (Acid Phosphatase 5), PLA2G15 (Lysosomal Phospholipase A2 Group XV), PIK3R2 (Phosphoinositide-3-Kinase Regulatory Subunit 2), and ATP6V0D2 (ATPase H+ Transporting V0 Subunit D2) (Figure 6; Table S9).

There was also downregulation of critical transcriptional factors, such as TFEB (Transcription Factor EB - master regulator of lysosomal biogenesis, autophagy, lysosomal exocytosis, lipid catabolism, energy metabolism, and immune response), proteins such as Deptor (DEP domain-containing mTOR-interacting protein – mTOR inhibitor), Stx17 (Syntaxin 17 – SNARE essential for fusion of cellular membranes), Atg14 (Autophagy Related 14 - determines the autophagy-specific PI3-kinase complex PI3KC3-C1 localization), Snx14 (Sorting Nexin 14 - intracellular trafficking and required for autophagosome clearance), and receptors, such as TLR9 (intracellular DNA recognition), H2-DMa (a subunit of a heterodimeric H2-DM chaperone molecule), Fcgrt (Fc Fragment Of IgG Receptor And Transporter), HFE (Homeostatic Iron Regulator - membrane protein similar to MHC class I-type proteins and associates with beta2-microglobulin (beta2M)), NBR1 (NBR1 Autophagy Cargo Receptor) (Figure 6; Table S9).

Considering processes related to antigen processing and presentation, one of the main DCs activities, most components of MHC (Major histocompatibility complex) class I and MHC class II components were not significantly altered in the resistant mice (Figure 6C; Table S9). Notwithstanding, we observed an enrichment in GO terms related to antigen cross-presentation by those DCs, such as the "antigen processing and presentation of endogenous peptide antigen via MHC class I/via ER pathway, TAP-independent" (Figure 2), and "Antigen processing and presentation of endogenous peptide antigen via MHC class Ib" (Table S6). In contrast, in BMDCS from the susceptible mice, there was enrichment in several components of GO terms and KEGG pathways related to antigen processing and presentation (Figures 2 and 5), including the ones observed in the resistant strain, but also of other components of MHC class I, such as "MHC class I peptide loading complex" and "TAP binding" followed by downregulation of some MHC II components such as H2-DMa (MHC-IIb). This chaperone is critical for the release of class II HLA-associated invariant chain-derived peptides (CLIP) from the MHC II groove, freeing the peptide binding site, which might compromise MHC class II availability in the susceptible mouse [62] (Figure 6C; Table S9).

3.4. PCM-susceptible mouse strain shows a deficiency in performing LC3-associated phagocytosis of P. brasiliensis

The susceptible strain transcriptional profile suggested a possible impairment of autophagy in the mouse model. Given the role of autophagy in the immune response against several microbes and our work regarding macrophages after the interaction with several fungal pathogens [40,63–65], including *P. brasiliensis* [66], experiments were performed to assess differences in LC3-associated phagocytosis (LAP) after *P. brasiliensis* infection between the two mouse strains. For this, we infected murine BMMs

and BMDCs with the virulent strain Pb18, and after 12 h of interaction, we performed immunofluorescence experiments with antibodies to LC3, an autophagosome marker which is also a marker for LAP [67] (Figure 7A). We observed a significant difference in LAP induction after *P. brasiliensis* infection between both macrophages and DCs derived from A/J and B10.A mouse strains ($p < 0.0001$). The percentage for LAP-positive cells decreased from 10.4% in resistant BMMs to 4.6% in susceptible BMMs, while the percentage of LAP-positive cells decreased from 14.1% in resistant BMDCs to 7.4% in susceptible BMDCs (Figure 7B). These differences suggest a possible link between the macrophages and dendritic cells' ability to perform LC3-associated phagocytosis and susceptibility/resistance to *P. brasiliensis* infection.

4. Discussion

In several systemic mycoses, host resistance is associated with cellular immunity and proper activation of phagocytes, while susceptibility is associated with polarization towards type-2 immunity (Th2/Th9) and a marked impairment/depression of cellular-mediated immunity [15,68]. In the murine PCM model, the A/J (resistant) strain portrays an initial more controlled (mild) response to infection that evolves for activation of cellular immunity and phagocytes, resulting in a limited number of well-organized granulomatous lesions that evolve into self-healing, abundant neutrophil infiltration, and fungal destruction [15,20,26,68]. Meanwhile, B10.A (susceptible) shows greater activation of the innate immune response, leading to excessive NO secretion, which might lead to deletion and anergy of $CD4^+$ cells, defective activation of cellular immunity, culminating in disseminated nonorganized inflammatory lesions containing high fungal loads [15,20,26,68,69]. Considering those differences, we decided to further investigate possible differences in the global transcriptional profile of BMDCs from both strains, focusing on their innate immune response against *P. brasiliensis* infection after 6 h of interaction.

We observed that BMDCs from the susceptible mouse presented a more intense and apparently disorganized gene modulation in response to infection in comparison to cells from the resistant mouse. Overall, the disparity in the numbers and terms of GO processes and KEGG pathways enriched upon infection in both groups agree with previous models of PCM resistance/susceptibility [15,69]. Although A/J and B10.A clustered genes in similar categories when using the immune system process GO database, the BMDCs in PCM-resistant mice (A/J) are probably mounting a more controlled and precise response, up-regulating monocyte's and neutrophil's recruitment, apoptotic process, cell killing, response to interferon-beta, and type I interferon and cytokine production. In comparison, PCM-susceptible mice (B10.A) induces an inadequate and disproportionate response by direct or indirectly down-regulating several catabolic processes, essential for lysosomal function, and possibly to antigen presentation and the PPAR pathway, important in the modulation of inflammatory processes [70,71], while up-regulating macrophage migration but not neutrophil or monocyte recruitment.

Our transcriptomic results revealed that BMDCs from the resistant mice strain induce gene expression that, according to the literature, reinforces the idea of differential migration of neutrophils, while BMDCs from the susceptible mice strain induce macrophage migration during early interaction with *P. brasiliensis*. Neutrophils are seen in lesions of PCM patients and experimentally infected mice; and, when appropriately activated (IFN-γ, TNF-α, GM-CSF, IL15), they are able to limit infection and fungal burden and are important sources of INF-γ and IL-17, especially at early stages of *P. brasiliensis* infection [72–74]. Neutrophil depletion at chronic PCM phases might attenuate lung fibrosis and inflammation. However, the absence of those cells at the initial acute phase of PCM exacerbates the inflammatory response indicating an important role of neutrophils in the early response to *P. brasiliensis* infection [75,76].

On the other hand, despite their role in resistance to *P. brasiliensis* infection, confirmed both in susceptible and resistant models of infection [77], macrophages can also be a relevant site of fungal replication and dissemination. Non-activated alveolar macrophages, despite their ability to internalize yeasts both *in vivo* and *in vitro*, are frequently permissive to the multiplication of *P. brasiliensis*, while their activation by INFγ enhances their microbicidal activity [78]. In conclusion, both phagocytes play

vital roles in the immune response against *P. brasiliensis*, albeit in different moments of the host-pathogen interaction.

Another critical difference observed between BMDCs from susceptible and resistant mouse models of PCM relies on the modulation of genes related to antigen processing and presentation, a key function of DCs. Recognition, processing, and presentation of antigens by these cells determine adaptative response polarization and ultimately define the outcomes of host-pathogen interaction [7]. The differences in antigen processing and presentation in APCs is dependent, among other factors, on the rate of lysosomal proteolysis and the proper selection of epitopes [79]. Most genes of MHC class I and MHC class II components were not significantly modulated in the resistant mice. In contrast, BMDCs from the susceptible mouse had a broader enrichment in several GO term and KEGG pathway components related to antigen processing and presentation, especially in the MHC class I components; this seems to be in agreement with a disproportional early inflammatory profile of the susceptible mouse.

BMDCs from the susceptible strain also displayed enrichment of GO and KEGG categories related to the repression of different lysosomal pathway elements. This catabolic repression in the susceptible strain might impact several processes related to fungal destruction and development of protective adaptive immune response, such as phagosomal activity, reactive oxygen species production, antigen presentation, and autophagy [62]. Taken together, these features indicate that fungal cells might remain longer inside DCs, avoiding effector functions of the immune system in the susceptible mice. In agreement with this hypothesis, Ferreira et al. (2007)) had previously described that DCs from PCM-susceptible mice had a higher phagocytic index but also higher fungal viability after the interaction with *P. brasiliensis* than cells from the PCM-resistant mouse model [8].

Another transcriptional difference between BMDCs from both mouse models was the regulation of autophagy, a process closely related to several components of immunity to infection, including microbial killing, antigen presentation, and inflammation [80]. In the last two decades, several groups have described how autophagy can participate in innate and adaptative responses to different microbes. Furthermore, some pathogens developed ways to manipulate host autophagy for their benefit. LC3-associated phagocytosis (LAP) is a non-canonical form of autophagy, triggered by the engagement of surface recognition receptors, and a link between phagocytosis and the autophagy machinery. This process impacts immune activation and inflammatory response, and it is believed to be a safe pathway to control the lysosomal degradation of microbial pathogens [81–83]. Despite the lack of a double membrane autophagosome, LAP shares several of the canonical autophagy components, including Beclin1, various Atg proteins, the PI3K complex, and the soluble LC3-I conversion into the membrane-bound LC3-II [81]. So far, LAP has been shown to play a role in the antifungal immunity to several fungal pathogens, including *Aspergillus fumigatus*, *Candida* spp, *Cryptococcus neoformans,* and *Histoplasma capsulatum* [40,63–65]; our group has also been involved in the characterization of this process in the interaction of *P. brasiliensis* and macrophages in the last few years [66].

In DCs, antigen processing via autophagy modulates T cell immunity by promoting both endogenous and exogenous antigen presentation. This process is believed to be the primary intracellular pathway involved in the non-conventional endogenous antigenic peptide presentation in MHC class II, making it important in DCs for both self and foreign antigens presentation [62,84]. Autophagy also contributes to the DCs regulation of cytokine production and cell death. Both autophagy proteins and NADPH oxidase 2 (NOX2) are required for LC3-associated phagocytosis (LAP), stabilize the phagosome, and are crucial for the efficiency of MHC class II presentation of extracellular antigens [84]. We observed the repression of several key autophagy genes in susceptible mice, and this autophagic function repression was confirmed by the reduced percentage of LC3-II recruitment in the phagosomes of B10.A DCs and macrophages infected with *P. brasiliensis* in comparison to those from A/J mice.

Among the differences in the autophagy/LAP regulation, there was a significant downregulation of Deptor transcript and the upregulation of Hif1α transcript after infection in BMDCs from the susceptible strain. Deptor is an inhibitor of mTORC activity and, consequently, an activator of autophagy. In multiple human myeloma cells, the knockdown of Deptor was shown to trigger apoptosis

and suppress autophagy [85]. The transcription factor Hif1α is a major regulator of innate immunity against pathogens and macrophage INF-γ dependent control of infection [86,87]. In the interaction of macrophages with *H. capsulatum*, Hif1α was shown to limit fungal intracellular survival by reducing the recruitment of LC3-II to the fungal phagosome. In this case, *H. capsulatum* exploits host autophagy to survive [87,88]. Contrastingly, results from a parallel project from our group suggest that, in the interaction of different macrophages with *P. brasiliensis*, LAP is detrimental for the fungus, reinforcing this process's potential role in macrophage ability to deal with this pathogen. In addition to its role in autophagy, Hif1α upregulates inducible nitric oxide synthase (iNOS). In our experiments, BMDCs from both mouse models up-regulated the NOS2 gene (Nitric oxide synthase 2, inducible); however, the upregulation in the susceptible mouse was significantly higher, and excessive NO production by the susceptible mouse was suggested to have a suppressive effect on T lymphocytes activation [69]. Our results suggest that the upregulation of Hif1α might be involved in the lower recruitment of LC3-II to the phagosome observed in the immunofluorescence assays and also in the increased accumulation of the iNOS transcript observed in BMDCs from the susceptible mouse.

In conclusion, our results corroborate the previously proposed intense activation of the inflammatory response in the susceptible PCM mouse model after infection with *P. brasiliensis*. In addition to that, we propose that suppression of highly interconnected processes, such as repression of lysosomal acidification, catalytic activity, and autophagy function, might negatively impact antigen processing and presentation by BMDCs from the susceptible mice leading to ineffective activation of the adaptive immune response and susceptibility to this fungal infection (Figure 8). What makes a host susceptible or resistant to infection is a crucial question for most infectious diseases, and many factors have been implicated in disease development, such as sex, nutritional status, smoking habits, pollution, and genetics [89]. Our work reinforces the significance of host genetic background in susceptibility to fungal infections. These findings might help develop strategies to prevent or treat PCM, such as the use of DC biomarker detection to predict people with higher risks of developing the disease, information with significant prognostic impact. Therefore, further in-depth exploration and assessment of these processes, for example, *in vivo*, with other cells or different time points of interaction, should help deepen the comprehension of the molecular mechanisms behind susceptibility/resistance not only for this neglected fungal infection but also for other infectious diseases.

Supplementary Materials: The following are available online at www.mdpi.com/xxx/s1, Figure S1: Transcripts levels detected by RNA-seq compared to RT-qPCR assay, Figure S2: Cytokines and chemokine profile from *P. brasiliensis*-infected Dendritic cells, Table S1: Primer's sequences used in RT-qPCR experiments, Table S2: General results from high-throughput sequencing, filtering and mapping steps, Table S3: General results from differential expression analysis by the edgeR software package in A/J BMDCs upon infection with *P. brasiliensis*, Table S4: General results from differential expression analysis by the edgeR software package in B10.A BMDCs upon infection with *P. brasiliensis*, Table S5: Enriched GO terms in B10.A BMDCs upon infection with *P. brasiliensis*, Table S6: Enriched GO terms in A/J BMDCs upon infection with *P. brasiliensis*, Table S7: Enriched KEGG pathways in B10.A BMDCs upon infection with *P. brasiliensis*, Table S8: Enriched KEGG pathways in A/J BMDCs upon infection with *P. brasiliensis*. Table S9: Comparison of the modulation of selected fungal immune-related genes in *P. brasiliensis* infected dendritic cells from A/J and B10.A mice strains.

Author Contributions: C.M.S.S., F.A.H., G.P.O.J., C.N., D.P.A., N.F.A., conducted the experiments; C.M.S.S., F.A.H., T.R., G.P.O.J., C.N., N.F.A., A.M.N and M.E.M.T.W. analyzed the data; C.M.S.S., F.A.H. and P.A. writing-original draft preparation; P.A., I.S.P, A.M.N., A.H.T. and A.L.B. writing-review and editing; A.L.B., P.A. and I.S.P conceived and supervised the project. All authors have read and agreed to the published version of the manuscript.

Funding: This work was supported by the National Council for Scientific and Technological Development (CNPq) (CNPq 564507/2010-5 to 2018) and the "Fundação de Apoio à Pesquisa do Distrito Federal (FAP-DF)/CNPq PRONEX (Grants: 0193.000.571/2009, 0193.000.496/2009, and 0193.001.200/2016) grants.

Acknowledgments: We thank the Professors Dr. Karen Spadari Ferreira (UNIFESP) and Dr. Sandro Almeida (USP), and their then Masters' degree student Grasielle Pereira Jannuzzi (USP) for their support and help. Special thanks to all members of the Laboratory of Molecular Biology of Pathogenic Fungi and Laboratory of Applied Immunology; we are grateful for the support and help with setting up the experiments. Finally, we are thankful to

the Molecular Biology and Molecular Pathology Graduate Programs (UnB) for their fellowship support of C.M.S.S. and F.A.H.

Conflicts of Interest: The authors declare no conflict of interest. The funders had no role in the design of the study; in the collection, analyses, or interpretation of data; in the writing of the manuscript, or in the decision to publish the results.

5. References

1. Martinez, R. New trends in paracoccidioidomycosis epidemiology. *J. Fungi* **2017**, *3*, doi:10.3390/jof3010001.

2. De Macedo, P.M.; De Melo Teixeira, M.; Barker, B.M.; Zancopé-Oliveira, R.M.; Almeida-Paes, R.; Do Valle, A.C.F. Clinical features and genetic background of the sympatric species *Paracoccidioides brasiliensis* and *Paracoccidioides americana*. *PLoS Negl. Trop. Dis.* **2019**, *13*, doi:10.1371/journal.pntd.0007309.

3. Negroni, R. Paracoccidioidomycosis. In *Hunter's Tropical Medicine and Emerging Infectious Diseases*; Elsevier, 2020; pp. 674–677 ISBN 978-0-323-55512-8.

4. Griffiths, J.; Colombo, A.L.; Denning, D.W. The case for paracoccidioidomycosis to be accepted as a neglected tropical (Fungal) disease. *PLoS Negl. Trop. Dis.* **2019**, *13*, doi:10.1371/journal.pntd.0007195.

5. de Almeida, J.N.; Peçanha, P.M.; Colombo, A.L. Paracoccidioidomycosis in immunocompromised patients: A literature review. *J. Fungi* **2019**, *5*, doi:10.3390/jof5010002.

6. Prado, M.; da Silva, M.B.; Laurenti, R.; Travassos, L.R.; Taborda, C.P. Mortality due to systemic mycoses as a primary cause of death or in association with AIDS in Brazil: A review from 1996 to 2006. *Mem. Inst. Oswaldo Cruz* **2009**, *104*, 513–521, doi:10.1590/S0074-02762009000300019.

7. Ferreira, K.S.; Lopes, J.D.; Almeida, S.R. Regulation of T helper cell differentiation in vivo by GP43 from *Paracoccidioides brasiliensis* provided by different antigen-presenting cells. *Scand. J. Immunol.* **2003**, *58*, 290–297, doi:10.1046/j.1365-3083.2003.01291.x.

8. Ferreira, K.S.; Bastos, K.R.; Russo, M.; Almeida, S.R. Interaction between *Paracoccidioides brasiliensis* and Pulmonary Dendritic Cells Induces Interleukin-10 Production and Toll-Like Receptor–2 Expression: Possible Mechanisms of Susceptibility. *J. Infect. Dis.* **2007**, *196*, 1108–1115, doi:10.1086/521369.

9. de Araújo, E.F.; Medeiros, D.H.; Galdino, N.A. de L.; Condino-Neto, A.; Calich, V.L.G.; Loures, F.V. Tolerogenic Plasmacytoid Dendritic Cells Control *Paracoccidioides brasiliensis* Infection by Inducting Regulatory T Cells in an IDO-Dependent Manner. *PLoS Pathog.* **2016**, *12*, doi:10.1371/journal.ppat.1006115.

10. Moreira, A.L.E.; Oliveira, M.A.P.; Silva, L.O.S.; Inácio, M.M.; Bailão, A.M.; Parente-Rocha, J.A.; Cruz-Leite, V.R.M.; Paccez, J.D.; de Almeida Soares, C.M.; Weber, S.S.; et al. Immunoproteomic Approach of Extracellular Antigens From *Paracoccidioides* Species Reveals Exclusive B-Cell

Epitopes. *Front. Microbiol.* **2020**, *10*, doi:10.3389/fmicb.2019.02968.

11. Camacho, E.; Niño-Vega, G.A. *Paracoccidioides* Spp.: Virulence Factors and Immune-Evasion Strategies. *Mediators Inflamm.* **2017**, *2017*, doi:10.1155/2017/5313691.

12. de Castro, L.F.; Ferreira, M.C.; da Silva, R.M.; Blotta, M.H. de S.L.; Longhi, L.N.A.; Mamoni, R.L. Characterization of the immune response in human paracoccidioidomycosis. *J. Infect.* **2013**, *67*, 470–485, doi:10.1016/j.jinf.2013.07.019.

13. De Oliveira, H.C.; Assato, P.A.; Marcos, C.M.; Scorzoni, L.; De Paula E Silva, A.C.A.; Da Silva, J. de F.; Singulani, J. de L.; Alarcon, K.M.; Fusco-Almeida, A.M.; Mendes-Giannini, M.J.S. *Paracoccidioides*-host interaction: An overview on recent advances in the paracoccidioidomycosis. *Front. Microbiol.* **2015**, *6*, doi:10.3389/fmicb.2015.01319.

14. Calich, V.L.G.; Mamoni, R.L.; Loures, F. V. Regulatory T cells in paracoccidioidomycosis. *Virulence* **2019**, *10*, 810–821, doi:10.1080/21505594.2018.1483674.

15. Calich, V.L.G.; Da Costa, T.A.; Felonato, M.; Arruda, C.; Bernardino, S.; Loures, F.V.; Ribeiro, L.R.R.; De Cássia Valente-Ferreira, R.; Pina, A. Innate immunity to *Paracoccidioides brasiliensis* infection. *Mycopathologia* **2008**, *165*, 223–236, doi:10.1007/s11046-007-9048-1.

16. Iovannitti, C.A.; Finquelievich, J.L.; Negroni, R.; Elías Costa, M.R. Histopathological evolution of experimental paracoccidioidomycosis in Wistar rats. *Zentralblatt fur Bakteriol.* **1999**, *289*, 211–216, doi:10.1016/S0934-8840(99)80108-X.

17. Scorzoni, L.; de Lucas, M.P.; Singulani, J. de L.; de Oliveira, H.C.; Assato, P.A.; Fusco-Almeida, A.M.; Mendes-Giannini, M.J.S. Evaluation of Caenorhabditis elegans as a host model for *Paracoccidioides brasiliensis* and *Paracoccidioides lutzii*. *Pathog. Dis.* **2018**, *76*, doi:10.1093/femspd/fty004.

18. Albuquerque, P.; Nicola, A.M.; Magnabosco, D.A.G.; da Silveira Derengowski, L.; Crisóstomo, L.S.; Xavier, L.C.G.; de Oliveira Frazão, S.; Guilhelmelli, F.; De Oliveira, M.A.; do Nascimento Dias, J.; et al. A hidden battle in the dirt: Soil amoebae interactions with *Paracoccidioides* spp. *PLoS Negl. Trop. Dis.* **2019**, *13*, e0007742, doi:10.1371/journal.pntd.0007742.

19. Garcia Calich, V.L.; Singer-Vermes, L.M.; Siqueira, A.M.; Burger, E. Susceptibility and resistance of inbred mice to *Paracoccidioides brasiliensis*. *Br. J. Exp. Pathol.* **1985**, *66*, 585–594.

20. Singer-Vermes, L.M.; Caldeira, C.B.; Burger, E.; Calich, V.L.G. Experimental murine paracoccidioidomycosis: Relationship among the dissemination of the infection, humoral and cellular immune responses. *Clin. Exp. Immunol.* **1993**, *94*, 75–79, doi:10.1111/j.1365-

2249.1993.tb05980.x.

21. Calich V.L.G., Singer-Vermes L.M., Russo M., Vaz C., B.E. Immunogenetics in paracoccidioidomycosis. In *Paracoccidioidomycosis*; Franco M, Lacaz CS, Restrepo-Moreno A, Del Negro G, E., Ed.; CRC Press: Boca Raton, Florida, 1994; pp. 151–173 ISBN 0-8493-4868-4.

22. Cano, L.E.; Singer-Vermes, L.M.; Vaz, C.A.C.; Russo, M.; Calich, V.L.G. Pulmonary paracoccidioidomycosis in resistant and susceptible mice: Relationship among progression of infection, bronchoalveolar cell activation, cellular immune response, and specific isotype patterns. *Infect. Immun.* **1995**, *63*, 1777–1783, doi:10.1128/iai.63.5.1777-1783.1995.

23. Calich, V.L.G.; Kashino, S.S. Cytokines produced by susceptible and resistant mice in the course of *Paracoccidioides brasiliensis* infection. *Brazilian J. Med. Biol. Res.* **1998**, *31*, 615–623, doi:10.1590/S0100-879X1998000500003.

24. Nishikaku, A.S.; Molina, R.F.S.; Albe, B.P.; Cunha, C. da S.; Scavone, R.; Pizzo, C.R.P.; de Camargo, Z.P.; Burger, E. Immunolocalization of IFN-gamma in the lesions of resistant and susceptible mice to *Paracoccidioides brasiliensis* infection. *FEMS Immunol. Med. Microbiol.* **2011**, *63*, 281–288, doi:10.1111/j.1574-695X.2011.00851.x.

25. De Souza Silva, C.; Tavares, A.H.; Sousa Jeronimo, M.; Soares De Lima, Y.; Da Silveira Derengowski, L.; Lorenzetti Bocca, A.; Silva-Pereira, I. The Effects of *Paracoccidioides brasiliensis* Infection on GM-CSF-and M-CSF-Induced Mouse Bone Marrow-Derived Macrophage from Resistant and Susceptible Mice Strains. *Mediators Inflamm.* **2015**, *2015*, doi:10.1155/2015/605450.

26. Pina, A.; Bernardino, S.; Calich, V.L.G. Alveolar macrophages from susceptible mice are more competent than those of resistant mice to control initial *Paracoccidioides brasiliensis* infection. *J. Leukoc. Biol.* **2008**, *83*, 1088–1099, doi:10.1189/jlb.1107738.

27. Almeida, S.R.; Lopes, J.D. The low efficiency of dendritic cells and macrophages from mice susceptible to *Paracoccidioides brasiliensis* in inducing a Th1 response. *Brazilian J. Med. Biol. Res.* **2001**, *34*, 529–537, doi:10.1590/S0100-879X2001000400014.

28. Ferreira, K.S.; Almeida, S.R. Immunization of susceptible mice with gp43-pulsed dendritic cells induce an increase of pulmonary Paracoccidioidomycosis. *Immunol. Lett.* **2006**, *103*, 121–126, doi:10.1016/j.imlet.2005.10.014.

29. Alves da Costa, T.; Di Gangi, R.; Martins, P.; Longhini, A.L.F.; Zanucoli, F.; de Oliveira, A.L.R.; Stach-Machado, D.R.; Burger, E.; Verinaud, L.; Thomé, R. Protection against *Paracoccidioides brasiliensis* infection in mice treated with modulated dendritic cells relies on inhibition of

interleukin-10 production by CD8+ T cells. *Immunology* **2015**, *146*, 486–495, doi:10.1111/imm.12526.

30. Fernandes, R.; Rodrigues, D.; Romagnoli, G.; Vieira, I.; Dias-Melicio, L.; Angela, R.; Soares, M. In vitro challenge of human dendritic cells with *Paracoccidioides brasiliensis* induces preferential generation of Treg cells. *Med. Res. Arch.* **2017**, *5*, doi:10.18103/mra.v5i12.1664.

31. Silva, L.B.R.; Taira, C.L.; Dias, L.S.; Souza, A.C.O.; Nosanchuk, J.D.; Travassos, L.R.; Taborda, C.P. Experimental therapy of Paracoccidioidomycosis using p10-primed monocyte-derived dendritic cells isolated from infected mice. *Front. Microbiol.* **2019**, *10*, doi:10.3389/fmicb.2019.01727.

32. de Araújo, E.F.; Feriotti, C.; de Lima Galdino, N.A.; Preite, N.W.; Calich, V.L.G.; Loures, F.V. The IDO-AhR axis controls Th17/Treg immunity in a pulmonary model of fungal infection. *Front. Immunol.* **2017**, *8*, doi:10.3389/fimmu.2017.00880.

33. Goihman-Yahr, M.; Pine, L.; Albornoz, M.C.; Yarzabal, L.; De Gomez, M.H.; Martin, B.S.; Ocanto, A.; Molina, T.; Convit, J. Studies on plating efficiency and estimation of viability of suspensions of *Paracoccidioides brasiliensis* yeast cells. *Mycopathologia* **1980**, *71*, 73–83, doi:10.1007/BF00440612.

34. Singer-Vermes, L.M.; Sakamoto, T.N.; Vaz, C.A.C. Influence of the genetic pattern and sex of mice in experimental paracoccidioidomycosis. *Clin Exp Immunol* **1995**, *101*, 1–14, doi:10.1111/j.1365-2249.1995.tb02286.x.

35. Lutz, M.B.; Kukutsch, N.; Ogilvie, A.L..; Rößner, S.; Koch, F.; Romani, N.; Schuler, G. An advanced culture method for generating large quantities of highly pure dendritic cells from mouse bone marrow. *J. Immunol. Methods* **1999**, *223*, 77–92, doi:10.1016/S0022-1759(98)00204-X.

36. Tavares, A.H.; Derengowski, L.S.; Ferreira, K.S.; Silva, S.S.; Macedo, C.; Bocca, A.L.; Passos, G.A.; Almeida, S.R.; Silva-Pereira, I. Murine dendritic cells transcriptional modulation upon *Paracoccidioides brasiliensis* infection. *PLoS Negl. Trop. Dis.* **2012**, *6*, doi:10.1371/journal.pntd.0001459.

37. Siqueira, I.M.; Fraga, C.L.F.; Amaral, A.C.; Souza, A.C.O.; Jerônimo, M.S.; Correa, J.R.; Magalhães, K.G.; Inácio, C.A.; Ribeiro, A.M.; Burguel, P.H.; et al. Distinct patterns of yeast cell morphology and host responses induced by representative strains of *Paracoccidioides brasiliensis* (Pb18) and *Paracoccidioides lutzii* (Pb01). *Med. Mycol.* **2016**, *54*, 177–188, doi:10.1093/mmy/myv072.

38. Tavares, A.H.F.P.; Silva, S.S.; Dantas, A.; Campos, É.G.; Andrade, R. V.; Maranhão, A.Q.; Brígido, M.M.; Passos-Silva, D.G.; Fachin, A.L.; Teixeira, S.M.R.; et al. Early transcriptional response of *Paracoccidioides brasiliensis* upon internalization by murine macrophages. *Microbes Infect.* **2007**, *9*, 583–590, doi:10.1016/j.micinf.2007.01.024.

39. Silva, S.S.; Tavares, A.H.F.P.; Passos-Silva, D.G.; Fachin, A.L.; Teixeira, S.M.R.; Soares, C.M.A.;

Carvalho, M.J.A.; Bocca, A.L.; Silva-Pereira, I.; Passos, G.A.S.; et al. Transcriptional response of murine macrophages upon infection with opsonized *Paracoccidioides brasiliensis* yeast cells. *Microbes Infect.* **2008**, *10*, 12–20, doi:10.1016/j.micinf.2007.09.018.

40. Nicola, A.M.; Albuquerque, P.; Martinez, L.R.; Dal-Rosso, R.A.; Saylor, C.; De Jesus, M.; Nosanchuk, J.D.; Casadevall, A. Macrophage autophagy in immunity to *Cryptococcus neoformans* and *Candida albicans*. *Infect. Immun.* **2012**, *80*, 3065–3076, doi:10.1128/IAI.00358-12.

41. Cock, P.J.A.; Fields, C.J.; Goto, N.; Heuer, M.L.; Rice, P.M. The Sanger FASTQ file format for sequences with quality scores, and the Solexa/Illumina FASTQ variants. *Nucleic Acids Res.* **2010**, *38*, 1767–1771, doi:10.1093/nar/gkp1137.

42. Andrews, S.; Krueger, F.; Seconds-Pichon, A.; Biggins, F.; Wingett, S. FastQC. A quality control tool for high throughput sequence data. Babraham Bioinformatics 2015.

43. Martin, M. Cutadapt removes adapter sequences from high-throughput sequencing reads. *EMBnet.journal* **2011**, *17*, 10, doi:10.14806/ej.17.1.200.

44. Schmieder, R.; Edwards, R. Quality control and preprocessing of metagenomic datasets. *Bioinformatics* **2011**, *27*, 863–864, doi:10.1093/bioinformatics/btr026.

45. Kim, D.; Pertea, G.; Trapnell, C.; Pimentel, H.; Kelley, R.; Salzberg, S.L. TopHat2: Accurate alignment of transcriptomes in the presence of insertions, deletions and gene fusions. *Genome Biol.* **2013**, *14*, R36, doi:10.1186/gb-2013-14-4-r36.

46. Li, H.; Handsaker, B.; Wysoker, A.; Fennell, T.; Ruan, J.; Homer, N.; Marth, G.; Abecasis, G.; Durbin, R. The Sequence Alignment/Map format and SAMtools. *Bioinformatics* **2009**, *25*, 2078–2079, doi:10.1093/bioinformatics/btp352.

47. Anders, S.; Pyl, P.T.; Huber, W. HTSeq-A Python framework to work with high-throughput sequencing data. *Bioinformatics* **2015**, *31*, 166–169, doi:10.1093/bioinformatics/btu638.

48. Robinson, M.D.; McCarthy, D.J.; Smyth, G.K. edgeR: A Bioconductor package for differential expression analysis of digital gene expression data. *Bioinformatics* **2010**, *26*, 139–140, doi:10.1093/bioinformatics/btp616.

49. Benjamini, Y.; Hochberg, Y. Controlling the False Discovery Rate: A Practical and Powerful Approach to Multiple Testing. *J. R. Stat. Soc. Ser. B* **1995**, *57*, 289–300, doi:10.1111/j.2517-6161.1995.tb02031.x.

50. Yu, G.; Wang, L.G.; Han, Y.; He, Q.Y. ClusterProfiler: An R package for comparing biological themes among gene clusters. *Omi. A J. Integr. Biol.* **2012**, *16*, 284–287, doi:10.1089/omi.2011.0118.

51. Blake, J.A.; Christie, K.R.; Dolan, M.E.; Drabkin, H.J.; Hill, D.P.; Ni, L.; Sitnikov, D.; Burgess, S.; Buza, T.; Gresham, C.; et al. Gene ontology consortium: Going forward. *Nucleic Acids Res.* **2015**, *43*, D1049–D1056, doi:10.1093/nar/gku1179.

52. Livak, K.J.; Schmittgen, T.D. Analysis of relative gene expression data using real-time quantitative PCR and the 2-ΔΔCT method. *Methods* **2001**, *25*, 402–408, doi:10.1006/meth.2001.1262.

53. Spandidos, A.; Wang, X.; Wang, H.; Seed, B. PrimerBank: A resource of human and mouse PCR primer pairs for gene expression detection and quantification. *Nucleic Acids Res.* **2009**, *38*, doi:10.1093/nar/gkp1005.

54. Panganiban, R.P.; Vonakis, B.M.; Ishmael, F.T.; Stellato, C. Coordinated post-transcriptional regulation of the chemokine system: Messages from CCL2. *J. Interf. Cytokine Res.* **2014**, *34*, 255–266, doi:10.1089/jir.2013.0149.

55. Das, A.S.; Basu, A.; Kumar, R.; Borah, P.K.; Bakshi, S.; Sharma, M.; Duary, R.K.; Ray, P.S.; Mukhopadhyay, R. Post-transcriptional regulation of C-C motif chemokine ligand 2 expression by ribosomal protein L22 during LPS-mediated inflammation. *FEBS J.* **2020**, doi:10.1111/febs.15362.

56. Ren, J.; Wang, Q.; Morgan, S.; Si, Y.; Ravichander, A.; Dou, C.; Kent, K.C.; Liu, B. Protein kinase C-δ (PKCδ) regulates proinflammatory chemokine expression through cytosolic interaction with the NF-κB subunit p65 in vascular smooth muscle cells. *J. Biol. Chem.* **2014**, *289*, 9013–9026, doi:10.1074/jbc.M113.515957.

57. Nakatsumi, H.; Matsumoto, M.; Nakayama, K.I. Noncanonical Pathway for Regulation of CCL2 Expression by an mTORC1-FOXK1 Axis Promotes Recruitment of Tumor-Associated Macrophages. *Cell Rep.* **2017**, *21*, 2471–2486, doi:10.1016/j.celrep.2017.11.014.

58. Bansal, K.; Sinha, A.Y.; Ghorpade, D.S.; Togarsimalemath, S.K.; Patil, S.A.; Kaveri, S. V.; Balaji, K.N.; Bayry, J. Src homology 3-interacting domain of Rv1917c of *Mycobacterium tuberculosis* induces selective maturation of human dendritic cells by regulating PI3K-MAPK-NF-κB signaling and drives Th2 immune responses. *J. Biol. Chem.* **2010**, *285*, 36511–36522, doi:10.1074/jbc.M110.158055.

59. Ji, W.-T.; Liu, H. PI3K-Akt Signaling and Viral Infection. *Recent Pat. Biotechnol.* **2008**, *2*, 218–226, doi:10.2174/187220808786241042.

60. Roca, H.; Varsos, Z.S.; Mizutani, K.; Pienta, K.J. CCL2, survivin and autophagy: New links with implications in human cancer. *Autophagy* **2008**, *4*, 969–971, doi:10.4161/auto.6822.

61. Knight, M.; Stanley, S. HIF-1α as a central mediator of cellular resistance to intracellular pathogens. *Curr. Opin. Immunol.* **2019**, *60*, 111–116, doi:10.1016/j.coi.2019.05.005.

62. Kotsias, F.; Cebrian, I.; Alloatti, A. Antigen processing and presentation. In *International Review of Cell and Molecular Biology*; Elsevier Inc., 2019; Vol. 348, pp. 69–121 ISBN 9780128183519.

63. Ma, J.; Becker, C.; Lowell, C.A.; Underhill, D.M. Dectin-1-triggered recruitment of light chain 3 protein to phagosomes facilitates major histocompatibility complex class II presentation of fungal-derived antigens. *J. Biol. Chem.* **2012**, *287*, 34149–34156, doi:10.1074/jbc.M112.382812.

64. Martinez, J.; Malireddi, R.K.S.; Lu, Q.; Cunha, L.D.; Pelletier, S.; Gingras, S.; Orchard, R.; Guan, J.L.; Tan, H.; Peng, J.; et al. Molecular characterization of LC3-associated phagocytosis reveals distinct roles for Rubicon, NOX2 and autophagy proteins. *Nat. Cell Biol.* **2015**, *17*, 893–906, doi:10.1038/ncb3192.

65. Huang, J.H.; Liu, C.Y.; Wu, S.Y.; Chen, W.Y.; Chang, T.H.; Kan, H.W.; Hsieh, S.T.; Ting, J.P.Y.; Wu-Hsieh, B.A. NLRX1 Facilitates *Histoplasma capsulatum*-Induced LC3-Associated Phagocytosis for Cytokine Production in Macrophages. *Front. Immunol.* **2018**, *9*, 2761, doi:10.3389/fimmu.2018.02761.

66. Pereira de Oliveira Júnior, G.; Renney de Sousa, H.; César de Melo Gorgo-, K.; Karla dos Santos Borges, T.; Teixeira Rangel, K.; Fabricant, S.; Koser Gustavo, C.; Fraga Friaça, L.; Rossi Neto, A.; Andrés Hurtado, F.; et al. Molecular mechanisms of LC3-associated phagocytosis in the macrophage response to *Paracoccidioides* spp. *bioRxiv* **2020**, 2020.10.30.362681, doi:10.1101/2020.10.30.362681.

67. Sanjuan, M.A.; Dillon, C.P.; Tait, S.W.G.; Moshiach, S.; Dorsey, F.; Connell, S.; Komatsu, M.; Tanaka, K.; Cleveland, J.L.; Withoff, S.; et al. Toll-like receptor signalling in macrophages links the autophagy pathway to phagocytosis. *Nature* **2007**, *450*, 1253–1257, doi:10.1038/nature06421.

68. Mendes, R.P.; Cavalcante, R. de S.; Marques, S.A.; Marques, M.E.A.; Venturini, J.; Sylvestre, T.F.; Paniago, A.M.M.; Pereira, A.C.; da Silva, J. de F.; Fabro, A.T.; et al. Paracoccidioidomycosis: Current Perspectives from Brazil. *Open Microbiol. J.* **2017**, *11*, 224–282, doi:10.2174/1874285801711010224.

69. Pina, A.; de Araujo, E.F.; Felonato, M.; Loures, F. V.; Feriotti, C.; Bernardino, S.; Barbuto, J.A.M.; Calich, V.L.G. Myeloid dendritic cells (DCs) of mice susceptible to paracoccidioidomycosis suppress T cell responses whereas myeloid and plasmacytoid DCs from resistant mice induce effector and regulatory T cells. *Infect. Immun.* **2013**, *81*, 1064–1077, doi:10.1128/IAI.00736-12.

70. Daynes, R.A.; Jones, D.C. Emerging roles of PPARs in inflammation and immunity. *Nat. Rev. Immunol.* **2002**, *2*, 748–759, doi:10.1038/nri912.

71. Ricote, M.; Glass, C.K. PPARs and molecular mechanisms of transrepression. *Biochim. Biophys. Acta - Mol. Cell Biol. Lipids* **2007**, *1771*, 926–935, doi:10.1016/j.bbalip.2007.02.013.

72. Pina, A.; Saldiva, P.H.N.; Cano Restrepo, L.E.; Calich, V.L.G. Neutrophil role in pulmonary paracoccidioidomycosis depends on the resistance pattern of hosts. *J. Leukoc. Biol.* **2006**, *79*, 1202–1213, doi:10.1189/jlb.0106052.

73. Rodrigues, D.R.; Dias-Melicio, L.A.; Calvi, S.A.; Peraçoli, M.T.S.; Soares, A.M.V.C. *Paracoccidioides brasiliensis* killing by IFN-γ, TNF-α and GM-CSF activated human neutrophils: Role for oxygen metabolites. *Med. Mycol.* **2007**, *45*, 27–33, doi:10.1080/13693780600981676.

74. Acorci-Valério, M.J.; Bordon-Graciani, A.P.; Dias-Melicio, L.A.; De Assis Golim, M.; Nakaira-Takahagi, E.; De Campos Soares, Â.M.V. Role of TLR2 and TLR4 in human neutrophil functions against *Paracoccidioides brasiliensis*. *Scand. J. Immunol.* **2010**, *71*, 99–108, doi:10.1111/j.1365-3083.2009.02351.x.

75. Puerta-Arias, J.D.; Pino-Tamayo, P.A.; Arango, J.C.; González, Á. Depletion of neutrophils promotes the resolution of pulmonary inflammation and fibrosis in Mice infected with *Paracoccidioides brasiliensis*. *PLoS One* **2016**, *11*, doi:10.1371/journal.pone.0163985.

76. Pino-Tamayo, P.A.; Puerta-Arias, J.D.; Lopera, D.; Urán-Jiménez, M.E.; González, Á. Depletion of Neutrophils Exacerbates the Early Inflammatory Immune Response in Lungs of Mice Infected with *Paracoccidioides brasiliensis*. *Mediators Inflamm.* **2016**, *2016*, doi:10.1155/2016/3183285.

77. Kashino, S.S.; Fazioli, R. dos A.; Moscardi-Bacchi, M.; Franco, M.; Singer-Vermes, L.M.; Burger, E.; Calich, V.L.G. Effect of macrophage blockade on the resistance of inbred mice to *Paracoccidioides brasiliensis* infection. *Mycopathologia* **1995**, *130*, 131–140, doi:10.1007/BF01103095.

78. Brummer, E.; Hanson, L.H.; Restrepo, A.; Stevens, D.A. Intracellular multiplication of *Paracoccidioides brasiliensis* in macrophages: Killing and restriction of multiplication by activated macrophages. *Infect. Immun.* **1989**, *57*, 2289–2294, doi:10.1128/iai.57.8.2289-2294.1989.

79. Delamarre, L.; Pack, M.; Chang, H.; Mellman, I.; Trombetta, E.S. Differential lysosomal proteolysis in antigen-presenting cells determines antigen fate. *Science (80-.).* **2005**, *307*, 1630–1634, doi:10.1126/science.1108003.

80. Deretic, V.; Saitoh, T.; Akira, S. Autophagy in infection, inflammation and immunity. *Nat. Rev. Immunol.* **2013**, *13*, 722–737, doi:10.1038/nri3532.

81. Tam, J.M.; Mansour, M.K.; Acharya, M.; Sokolovska, A.; Timmons, A.K.; Lacy-Hulbert, A.; Vyas, J.M. The role of autophagy-related proteins in *Candida albicans* infections. *Pathogens* **2016**, *5*, doi:10.3390/pathogens5020034.

82. Oikonomou, V.; Renga, G.; De Luca, A.; Borghi, M.; Pariano, M.; Puccetti, M.; Paolicelli, G.;

Stincardini, C.; Costantini, C.; Bartoli, A.; et al. Autophagy and LAP in the fight against fungal infections: Regulation and therapeutics. *Mediators Inflamm.* **2018**, *2018*, doi:10.1155/2018/6195958.

83. Heckmann, B.L.; Green, D.R. LC3-associated phagocytosis at a glance. *J. Cell Sci.* **2019**, *132*, jcs222984, doi:10.1242/jcs.222984.

84. Matsuzawa-Ishimoto, Y.; Hwang, S.; Cadwell, K. Autophagy and Inflammation. *Annu. Rev. Immunol.* **2018**, *36*, 73–101, doi:10.1146/annurev-immunol-042617-053253.

85. Zhang, H.; Chen, J.; Zeng, Z.; Que, W.; Zhou, L. Knockdown of DEPTOR induces apoptosis, increases chemosensitivity to doxorubicin and suppresses autophagy in RPMI-8226 human multiple myeloma cells in vitro. *Int. J. Mol. Med.* **2013**, *31*, 1127–1134, doi:10.3892/ijmm.2013.1299.

86. Braverman, J.; Sogi, K.M.; Benjamin, D.; Nomura, D.K.; Stanley, S.A. HIF-1α Is an Essential Mediator of IFN-γ–Dependent Immunity to *Mycobacterium tuberculosis*. *J. Immunol.* **2016**, *197*, 1287–1297, doi:10.4049/jimmunol.1600266.

87. Friedrich, D.; Zapf, D.; Lohse, B.; Fecher, R.A.; Deepe, G.S.; Rupp, J. The HIF-1/LC3-II axis impacts fungal immunity in human macrophages. *Infect. Immun.* **2019**, *87*, doi:10.1128/IAI.00125-19.

88. Quäschling, T.; Friedrich, D.; Deepe, G.S.; Rupp, J. Crosstalk Between Autophagy and Hypoxia-Inducible Factor-1α in Antifungal Immunity. *Cells* **2020**, *9*, 2150, doi:10.3390/cells9102150.

89. Casadevall, A.; Pirofski, L. anne What is a host? Attributes of individual susceptibility. *Infect. Immun.* **2018**, *86*, doi:10.1128/IAI.00636-17.

6. Figures and legends

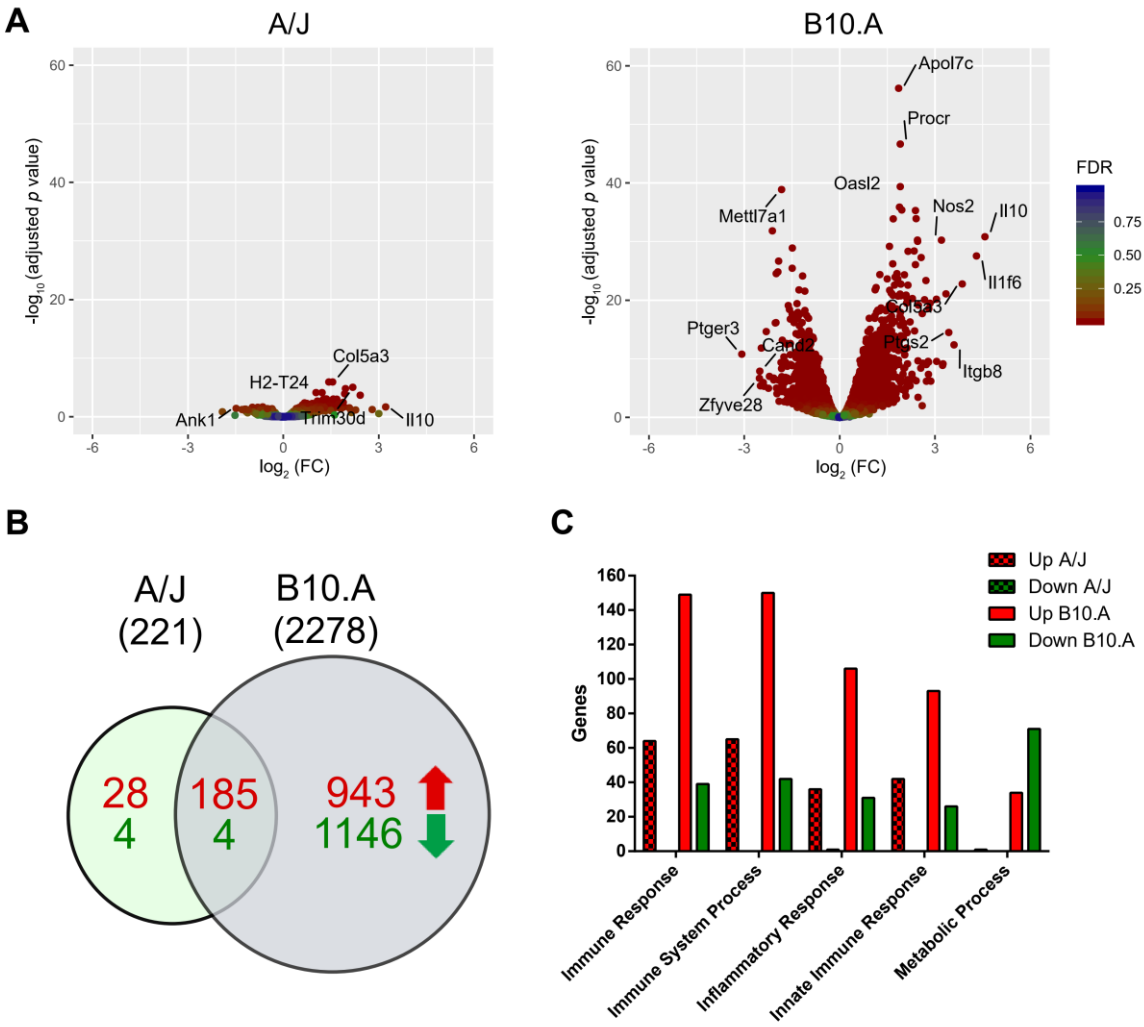

Figure 1. Differential Gene Expression of BMDCs from PCM-resistant and -susceptible strains upon *P. brasiliensis* infection.

A) Volcano plot showing gene expression changes comparing *P. brasiliensis* infected BMDCs derived from the resistant A/J (left) and the susceptible B10.A (right) mouse strains vs. control (non-infected) samples. The y-axis represents the -log10 values of the adjusted *p*-value and the x-axis represents the log2 values of the fold change observed for each transcript. The top differentially expressed genes (DEGs: adjusted *p*-value < 0.05 and fold change ≥ ±1.4) are indicated. **B)** Venn diagram of positively (red) and negatively (green) regulated genes of A/J and B10.A mice strains. **C)** Number of DEGs correlated to different GO terms in A/J and B10.A mouse strains infected with *P. brasiliensis*.

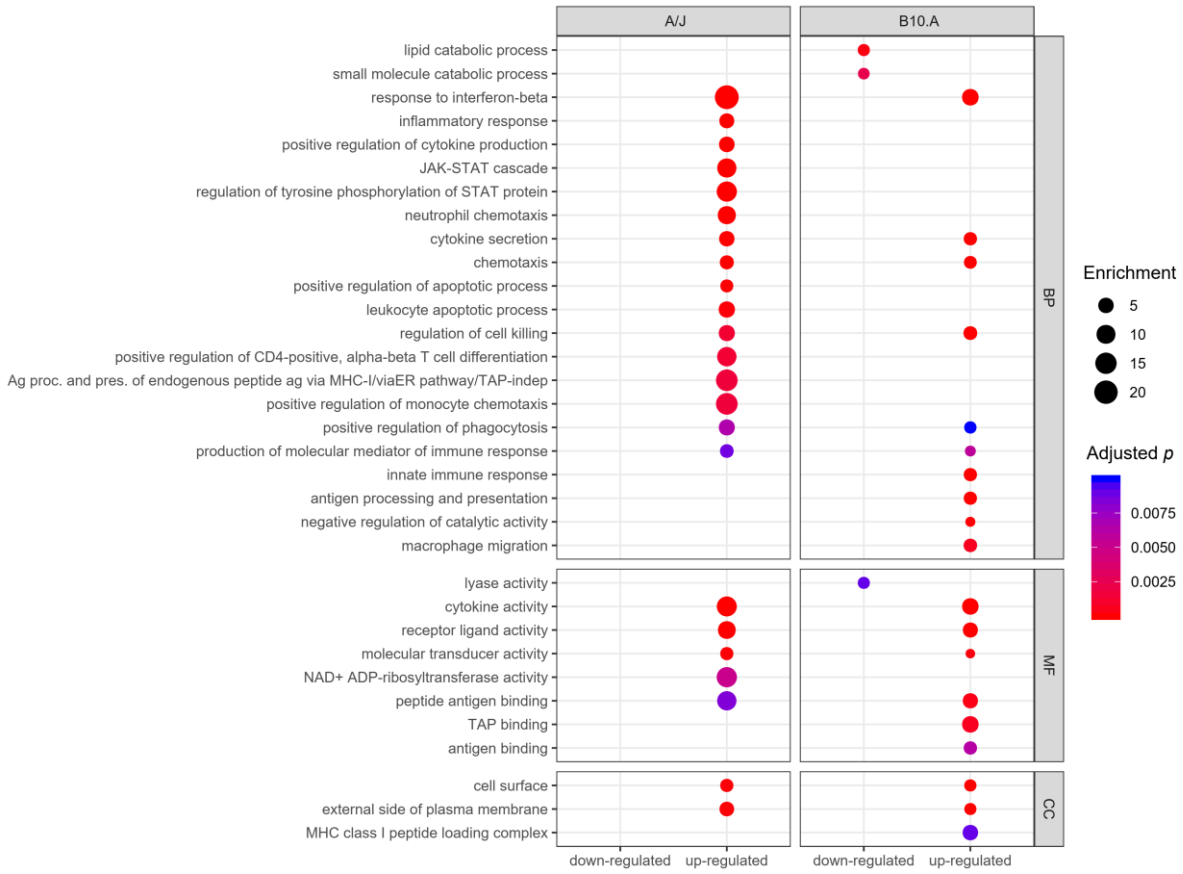

Figure 2. Gene ontology enrichment of differentially expressed genes in BMDCs after *P. brasiliensis* infection.

Enriched ontological categories (adjusted *p*-value < 0.01) associated with up- or down-regulated DEG in BMDCs derived from the resistant A/J (left) and the susceptible B10.A (right) mice strains. Dot size represents the enrichment (gene modulated ratio/gene background ratio) for each GO term. BP: biological process, MF: molecular function, CC: cellular component.

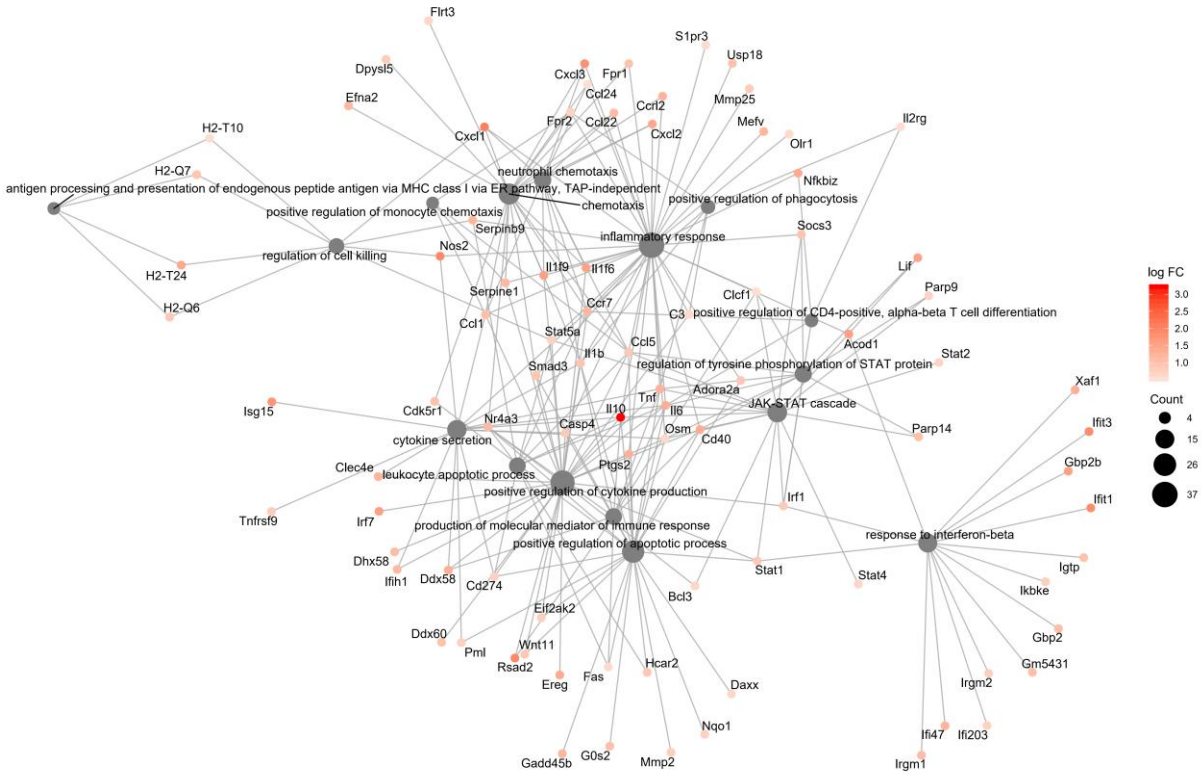

Figure 3. Functional interaction networks related to biological process Gene Ontology terms enriched by genes upregulated in response to *P. brasiliensis* infection in BMDCs from the resistant mouse strain, A/J.

ClusterProfiler was used to generate the functional interaction networks formed by up-regulated genes related to the GO Biological Process terms. Dot size represents the number of genes in each GO term.

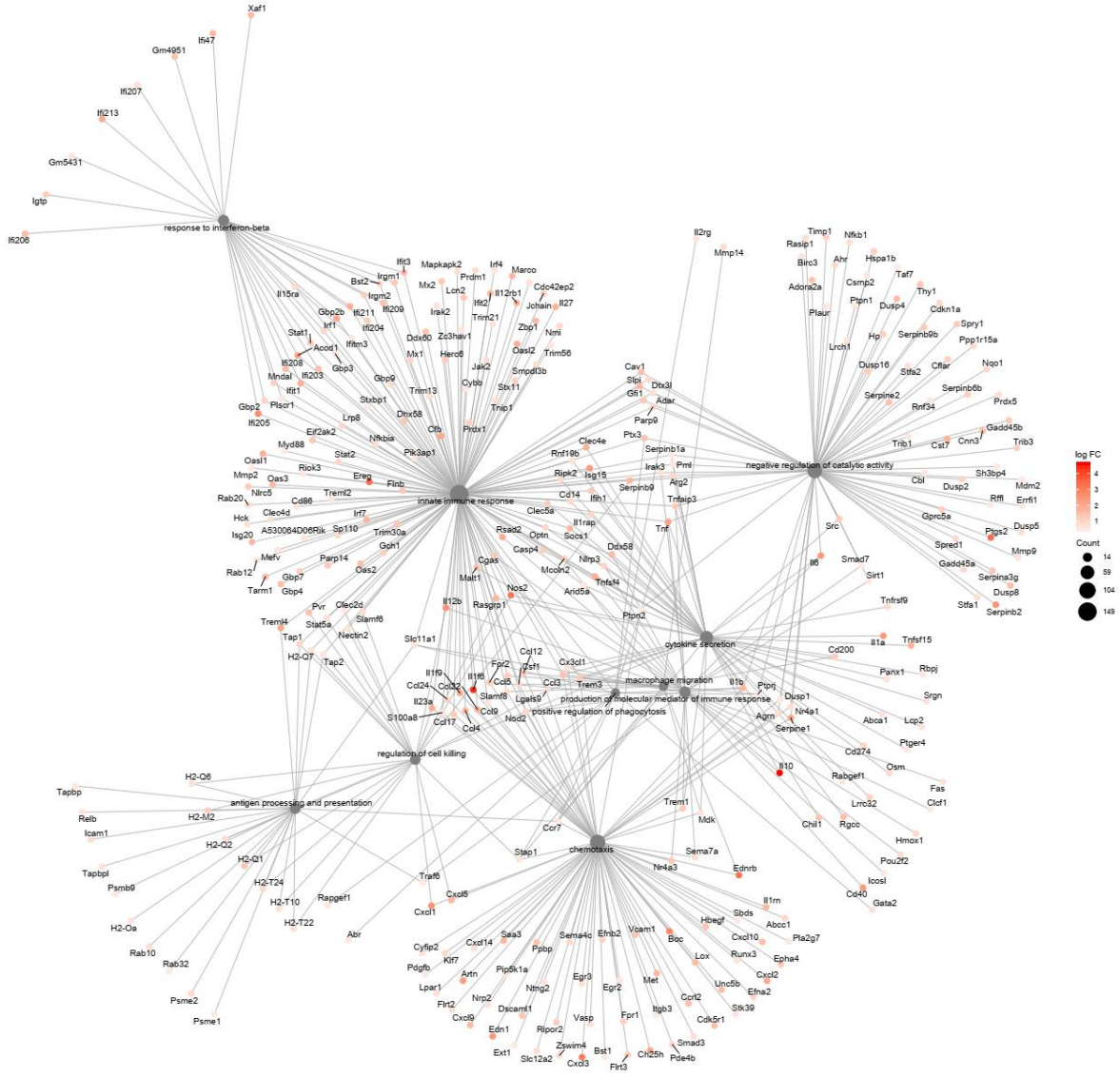

Figure 4. Functional interaction networks related to biological process Gene Ontology terms enriched by genes upregulated in response to *P. brasiliensis* infection in BMDCs from the susceptible mouse strain, B10.A.

ClusterProfiler was used to generate the functional interaction networks formed by up-regulated genes related to the GO Biological Process terms. Dot size represents the number of genes in each GO term.

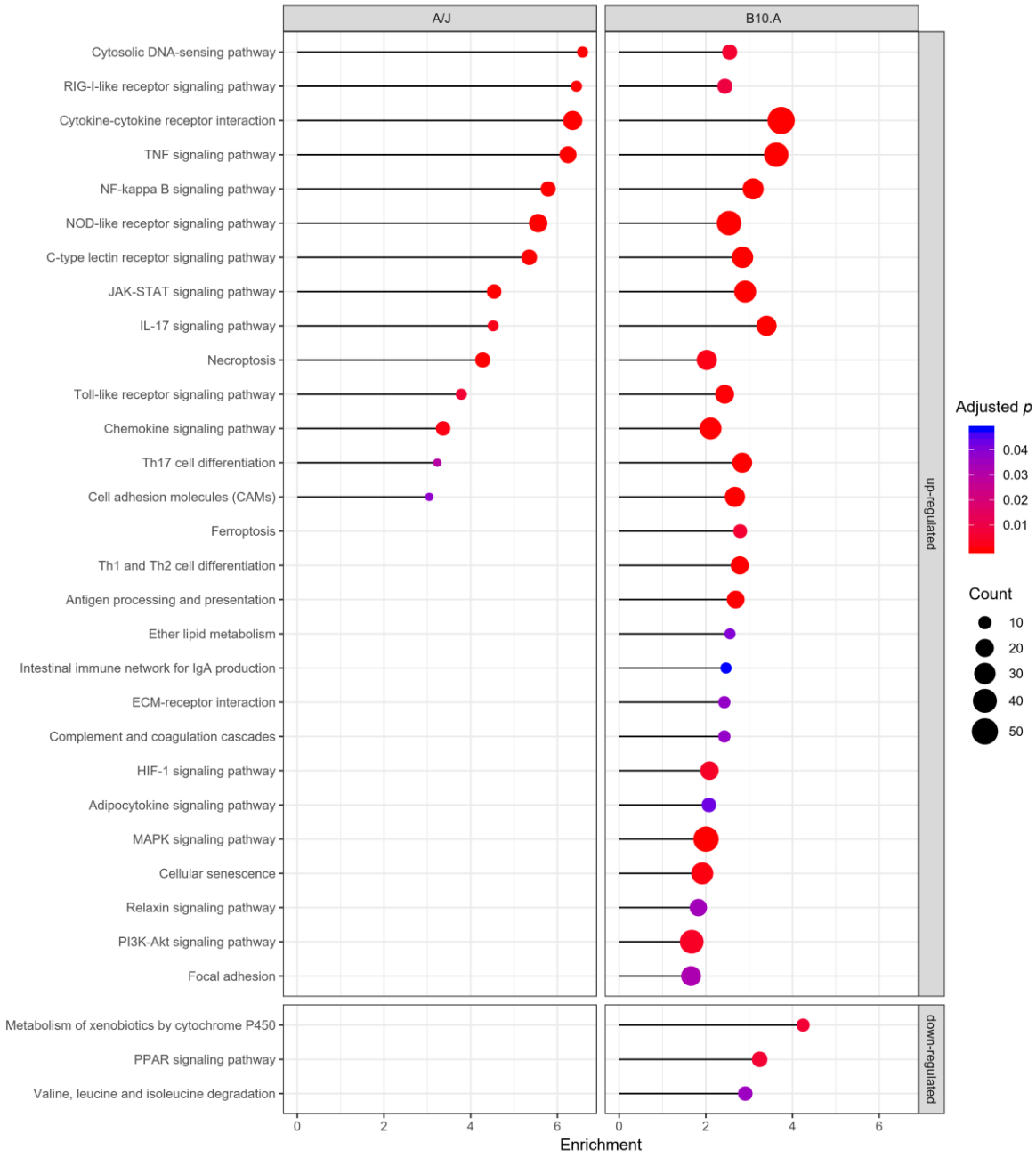

Figure 5. KEGG pathway enrichment of differentially expressed genes in BMDCs derived from resistant (A/J) and susceptible (B10.A) mouse strains in response to *P. brasiliensis* infection.

Enriched pathways (adjusted *p*-value < 0.05) associated with up-regulated or down-regulated DEG for the two murine strains. The x-axis represents the enrichment in each pathway. Dot size represents the number of genes in each pathway.

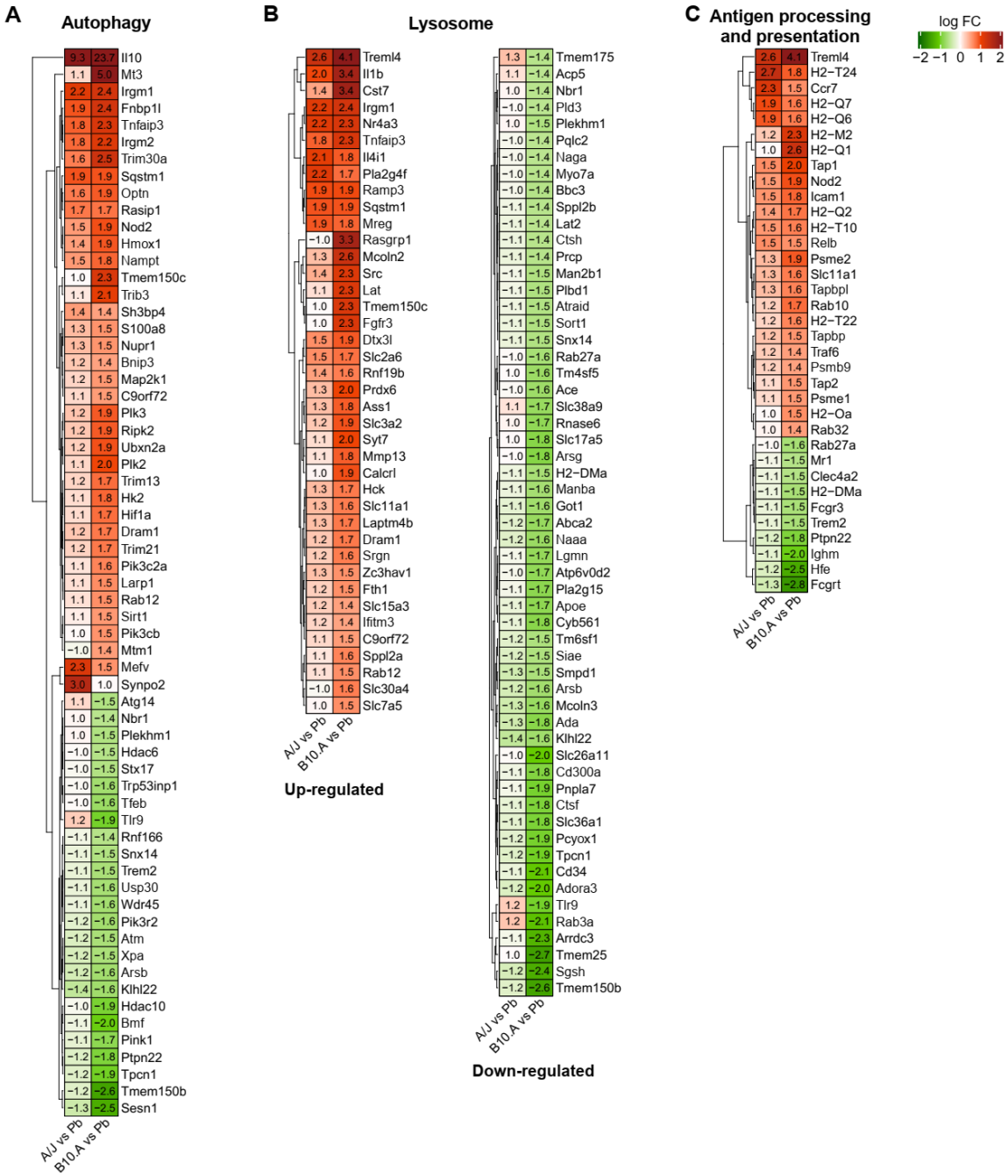

Figure 6. Comparison of selected DEG modulation related to antigen presentation, autophagy, and lysosome function Gene Ontology terms in BMDCs from resistant (A/J) and susceptible (B10.A) mouse strains upon infection with *P. brasiliensis*.

A to **C**) The values in heatmaps represent the fold change for each gene. DEGs: adjusted *p*-value < 0.05, and fold change ≥ ±1.4.

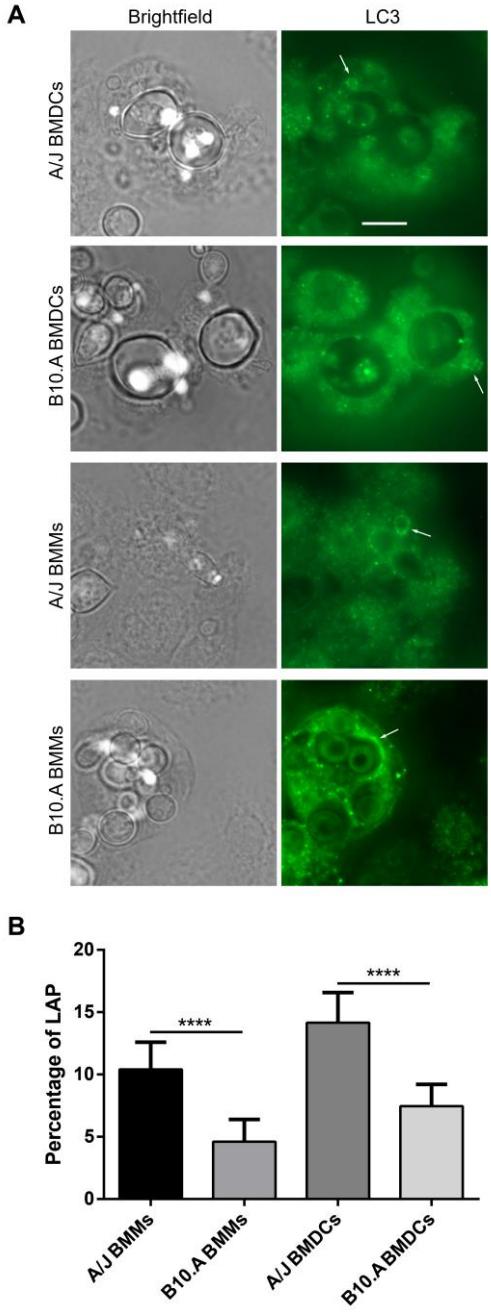

Figure 7. LC3-associated phagocytosis of BMMs and BMDCs from A/J and B10.A mice upon *P. brasiliensis* infection.

BMMs and BMDCs were co-cultured with *P. brasiliensis* at a MOI 1:1 for 12 h and treated with anti-LC3 fluorescent antibody. **A**) The localization of LC3-associated phagocytosis (LAP) was assessed by fluorescence microscopy. The fluorescence images were processed by deconvolution using a constrained iterative algorithm. The arrows point to cells that are surrounded by the autophagosome marker LC3. Scale bar: 10 μm. **B**) The percentage of LC3-associated phagocytosis (LAP) was measured by the number of phagocytosed fungal cells positive for LC3 divided by the total number of phagocytosed fungal cells. Data are presented as mean ± 95% C.I. (n=3 independent experiments, **** $p < 0.0001$ using Fisher's exact test).

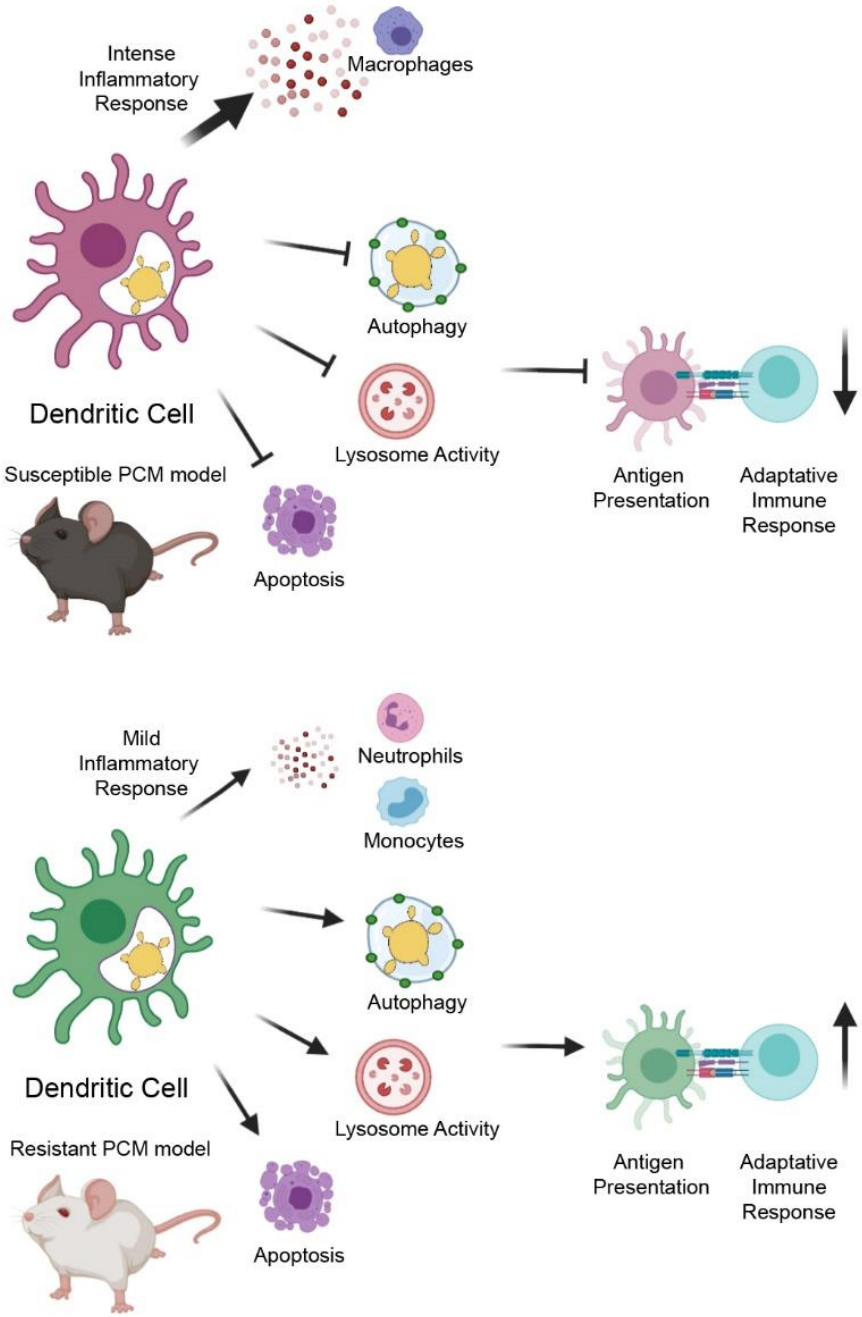

Figure 8. Schematic model of major transcriptional differences of BMDCs from resistant (A/J) and susceptible (B10.A) mouse strains upon infection with *P. brasiliensis*.

BMDCs from the susceptible strain displayed a more intense activation of inflammatory response followed by the downregulation of autophagy, lysosome activity and apoptosis, all processes involved in antigen processing and presentation and the activation of adaptive immune response. In contrast, BMDCs from the resistant mouse induce a mild inflammatory response with preserved functionality of autophagy, lysosome activation and apoptosis which might lead to more efficient antigen processing and presentation and proper activation of adaptative immune response.

Capítulo III:

Análise transcritômica comparativa da resposta imune de macrófagos murinos à infecção por duas linhagens de *Cryptococcus neoformans*

Este capítulo refere-se ao trabalho cujo manuscrito se encontra em fase final de preparação. O foco desse capítulo é apresentar os principais resultados e discussão parcial.

Título provisório:

Capsule Matters: Cryptococcus neoformans' capsule effect on the macrophages' immune response landscape

Capsule Matters: Cryptococcus neoformans' capsule effect on the macrophages' immune response landscape

Abstract: Polysaccharide capsule is a relevant virulence factor in cryptococcal infection. This structure has been previously associated with many protective functions, including the inhibition of phagocytosis, reduction of host immune responses, and depletion of complement components. The main components of capsular material are glucuronoxylomannan and galactoxylomannan, two polymers with potent immunomodulatory properties *in vivo* and *in vitro*, such as the suppression of both innate and adaptive immune mechanisms. In this study, we employed *in vitro* primary murine macrophages infection, qPCR-array of micro-RNAs, and high-throughput RNA sequencing to compare the macrophages responses to genetically equivalent encapsulated (B3501) and nonencapsulated (Cap67) *Cryptococcus neoformans* strains. We analyzed the data in terms of subset composition, gene, and microRNAs signatures, enriched pathways, and transcriptional regulatory networks. Although, both infection models induced modulation of genes related to inflammation and adaptive immune responses there was a significant delay in the transcriptomic response of the encapsulated yeasts-infected macrophages. Interestingly, an increased diversity of differentially expressed miRNAs was detected in the early stage of macrophages infection with the encapsulated strain. Considering the multiples roles of miRNAs in regulating gene expression, these findings provide some insights into the molecular mechanisms behind the immunomodulatory role of *C. neoformans* capsule during its interaction with macrophages.

1. Introduction

Over the last decades, epidemiological studies pointed out that the prevalence and mortality by pathogenic fungal infections have increased worldwide (1–3). The cryptococcosis is a systemic mycosis caused by the *Cryptococcus neoformans* and *Cryptococcus gattii* species complex, mainly in immunosuppressed individuals (4). Approximately 112,000 annual deaths are related to *Cryptococcus* spp. infections in HIV/AIDS patients worldwide (5).

Macrophages and dendritic cells are crucial components of the innate immune system in the lungs and are considered key effectors in the immune response against *C. neoformans*. These cells recognize the *C. neoformans* yeasts, phagocytize them, and promote their destruction inside the phagosomes. Cytokines and chemokines, such as interferon-gamma (INF-γ), tumor necrosis factor-alpha (TNF-α), interleukin-12 (IL12), IL17A, IL23, C-X-C motif ligand 9 (CXCL9), CXCL10, and CXCL11 are released by infected cells (6–10). Phagocytic cells also produce reactive oxygen (ROS) and nitrogen species (RNS), among myriad antimicrobial molecules, and present antigens to T cells, thus triggering the adaptive immune response that leads to the induction of a protective Th1-type immunity (10,11). Conversely, *C. neoformans* evolution selected sophisticated defense mechanisms to evade the host innate and adaptive immune responses. This fungus can survive and persist in both intracellular and extracellular mammalian hosts environments, which hampers its eradication from mammalian host organs (12–15).

In the environment and inside the host, *C. neoformans* produces a characteristic polysaccharide capsule, composed primarily by glucuronoxylomannan (GXM) and minor components such as galactoxylomannan (GalXM), mannoproteins, and some lipids (16–19). This structure hinders phagocytosis preventing fungal recognition by the PRRs. The capsule also depletes complement components, and prevent dendritic cells maturation, antigen presentation, and the production proinflammatory cytokines (20–25). In addition to the capsule, laccases and melanin production confer protection to *C. neoformans* from ROS and antimicrobial drugs (21,26,27). Other enzymes, such as ureases, proteases and phospholipases increase the resistance to the host defenses (27).

The refined understanding of the host-pathogen interaction is crucial to the development of efficient strategies for controlling fungal infections. This requires the elucidation of the molecular mechanisms underlying fungal pathogenesis. The capsule seems to be essential for fungal survival in the host's cells, and acapsular *C. neoformans* strains are normally avirulent

(28–30). However, little is known about the molecular mechanisms behind the immunomodulatory effects of this fungal structure during host-pathogen interactions. The present work aimed to compare the macrophages transcriptomic expression profiles after infection by genetically equivalent encapsulated and nonencapsulated *C. neoformans* strains. Gene ontology and KEGG enrichment analyses were performed to evaluate potentially different signaling pathways activated by the fungal infection. Our results revealed strain-specific gene expression profiles. A response consistent with a delay in triggering an adequate innate and adaptive immune responses was observed in macrophages infected by the encapsulated strain. Conversely, there was an increased modulation of several miRNAs by macrophages infected with encapsulated strain. These findings contributed to the understanding of host-pathogen interaction mechanisms between mammalian cells and *C. neoformans*.

2. Materials and methods

2.1. Ethics statement

All animal procedures were performed per national and institutional guidelines for animal care and were approved by the University of Brasilia (UnB)'s Animal Ethics Committee (Proc. UnB Doc 52657/2011) (31).

2.2. Fungal Cells and Growth Conditions

C. neoformans strains used for these experiments were the encapsulated B3501-A (B3501) and the non-encapsulated mutant *cap67*Δ (Cap67) (32). Yeast cells were grown by streaking to single colonies on YPD agar plates (containing 1.0% yeast extract, 2.0% peptone, 2.0% dextrose, and 1.5% agar; pH 7.2) and incubation for 2 or 3 days at 30 °C. All the strains were stored in 35% glycerol at -80 °C. For the infection assays, a single colony was seeded in YPD liquid medium and incubated at 30 °C for 24 h with shaking (150 rpm). The culture was then centrifuged at 1000 x *g* for 5 min at room temperature and washed thrice with phosphate-buffered saline (PBS; 1X). Yeasts were counted in a hemocytometer, and the cell density of the suspension was adjusted to 1 x 10^7 cells/mL. Before infection, opsonization of yeast cells was performed in RPMI-1640 medium (Gibco) containing 20% fresh mouse serum at 37 °C in 150 rpm for 30 min.

2.3. Bone Marrow-derived Macrophages cultivation

Bone marrow-derived macrophages (BMDMs) were obtained, as previously described (33), by extracting the bone marrow from femurs and tibiae of 8 to 12 weeks old BALB/c mice

(Animal Center of the Institute of Biological Sciences - University of Brasilia) and culturing the cells *in vitro* on non-treated culture 100 mm Petri dishes, containing complete RPMI 1640 medium (Gibco) supplemented with 10% heat-inactivated fetal bovine serum (FBS; Gibco), 50 µg/mL of gentamicin, 50 µM 2-mercaptoethanol (Sigma-Aldrich) and 20 ηg/mL recombinant GM-CSF (PeproTech). The cultures were incubated for 8 days at 37 °C in a humidified 5% CO_2 atmosphere. Complete RPMI 1640 medium (10 mL) was added to the culture on day 3. On day 6, half of the volume was replaced by 10 mL fresh medium. On day 8, BMDMs were detached from the plates with the TrypLE™ Express reagent (Gibco) and collected.

BMDM cells were then centrifuged at 300 x *g* for 5 min and washed twice with PBS. The supernatant was discarded, and the cells were resuspended in PBS/2% FBS (blocking/washing solution) for 30 min to block non-specific antibody interactions. For macrophage surface markers identification, cells were incubated for 1 h with the monoclonal antibodies anti-CD11b, conjugated to the APC fluorophore (eBioscience), and anti-F4/80, conjugated to the PE fluorophore (Abcam), according to the manufacturer's instructions. As control for non-specific labeling, isotypic antibodies conjugated to APC were used. Subsequently, the cells were washed twice with a blocking/washing solution, acquired in the flow cytometer (BD FACSVerse™), and analyzed using the FlowJo software, version X. Around 85% of these cells expressed F4/80 and CD11b markers, which characterize bone marrow-derived macrophages (Additional information: **Figure A1**).

2.4. Host-pathogen interaction experiments

Approximately 5×10^4 BMDMs were plated onto each well of 96-well polystyrene microplates containing 100 µL of RPMI medium supplemented with 10% FBS. The cultures were incubated for 24 h at 37 °C in a humidified 5% CO_2 atmosphere. The supernatant was removed, and the cells were infected with 1×10^5 yeast cells previously opsonized with 20% mouse serum, using a multiplicity of infection of 2 (MOI = 2), in 100 µL of RPMI medium supplemented with 10% FBS. Phagocytosis assays were performed at 2-, 4-, 6-, and 24-hours post-infection (hpi). For the quantification of phagocytosis, cells were fixed and stained with a Fast Panoptic kit (Laborclin). Under an Axio Observer GmbH microscope (Carl Zeiss Microscopy), two hundred macrophages were counted per well to determine the number of macrophages that phagocytosed one or more yeasts, considering the total number of counted cells.

Fungal survival after the interaction with BMDMs was performed after 4 or 24 h of co-culture. After 4 h of incubation, the macrophages were washed with PBS to remove extracellular and loosely attached yeasts. Internalized yeast cells were released by macrophages lysis with 0.05% SDS and plating fungal cells in YPD agar for colony forming units counting. For the 24 h assay, supernatant and lysate were pooled together to contemplate non-lytic exocytosis.

For RNA extraction assays, approximately 1×10^6 BMDMs were plated onto each well in 6-well tissue culture plates containing 2 mL RPMI medium supplemented with 10% FBS and incubated at 37 °C in a humidified 5% CO_2 atmosphere for 24 h. The culture supernatant was removed, and 2×10^6 mouse serum opsonized yeast cells, in RPMI medium/10% FBS, were transferred to each well. The co-cultures were then incubated for 4 and 24 h at 37 °C in a humidified 5% CO_2 atmosphere. After 4 h, noninternalized yeast cells were removed by washes with PBS. For the 24 hpi assays, 2 mL of fresh pre-warmed RPMI medium/10% FBS were added to wells.

2.5. RNA extraction

After 4 and 24 h of infection, co-cultures were washed with PBS, and BMDMs total RNA was extracted by using the mirVana™ miR isolation kit (Ambion, LifeTechnologies), according to the manufacturer's instructions. The total RNA fraction, depleted of small RNAs (< 200 nt), and the miRNAs enriched fraction, were recovered in different tubes. The samples were stored at -20 °C, quantified by NanoDrop ND-2000 (NanoDrop technologies) and evaluated by Bioanalyzer 2100 (Agilent Technologies). All samples showed high quality and integrity (RNA Integrity Number - RIN > 9) (**Figure A2 and Table A1**).

2.6. High-throughput RNA-sequencing and transcriptomic data analysis

RNA-seq libraries were prepared by the rRNA negative selection and barcode technology, in order to generate 100-bp paired-end cDNA reads. RNA was sequenced by the Illumina HiSeq 2000 system (Macrogen Inc, Korea) using the standard Illumina protocol for high-throughput sequencing. Approximately 16 to 28 million paired reads were obtained for each library (**Table A1**).

The FASTQC software was employed for the sequenced reads quality determination (34,35). After clipping and trimming by the CUTADAPT software (36), the reads were mapped to the *Mus musculus* reference genome (GRCm38.74) using TopHat, and HTSeq software estimated the transcripts abundance in each sample (37,38). The differentially expressed genes

(DEG) were identified by the edgeR package, applying TMM library size normalization and likelihood ratio test, implemented in R version 5.1 (39). Transcripts present in low counts (CPM < 1) and not present in at least two libraries were removed from the analysis. The DEG cutoff criteria were a fold change level ≥ 2.0 and an adjusted *p*-value < 0.05. The false discovery rate (FDR) from obtained *p*-values was controlled by Benjamini-Hochberg algorithm (40).

2.7. Functional enrichment analysis

Differentially expressed genes were annotated with their gene ontology using data from org.Mm.eg.db R package and located within biochemical pathways. Genes considered differentially expressed were used for Gene Ontology and KEGG (Kyoto Encyclopedia of Genes and Genomes) (41) enrichment analysis by clusterProfiler (42). Only nodes with FDR-adjusted *p-value* < 0.05 were considered statistically significant, unless otherwise stated. The Simplify method from clusterProfiler was used to reduce the enriched GO terms redundancy. The inflammatory response score was determined by calculating the average expression of genes in the GO term inflammatory response (GO: 0006954), and the significance was calculated using a two-sided Wilcoxon test. Plots were produced in R using the package ggplot2.

2.8. Quantitative Real-Time Polymerase Chain Reaction

The mRNA levels of multiple genes related to the innate immunity were evaluated using RT-qPCR. After DNase I treatment (DNase I Amplification Grade, Invitrogen), total RNA was reverse transcribed from 500 ηg of total RNA employing the High-capacity cDNA reverse transcription kit (Applied Biosystems). The qPCR reactions were performed on a 7500-Fast thermal cycler (Applied Biosystems), with the fast SYBR-green PCR master mix (Applied Biosystems) following the manufacturer's instructions. The 40S ribosomal protein S9 gene (RPS9) served as housekeeping control. The fold change in co-cultures was compared to the control groups for 4 and 24 hpi, by the $2^{-\Delta\Delta Ct}$ method (43). The primers sequences are listed in **Table S1**.

2.9. Quantitative Real-Time PCR-Array for miRNA expression analysis

The RNA fractions enriched with small RNAs, obtained in the host-pathogen interaction experiments at 4 hpi, were evaluated for the expression of miRNAs. Small RNA samples were reverse transcribed from 25 ηg using the miScript II RT kit (Qiagen). The qPCR reactions were performed on a 7500-Fast thermal cycler (Applied Biosystems) with the Immunopathology miRNA PCR Array kit (SYBR® Green; Qiagen), following the manufacturer's instructions.

The MIMM-104Z plates, which allow the simultaneous analysis of 84 miRNAs differentially expressed in control and infection conditions, were employed. The miRNAs accumulation analysis was performed by relative quantification by the $2^{-\Delta\Delta Ct}$ method (43), employing SNORD95 and SNORD96A as constitutive internal controls. Enrichment analysis for molecular pathways was performed with the experimentally validated miRNA targets from TarBase v7.0 database. KEGG enrichment analysis was carried out through Diana Tools mirPath, applying Fisher's exact test and the *p*-value adjusted by FDR was reported (44).

2.10. Cytokines measurements

Host-pathogen interaction assays were performed, as previously described, to evaluate the macrophages responsiveness to the stimulus by *C. neoformans* yeasts or by LPS (100 ηg/mL; *Escherichia* coli O111:B4; positive control). The culture supernatants were recovered and centrifuged at 1000 x *g* for 5 min, transferred to Eppendorf tubes and stored at -80 ºC. Noninfected macrophage cultures were used as negative control. The levels of the cytokines *Tumor Necrosis Factor-alpha* (TNF-α) and *Interleukin 10* (IL10) in the co-culture supernatants were quantified by a capture enzyme-linked immunosorbent assay (ELISA; DuoSet® kit - R&Dsystems). The absorbance values were determined with the SpectraMax M5 (Molecular Devices) spectrophotometer and analyzed by the SoftMax 5.2 software. Cytokine concentrations were determined from a standard curve, following the manufacturer's recommendations.

2.11. Statistical analysis

Data are presented as the mean ± standard deviation (SD), unless otherwise stated. Three independent experiments were performed in technical triplicate. The multiple group comparisons were conducted by one-way analysis of variance (ANOVA), followed by the Dunnett's post-test. The comparison of proportions was performed by the Chi-square test. The *p*-value < 0.05 indicated statistically significant difference. The statistical analyses were conducted with the GraphPad Prism software, version 7.0.

3. Results

3.1. General aspects of host-pathogen interaction experiments

The present study focused on the interaction of bone marrow-derived macrophages with the *C. neoformans* strains B3501 (capsular) and *cap67Δ* (a B3501-derived acapsular mutant), characterizing differences in macrophages transcriptomic response to infection with each strain.

Initially, we analyzing the macrophages responsiveness to fungal strains by evaluating the phagocytic activity at 2-, 4-, 6-, and 24-hour post-infection (hpi) (**Figure 1A**). The phagocytosis rate increased from 80% at 2 hpi to 90% at 24 hpi for the B3501 strain. In contrast, no significant changes were observed for infection with Cap67 (92% phagocytosis rate throughout time). We defined the interaction time as 4 and 24 hpi for the subsequent experiments to represent the early- and late-stage responses between macrophages and fungal cells.

The fungicidal activity significantly differed between the B3501-infected and the Cap67-infected macrophages (**Figure 1B**). Fungal survival rate was higher for B3501 than for Cap67 at 4 and 24 hpi (p-value < 0.01). No major differences in the B3501 strain survival were detected between 4 and 24 hpi. A significant reduction in CFU counts was identified for Cap67 at 24 hpi (p-value < 0.05). Additionally, to confirm the macrophages activation, we quantified the cytokines TNF-α and IL10. An increment in TNF-α secretion by macrophages infected with both strains was verified (p-value < 0.01). The IL-10 secretion was not altered between strains (**Figure 1C, D**).

Principal Component Analysis (PCA) was used to generate a genome-wide overview of macrophages response to infection by *C. neoformans* B3501 and Cap67 strains, as well as for uninfected macrophages. At 4 hpi, the first principal component (PC1) separated uninfected cells from infected macrophages. The Cap67-infected group differed from uninfected and B3501 groups, corresponding to 87% of the variance (**Figure S1A**). This indicated that the B3501-infected group is transcriptionally more similar to the uninfected control than to the Cap67-infected group. Clear and distinct clusters were formed at 24 hpi, separating the infected and uninfected groups, thus suggesting that the variation in gene expression results from the interaction with yeast cells (82% of the variance in the PC1; **Figure S1B**). The second PC (PC2) separated macrophages infected by B3501 from the ones infected by the Cap67 strain (15% of the variance), indicating different responses elicited by each strain. One of the B3501-infected biological samples presented a quite different PCA and was excluded from the following analyses (**Figure S2**).

3.2. Differential gene expression analysis of macrophages infected by C. neoformans

To better understand transcriptional changes at the gene level, we used a differential gene expression analysis to identify the group of genes that were significantly modulated in response to the infection by each strain. Significantly differentially expressed genes (DEG) were defined as those with a fold-change threshold of $\geq \pm 2$ between the fungal-infected cells and the controls

and an adjusted *p*-value < 0.05 to control the false discovery rate (FDR). Considering this, at 4 hpi, a global DEG overview displayed different transcription patterns between macrophages infected by *C. neoformans* B3501 and Cap67 strains (**Figure 2A**). We identified 187 DEG in macrophages infected by B3501. Among these, 136 genes were upregulated and 51 downregulated. On the other hand, 957 and 458 genes were up and downregulated, respectively, upon infection with Cap67 (**Figure 2B**). The infection with B3501 evoked less genes related to innate immune, inflammatory responses and metabolic processes than the infection with Cap67 (**Figures 2C**). The B3501 pattern was more similar to the one of uninfected macrophages, while infection with Cap67 was characterized by an intense accumulation of several transcripts related to immune system processes.

At 24 hpi, we identified 2006 genes differentially expressed by macrophages after the infection with B3501, and 2058 upon the infection with Cap67 (**Figures 3A and 3B**). The infection by two strains presented 508 genes upregulated and 510 DEG downregulated in common (**Figure 3B**). Notably, there is less variation in the number of genes upregulated between the infection by two strains concerning to functional categories compared to 4 hpi (**Figure 3C**). At 24 hpi, there was an enrichment of categories related to immunity and a marked negative regulation for genes related to metabolic processes (**Figure 3C**).

The RNA-seq results were validated by RT-qPCR to assess transcript levels of several genes related to the immune response (*Tnf-α*, *Il10*, *Il1β*, *Cxcl10, Myd88*, *Ikbke*, *Stat1*, *Clec7a*, *Socs1*, and *Socs3*). As shown in **Figure S3**, the data of transcripts accumulation matched the transcription counts, supporting the RNA-seq results.

Based on the number of DEGs, the macrophages infected by the encapsulated (B3501) and the nonencapsulated mutant *cap67*Δ (Cap67) *C. neoformans* strains revealed differential transcriptional changes, in which infection with nonencapsulated strain inducing a higher reprogramming of macrophage transcriptome at 4 hpi. On the other hand, B3501-infected macrophages showed a mild activation response to the infection at the same time point. Interestingly, macrophages response to both strains was very similar at 24 hpi.

3.3. Comparison of macrophage transcriptomic profile between B3501 and Cap67 strains' infections

To better comprehend transcriptional differences of macrophages infected by B3501 or Cap67, the bidirectional transcripts fold changes were compared. At 4 hpi, a weak correlation between the infections with B3501 or Cap67 was observed (r = 0.53; *p* < 2.2e-16; **Figure 4A**).

The mean fold change (FC) was four times lower for macrophages infected with B3501 (FC = 1.3) in comparison to Cap67 (FC = 5.1). On the other hand, at 24 hpi, a high correlation (r = 0.78; p < 2.2e-16; **Figure 4B**) and similar mean fold change (2.1) was verified, indicating that the macrophages response to the infection by the different strains is more similar. A clear difference in the magnitude of the macrophage's response to B3501 or Cap67 was observed at earlier infection (p = 2.2e-16, Wilcoxon rank sum test), while a convergence in response occurred at longer interaction period (p = 0.2875, Wilcoxon rank sum test).

Most genes showed directionally consistent fold changes (n = 1166, 78.2% at 4 hpi; n = 2730, 89.9% at 24 hpi). Nevertheless, there were 326 genes at 4 hpi and 308 genes at 24 hpi that showed opposite fold changes (**Figure 4A and B**); that is, increased expression with B3501-infection and decreased expression with Cap67-infection, or vice versa.

Notably, several genes related to cell migration and inflammation displayed opposite directional gene expression. The CXC receptor 4 gene (*Cxcr4*) was highly upregulated in the macrophage's response to B3501-infection at 24 hpi, while it was downregulated upon infection with Cap67 (4 and 24 hpi) (45). After infection with B3501, the *Tnfsf8* gene, which encodes a cytokine related to the tumor necrosis factor ligand family (46), presented a shift from downregulated (4 hpi) to upregulated (24 hpi). Infection with Cap67 resulted in upregulation of this gene throughout the interaction period (**Figure 4**). The *Med12l* gene (mediator complex subunit 12-like), which is involved in transcriptional activation, was significantly downregulated in the B3501 infection model (4 hpi), but upregulated in the macrophage's infection by Cap67.

At 24 hpi, genes related to different biological processes, including cell proliferation and migration (*Rassf10*) (47), immune response (*Dusp18*) (48), metabolism (*Vnn3*, *Rcn1*), cell growth and wound healing (*Dcbld2*), and non-coding RNA species (*Rnu3b1*) showed opposite directional gene expression in both infection models. The genes *Vnn3* and *Rassf10* were upregulated after macrophages infection with B3501 and downregulated by Cap67-infection. Likewise, the genes *Dcbld2*, *Dusp18*, *Rcn1*, and *Rnu3b1* were downregulated in macrophages response to B3501-infection, but upregulated by Cap67-infection (**Table S2**).

It was also observed that the Toll-like receptor 2 gene (*Tlr2*) was downregulated in B3501-infected macrophages, while *Tlr3* was upregulated only at 24 hpi. In Cap67-infected macrophages the *Tlr2*, *Tlr3*, and *Tlr7* encoding genes were upregulated. These genes are crucial for recognizing pathogens and initiating the responses by phagocytic cells.

Several key genes for the regulation of innate and adaptive immune responses and inflammatory activation, such as *Myd88*, *Nlrp3*, *Aim2*, *Gsdmd*, including chemokines (*Ccl*3), cytokines (*Tnf*, *Il6*), caspases *Casp1*, *Casp4*, *Casp8*, and the transcription factors *NF-κB1* (p50/p105) and *NF-κB2* (p52/p100), were upregulated exclusively in Cap67-infected macrophages at 4 hpi (**Table S2**). The expression of the other proinflammatory genes (*Il1β*, *Il18*, and *Ccl*2) were strongly induced (FC > 6) in this condition.

The expression of iNOS (inducible nitric oxide synthase 2; *Nos2*) and arginase (*Arg1*) genes, which encode enzymes related to the macrophages microbicidal potential, was increased by the infection with both strains. Nevertheless, a lower *Nos2-Arg1* (4,2) ratio was observed in macrophages infected by B3501 at 4 hpi in comparison to Cap67-infection (177,6). The *Nos2* and *Arg1* genes expression increased at the same proportion at 24 hpi for the B3501 strain-infection, leading to a *Nos2-Arg1* ratio (4,2) similar to the early stage of infection (**Table S2**).

The increase in specific gene expression associated with an inflammatory activity after *C. neoformans* infection demonstrates that the interaction with the fungal yeast stimulates this process. To assess the level of inflammation triggering, we calculated each strain's infection score. All the experimental conditions displayed an upregulation in the inflammatory response score, with Cap67 at 4 hpi showing the highest inflammatory response score (**Figure 4C**). No significant differences between the macrophage's response to B3501 and Cap67 was observed at 24 hpi.

Altogether, these results indicate that macrophages in interaction with *C. neoformans* showed specific transcriptional profiles related to the infection by each strain at 4 hpi. This transcriptional profile was associated with decreased inflammation and cytotoxic activity when infected by encapsulated (B3501) yeast, suggesting that *C. neoformans* capsule might activate specific mechanisms to avoid the activation of inflammasomes in macrophages.

3.4. Comparative functional enrichment analysis of differentially expressed genes from macrophages in response to C. neoformans

GO enrichment analysis

We next performed gene ontology (GO) and KEGG enrichment analysis to assesses whether the strain-related modulated genes in infected macrophages converged to the same biological functions. The enrichment analyses were performed for the 1494 DEGs at 4 hpi and 3046 DEG at 24 hpi, based on the annotations of GO biological processes category (Figures 5 and 6; adjusted *p*-value < 0.01) and KEGG pathways (Figure 7; adjusted *p*-value < 0.05). We found

132 enriched terms after B3501-infection and 129 terms in Cap67-infection. Thirty-nine terms were enriched for upregulated genes in both infection conditions, but no overlapping pathways for downregulated genes were detected at 4 hpi. The most divergent result for the GO analysis was the exclusive enrichment of terms related to the adaptive immune response, including antigen processing and presentation of endogenous peptide antigen via MHC class Ib and via ER pathway (GO:0002476 and GO:0002484; p < 7.42e-10), lymphocyte mediated immunity (GO:0002449; p = 6.98e-11), and regulation of T cell activation (GO:0050863; p < 1.10e-06) in macrophages infected with Cap67 strain (**Figure 5**).

At 24 hpi, there was a lower number of GO terms enriched for the B3501-infection (n = 112 terms) than for Cap67-infection (n = 161 terms). Seventy-eight terms were similarly upregulated. For macrophages infected with B3501, terms related to immune response were enriched, such as positive regulation of lymphocyte chemotaxis (GO:0140131; p = 5.06e-3), interferon-gamma production (GO:0032609; p = 4.32e-6), and mononuclear cell proliferation (GO:0032943; p = 1.22e-7) (**Figure 6**). On the other hand, some terms were enriched in the Cap67-infection: antimicrobial humoral immune response mediated by antimicrobial peptide (GO:0061844; p = 1.07e-4), interferon-alpha production (GO:0032607; p = 2.99e-3), and cytokine production involved in immune response (GO:0002367; p = 3.95e-5).

The GO analysis demonstrates different functional modules dominated by a large number of genes involved on a core of inflammatory/adaptive response's processes, which are significantly over-represented. Appealingly, the response to hypoxia (GO:0001666; $p \leq$ 1.76e-4) was only enriched in the B3501 infection model (**Figure 5 and 6**). Similarly, regulation of pattern recognition receptor signaling pathway (GO:0062207; p = 3.44e-3), processes involved in production and in cellular response to interferons (GO:0032609 and GO:0035458; $p \leq$ 2.11e-9), and processes related to antigen presentation via MHC class I (GO:0002476 and GO:0002484; p = 7.42e-10) were enriched just upon Cap67-infection at 4 hpi (**Figure 5**).

KEGG enrichment analysis

We next explored the biological implications of upregulated and downregulated DEGs through KEGG pathway enrichment analysis for both infection models. The signaling pathways (SPs) commonly enriched by upregulated genes at 4 hpi were TNF (mmu04668; p < 1.08e-6), IL-17 (mmu04657; p < 1.57e-6) and NOD-like receptor (mmu04621; p < 4.83e-4) (**Figure 7A**; **Table S3**). However, these pathways displayed a lower mean of $\log_2$ of fold change for the genes of core enrichment in response to infection by B3501 (FC = 1.06, FC = 1.21 and FC =

0.79) than by Cap67 (FC = 2.63, FC = 2.68 and FC = 2.52) (**Figure 7B**). Interestingly, the MAPK SP (mmu04010; p = 3.35e-5) was only activated in macrophages upon infection by B3501. Antigen processing and presentation pathway (mmu04612; p = 1.06e-4) was activated just by the Cap67-infection. These enriched pathways were in agreement with GO analysis (**Figure 7C**).

In the enrichment analysis for 24 hpi, several pathways were activated in macrophages upon infection by both strains. The cytokine-cytokine receptor interaction pathway (mmu04060; p < 1.63e-5) exhibited a lower mean of fold change for the B3501-infection (FC = 1.89) than for Cap67 (FC = 2.57). A similar result was observed for the antigen processing and presentation pathway (mmu04612; p < 5.54e-3; B3501-FC = 1.56; Cap67-FC = 1.99) (**Figure 7B and C**). Downregulated genes enriched multiple pathways involved in mismatch repair (mmu03430; p < 3.11e-3) and DNA replication (mmu03030; p < 1.80e-4) at both time frames. Contrarily, downregulated genes by infection with Cap67 did not show any enriched pathway (**Figure 7C**).

Interestingly, the Hif-1 signaling pathway (mmu04066; p < 1.02e-8) was ranked in the top-3 score of enriched pathways by upregulated genes only in B3501-infected macrophages (**Figure 7**). Cytosolic DNA-sensing (mmu04623; p < 8.42e-7), phagosome (mmu04145; p < 8.15e-4) and RIG-I-like receptor signaling pathway (mmu04622; p < 4.74e-3) were enriched by upregulated genes exclusively upon Cap67 infection for both interaction periods (**Figure 7C**; **Table S3**).

Activated pathways that were enriched in macrophages at 4 hpi displayed a lower fold change in the infection with B3501 than Cap67. The NF-kappa B (mmu04064; p < 2.66e-8; B3501-FC = 0.88; Cap67-FC = 1.89) and C-type lectin receptor (mmu04625; p < 6.23e-14; B3501-FC = 0.85; Cap67-FC = 2.20) signaling pathways illustrate this observation (**Figure 7; Table S3**).

Relevant pathways for an appropriated immune response to fungal infections were enriched for all the experimental conditions. The highest mean of fold change was verified for Cap67-infection at 4 hpi. Among them, the TNF signaling (mmu04668; p < 9.72e-4; B3501-FC = 1.06; Cap67-FC = 2.91), cytokine-cytokine receptor interaction (mmu04060; p < 3.30e-5; B3501-FC = 1.07; Cap67-FC = 2.91) and NOD-like receptor signaling pathways (mmu04621; p < 2.42e-5; B3501-FC = 0.79; Cap67-FC = 2.52).

KEGG-based analysis also revealed several enriched pathways associated to immune response in both infection's models. Nonetheless, the activation was more intense upon Cap67-

stimulation, particularly at 4 hpi, for the phagosome, cytosolic DNA-sensing, RIG-I-like receptor, and antigen processing and presentation pathways. The results above indicate that the two distinct strains evoke different transcriptional responses at the shorter interaction period, but a more similar pattern later on.

3.5. MicroRNAs expression profile in macrophages upon infection by C. neoformans capsulated and nonencapsulated strains

Next, we profiled the miRNAs that were modulated in the macrophage's interaction with *C. neoformans* strains at 4 hpi. Thus, we performed a miRNAs PCR array. We identified 21 miRNAs with significant differential expression in B3501-infection and three miRNAs in Cap67-infection, in comparison to the control condition (fold change $\geq \pm 2$ and p-value < 0.05; **Figure 8A and B**; **Table S4**). Interestingly, none of the 84 different miRNAs evaluated presented negative regulation on infected macrophages.

The expression of miR-155 (FC = 5.73; $p < 1.51e\text{-}3$) and miR-147 (FC = 5.63; $p < 2.01e\text{-}3$) were increased noticeably upon infection by B3501 (**Figure 8C**). The accumulations of miR-493 (FC = 3.00; $p < 9.84e\text{-}3$) and miR-30b (FC = 2.02; $p < 1.04e\text{-}2$) with B3501 infection were lower in comparation to Cap67 (miR-493: FC = 3.60; $p < 1.10e\text{-}3$; miR-30b: FC = 2.51; $p < 8.53e\text{-}5$). In addition, the expression of miR-493, -147 and -30b was upregulated in macrophages upon infection by each strain, when compared to the noninfected control.

In order to investigate the biological processes regulated by differentially expressed miRNAs in macrophages after *C. neoformans* infection, we selected the TarBase v7.0 database for the identification of the gene targets. This data base comprises only target genes which were experimentally investigated and proved to be modulated by the upregulation of miRNAs. We performed a KEGG enrichment analysis for the target genes of all miRNAs differentially expressed upon the infection by *C. neoformans*, in order to identified molecular pathways that could be altered. We identified statistically significant pathways related to inflammatory/immune response, such as endocytosis (mmu04144; $p < 8.24e\text{-}8$), T cell receptor (mmu04660; $p < 9.50e\text{-}4$), and TGF-beta signaling pathways (mmu04350; $p < 2.47e\text{-}3$). Intracellular signal transduction signaling pathways, including MAPK (mmu04010; $p < 9.43e\text{-}4$), and ErbB signaling pathway (mmu04012; $p < 7.19e\text{-}4$) were also enriched (**Figure 8D**). These pathways were also identified as targets for miR-155.

We focused on the miR-155 target genes for their extensively reported role in regulating the immune response (49–51). To verify whether this differentially expressed mature miRNA was

indeed modulated by *C. neoformans* infection, we conducted a qPCR experiment with miR-155 specific probes. The results confirmed a significant upregulation of miR-155 in macrophages infected by the B3501 strain (**Figure S4**). We then compared the expression of some relevant genes from the data set of differentially expressed genes between macrophages infected by B3501- and Cap67-strains. Inflammation process-related genes previously confirmed as direct targets of miR-155 (52,53), such as *Ikbke*, *Myd88*, and *Bach1* presented ~2.59 lower fold change in macrophages infected with B3501, when compared to Cap67-infection (**Table S2**). Post-transcriptional inhibition of these genes may be related to the miR-155 upregulation verified in macrophages infected by B3501 strain. Thus, miR-155 may dampen the pro-inflammatory gene expression in our infection model of the encapsulated strain. Our results indicated that the infection by the encapsulated strain B3501 activates a microRNA processing machinery, limiting the pro-inflammatory response in macrophages.

4. Discussion

In this work, we focused on comparing differences in the transcriptional response of BMDMs to the infection by *C. neoformans* encapsulated (B3501) and nonencapsulated (Cap67) strains. The capsule is a prominent virulence factor that shields *C. neoformans* from immune-mediated recognition and destruction (54). Several works explore the immunoregulatory properties of glucuronoxylomannan (GXM), the main capsular component that inhibits the T-cells responses (55–58). We analyzed the transcriptional landscape of macrophages' response to the capsular B3501 or acapsular mutant *cap67*Δ strains and identified different transcriptomic patterns for genes involved in the immune response.

Myeloid cells, including macrophages and dendritic cells, promote antigen presentation and inflammatory processes. In our transcriptomic results, the enrichment of pathways related to positive and negative regulation of mononuclear cells proliferation and innate immune response indicated that monocyte differentiation is restrained by infection with B3501 strain, primarily after 4 hpi. This impairment in innate and adaptive response against the infection is evidenced by the weakening of pathways, in terms of gene expression levels, associated with pattern recognition receptors, cytosolic DNA sensing, and antigen presentation. Upon B3501 infection, transcription factors of the EGR family members (*Egr*2), which negatively regulates the differentiation and inflammatory activation of myeloid cells were upregulated (59). Contrarily to the early stage of B3501-infection response, Cap67-infection was associated with the

upregulation of several inflammatory genes, including *Tnf*, *Il6*, *Il18*, *Ccl2*, *Ccl3*, and *Ccl12* (**Table S2**).

As previously demonstrated, in the differentiation/activation of macrophages the enzyme nitric oxide synthase II (NOS2) induction leads to the nitric oxide (NO) synthesis, which is vital for fungal killing inside of macrophages (60). In contrast, the expression of the enzyme arginase (ARG) is linked to the reduction of NO production and fungal survival (61). The microbicidal potential of activated macrophages is associated with the differential regulation of these enzymes (61). In this regard, we described an increased *Nos2* and *Arg1* transcript expression in both infection models. Nevertheless, *Nos2*/*Arg1* expression ratio at 4 hpi was significantly lower in macrophages infected by B3501 than by Cap67, suggesting that macrophages infected by the encapsulated strain presented a less pronounced activation. Furthermore, this effector mechanism is mostly triggered in a pro-inflammatory milieu with cytokines such as IFN-γ, TNF-α, and IL6 (62). These cytokines also help in mediating the protection against *C. neoformans* at the early stages of infection (63). However, in our data, macrophages infected by the encapsulated strain did not show increased *Tnf* and *Il6* gene expression associated with an inflammatory state, suggesting that cells were not properly activated.

Inflammasomes are cytosolic multiprotein complexes known as key inflammatory signaling platforms for the host defense mechanisms against pathogens (64). In this study, we found a robust proinflammatory response on macrophages after interaction with Cap67. This is mainly evidenced by the increase in NLRP3 inflammasome transcript and higher *Il-1β* and *Il18* mRNA levels. These cytokines are essential for the Th1/Th17 polarization and optimal activation of the macrophages' antifungal activity (65). Furthermore, the *Casp1* and *Casp4* genes expression levels were significantly upregulated by Cap67 at 4 hpi, when compared to B3501 infection. This probably impacts on the caspase activation and the cleavage of inactive IL-1*β* and IL18 precursors. The lower upregulation of those genes suggests that the B3501 *C. neoformans* strain employs specific mechanisms to avoid inflammasome activation in macrophages. Previously, the acapsular mutant strain *cap59*Δ was reported to activate the NLRP3 inflammasome, indicating that the capsule may directly or indirectly prevent the recognition of the fungus by the host NLRP3 inflammasome (66).

Recently, experiments with conditioned medium from B3501 and Cap67 cultures demonstrated that small molecules secreted by both these strains could modify the activation of the intracellular inflammasome pathway (67). This alters critical functions, such as

phagocytosis and intracellular killing, thus affecting the macrophages' protective response to infection. These results suggest that GXM alone is not sufficient to promote inflammasome inhibition (67).

Both infection models shared several upregulated biological categories, although some processes closely related to adaptive immune response were only activated in the infection by the nonencapsulated strain. This divergence was more prominent in the early stages of infection than for the later stages (**Figures 5 and 6**). For example, lymphocyte-mediated immunity, antigen processing and presentation, and T-cell activation categories were not enriched at the early time point in the encapsulated strain infection. Surprisingly, these or related functional categories were enriched in the latter stage of both infection models. It is possible that the capsule protects *C. neoformans* by delaying macrophages' immune response. In agreement to this, Neal *et al*. (2017) previously observed a delayed inflammatory response on a model of murine central nervous system infection by *Cryptococcus*.

The cellular immune system plays a crucial role in eradicating cryptococcal infections (7). Macrophages and dendritic cells are involved in the antigen presentation to the T cells and in the expression of costimulatory molecules (69). Nevertheless, the interaction between the antigen-presenting cells MHC-bound peptides and T cell receptors is insufficient for lymphocyte activation. The costimulatory molecules are required for a complete activation (69,70). Remarkably, *C. neoformans* infection is characterized by the depression of the immune system, affecting mainly those individuals with impaired pro-inflammatory responses. Previously, clinical and experimental data indicated that T-cell-mediated immunity, predominantly $CD4^+$ T lymphocytes, is necessary to effectively control cryptococcal infection (71–74).

Glucuronoxylomannan (GXM) has consistently been linked to the direct inhibition of T cell proliferation, or to the interference with the antigen uptake or processing. So, it improves the *C. neoformans* virulence and survival upon attack by variety of host immune cells (56).

In our model, we observed a delayed triggering of regulation of T cell activation category (**Figure 5 and 6**; upregulated genes in GO:0050863 pathway) upon macrophages stimulation with B3501, which occurred only at 24 hpi. On the other hand, this triggering was already observed at 4 hpi with Cap67. Supporting this, an increased expression of co-stimulatory molecules, like CD40 and CD86, was particularly verified in macrophages infected with Cap67 at 4 hpi. These molecules induce the proliferation of T cells in general and enhance the

generation of cytolytic T cells. Microbial pathogens can also negatively modulate the antigen-presenting cells function, leading to a defective maturation process that impairs the expression of costimulatory molecules (20,75).

Over the past decade, many studies focused the investigation of the roles of miRNAs in the regulation of the immune system after fungal infections (76). By inhibiting the translation of particular genes, microRNAs can rapidly intensify the host cells inflammatory responses to fungal infections (77). Nonetheless, we might consider that this gene regulation process is highly complex, and that miRNAs profiles may vary among cell types and pathogenic stimuli.

In this work, we observed significant differences in the qPCR array analysis of miRNA expression profiles between macrophages infected by encapsulated and nonencapsulated *C. neoformans* strains. Twenty-one miRNAs, specially miR-155, were upregulated upon encapsulated yeasts stimulation (**Figure 8**). Similar results were observed for the stimulation of different phagocytic cells by *Aspergillus fumigatus*, *Candida albicans*, and *C. neoformans* WN148 (51,78–81). These findings suggest that the upregulation of miR-155 is a common feature of the phagocyte's response to the infection by pathogenic fungi. Additional *in silico* analyses indicated that miR-155 is involved in the regulation of endocytosis, T-cell receptor, and TGF-beta and MAPK signaling pathways.

miR-155 evokes distinct responses in different cell types, tissues, physiological situations, and individual targets. Sometimes these responses are contradictory (82). A previously study reported the early expression of miR-155 in macrophages infected by *Mycobacterium tuberculosis*. This expression led to the transcriptional silencing of host protective genes, thus favoring the establishment of the infection. The miRNA-155 inhibition impaired the pathogen survival within macrophages (83). The negative regulation of inflammatory response by miR-155 was also described for other microbial infections, including *C. albicans*, by targeting keys molecules in inflammatory signaling pathways, including NF-κB p65, BCL10, MyD88, TAB2, IRAK1, and TARF6 (51,52,80,84).

We also described a clear difference in the macrophages miRNA profiles upon infection by encapsulated or nonencapsulated *C. neoformans* strains. Several Toll-like receptors were upregulated in macrophages infected by the Cap67 strain. These receptors are frequently associated with the activation of miRNAs expression (85–88).

In summary, we employed high-throughput approaches to identify transcriptome-level differences in macrophages infected by two *C. neoformans* strains. Our results show strain-

specific patterns of gene expressions during the infection and suggest that the adequate innate and adaptive immune response is delayed in the encapsulated-infected macrophages. This delay can improve the pathogen adaptation within the host, allowing the activation of the virulence factors necessary for a successful infection. Furthermore, we demonstrated the cryptococcal strain-specific miRNA expression patterns in macrophages. These data may reveal hitherto unknown gene regulation patterns in macrophages after cryptococcal infection that are potentially important to their function and defense mechanisms. Further experimental studies should explore and assess the differences observed in these transcriptomic landscapes, especially regarding antigen processing and presentation, as well as the miRNAs' role, particularly miR-155, on the phagocytosis process.

5. References

1. Dhandapani K, Sivarajan K, Ravindhiran R, Sekar JN. Fungal Infections as an Uprising Threat to Human Health: Chemosensitization of Fungal Pathogens With AFP From Aspergillus giganteus. Front Cell Infect Microbiol [Internet]. 2022 May 25 [cited 2022 Dec 15];12. Available from: https://pubmed.ncbi.nlm.nih.gov/35694549/
2. Dangarembizi R, Wasserman S, Hoving JC. Emerging and re-emerging fungal threats in Africa. Parasite Immunol [Internet]. 2022 [cited 2022 Dec 15]; Available from: https://pubmed.ncbi.nlm.nih.gov/36175380/
3. Ibe C, Okoye CA. Integrated healthcare approach can curb the increasing cases of cryptococcosis in Africa. PLoS Negl Trop Dis [Internet]. 2022 Aug 1 [cited 2022 Dec 15];16(8):e0010625. Available from: /pmc/articles/PMC9409514/
4. Kwon-Chung KJ, Fraser JA, Doering TÁL, Wang ZA, Janbon G, Idnurm A, et al. Cryptococcus neoformans and Cryptococcus gattii, the etiologic agents of cryptococcosis. Cold Spring Harb Perspect Med [Internet]. 2015 [cited 2022 Dec 15];4(7). Available from: https://pubmed.ncbi.nlm.nih.gov/24985132/
5. Rajasingham R, Govender NP, Jordan A, Loyse A, Shroufi A, Denning DW, et al. The global burden of HIV-associated cryptococcal infection in adults in 2020: a modelling analysis. Lancet Infect Dis [Internet]. 2022 Dec [cited 2022 Dec 15];22(12). Available from: https://pubmed.ncbi.nlm.nih.gov/36049486/
6. Fa Z, Xu J, Yi J, Sang J, Pan W, Xie Q, et al. TNF-α-Producing Cryptococcus neoformans Exerts Protective Effects on Host Defenses in Murine Pulmonary Cryptococcosis. Front Immunol [Internet]. 2019 [cited 2022 Dec 15];10:1725. Available from: https://pubmed.ncbi.nlm.nih.gov/31404168/
7. Leopold Wager CM, Hole CR, Wozniak KL, Wormley FL. Cryptococcus and phagocytes: Complex interactions that influence disease outcome. Front Microbiol. 2016;7(FEB):1–16.
8. Osterholzer JJ, Chen GH, Olszewski MA, Zhang YM, Curtis JL, Huffnagle GB, et al. Chemokine receptor 2-mediated accumulation of fungicidal exudate macrophages in mice that clear cryptococcal lung infection. Am J Pathol [Internet]. 2011 [cited 2022 Dec 15];178(1):198–211. Available from: https://pubmed.ncbi.nlm.nih.gov/21224057/
9. Chen Y, Shi ZW, Strickland AB, Shi M. Cryptococcus neoformans Infection in the Central Nervous System: The Battle between Host and Pathogen. J fungi (Basel, Switzerland) [Internet]. 2022 Oct 1 [cited 2022 Dec 15];8(10). Available from: https://pubmed.ncbi.nlm.nih.gov/36294634/
10. Nelson BN, Daugherty CS, Sharp RR, Booth JL, Patel VI, Metcalf JP, et al. Protective interaction of human phagocytic APC subsets with Cryptococcus neoformans induces genes associated with metabolism and antigen presentation. Front Immunol [Internet]. 2022 Nov 15 [cited 2022 Dec 15];13:1054477. Available from: /pmc/articles/PMC9709479/
11. Wormley FL, Perfect JR, Steele C, Cox GM. Protection against cryptococcosis by using a murine gamma interferon-producing Cryptococcus neoformans strain. Infect Immun [Internet]. 2007 Mar [cited 2022 Dec 15];75(3):1453–62. Available from: https://pubmed.ncbi.nlm.nih.gov/17210668/
12. Dromer F, Ronin O, Dupont B. Isolation of cryptococcus neoformans var. Gattii from an asian patient in France: Evidence for dormant infection in healthy subjects. Med Mycol [Internet]. 1992 [cited 2022 Dec 15];30(5):395–7. Available from: https://pubmed.ncbi.nlm.nih.gov/1469541/
13. Ristowi LC, Davisi JM. The granuloma in cryptococcal disease. PLoS Pathog [Internet]. 2021 Mar 1 [cited 2022 Dec 15];17(3). Available from: https://pubmed.ncbi.nlm.nih.gov/33735307/
14. García-Rodas R, Zaragoza O. Catch me if you can: Phagocytosis and killing avoidance by Cryptococcus neoformans. FEMS Immunol Med Microbiol. 2012;64(2):147–61.
15. Saha DC, Goldman DL, Shao X, Casadevall A, Husain S, Limaye AP, et al. Serologic evidence for reactivation of cryptococcosis in solid-organ transplant recipients. Clin Vaccine Immunol [Internet]. 2007 Dec [cited 2022 Dec 15];14(12):1550–4. Available from: https://pubmed.ncbi.nlm.nih.gov/17959819/
16. Vecchiarelli A. Immunoregulation by capsular components of Cryptococcus neoformans. Med Mycol [Internet]. 2000 Jan [cited 2022 Dec 15];38(6):407–17. Available from: https://pubmed.ncbi.nlm.nih.gov/11204878/
17. Gates-Hollingsworth MA, Kozel TR. Phenotypic heterogeneity in expression of epitopes in the Cryptococcus neoformans capsule. Mol Microbiol [Internet]. 2009 Oct [cited 2022 Dec 15];74(1):126–38. Available from:

https://pubmed.ncbi.nlm.nih.gov/19758241/

18. McFadden DC, De Jesus M, Casadevall A. The physical properties of the capsular polysaccharides from Cryptococcus neoformans suggest features for capsule construction. J Biol Chem [Internet]. 2006 Jan 27 [cited 2022 Dec 15];281(4):1868–75. Available from: https://pubmed.ncbi.nlm.nih.gov/16278213/

19. Sebolai OM, Pohl CH, Botes PJ, Strauss CJ, Van Wyk PWJ, Botha A, et al. 3-Hydroxy fatty acids found in capsules of Cryptococcus neoformans. Can J Microbiol [Internet]. 2007 Jun [cited 2022 Dec 15];53(6):809–12. Available from: https://pubmed.ncbi.nlm.nih.gov/17668042/

20. Monari C, Bistoni F, Casadevall A, Pericolini E, Pietrella D, Kozel TR, et al. Glucuronoxylomannan, a microbial compound, regulates expression of costimulatory molecules and production of cytokines in macrophages. J Infect Dis [Internet]. 2005 Jan 1 [cited 2022 Dec 15];191(1):127–37. Available from: https://pubmed.ncbi.nlm.nih.gov/15593014/

21. Zaragoza O, Chrisman CJ, Castelli MV, Frases S, Cuenca-Estrella M, Rodríguez-Tudela JL, et al. Capsule enlargement in Cryptococcus neoformans confers resistance to oxidative stress suggesting a mechanism for intracellular survival. Cell Microbiol [Internet]. 2008 Oct [cited 2019 Sep 12];10(10):2043–57. Available from: http://doi.wiley.com/10.1111/j.1462-5822.2008.01186.x

22. Vecchiarelli A, Pietrella D, Lupo P, Bistoni F, McFadden DC, Casadevall A. The polysaccharide capsule of Cryptococcus neoformans interferes with human dendritic cell maturation and activation. J Leukoc Biol [Internet]. 2003 Sep [cited 2022 Dec 15];74(3):370–8. Available from: https://pubmed.ncbi.nlm.nih.gov/12949240/

23. Mershon-Shier KL, Vasuthasawat A, Takahashi K, Morrison SL, Beenhouwer DO. In vitro C3 deposition on Cryptococcus capsule occurs via multiple complement activation pathways. Mol Immunol [Internet]. 2011;48(15–16):2009–18. Available from: http://dx.doi.org/10.1016/j.molimm.2011.06.215

24. Nakamura K, Kinjo T, Saijo S, Miyazato A, Adachi Y, Ohno N, et al. Dectin-1 is not required for the host defense to Cryptococcus neoformans. Microbiol Immunol [Internet]. 2007 [cited 2022 Dec 15];51(11):1115–9. Available from: https://pubmed.ncbi.nlm.nih.gov/18037789/

25. Casadevall A, Coelho C, Cordero RJB, Dragotakes Q, Jung E, Vij R, et al. The capsule of Cryptococcus neoformans. Virulence [Internet]. 2019 Jan 1 [cited 2022 Dec 15];10(1):822–31. Available from: https://pubmed.ncbi.nlm.nih.gov/29436899/

26. Van Duin D, Casadevall A, Nosanchuk JD. Melanization of Cryptococcus neoformans and Histoplasma capsulatum reduces their susceptibilities to amphotericin B and caspofungin. Antimicrob Agents Chemother [Internet]. 2002 Nov [cited 2022 Dec 15];46(11):3394–400. Available from: /pmc/articles/PMC128748/

27. Wang Y, Pawar S, Dutta O, Wang K, Rivera A, Xue C. Macrophage Mediated Immunomodulation During Cryptococcus Pulmonary Infection. Front Cell Infect Microbiol [Internet]. 2022 Mar 24 [cited 2022 Dec 15];12. Available from: /pmc/articles/PMC8987709/

28. Fromtling RA, Shadomy HJ, Jacobson ES. Decreased virulence in stable, acapsular mutants of Cryptococcus neoformans. Mycopathologia [Internet]. 1982 [cited 2019 Sep 11];79(1):23–9. Available from: http://link.springer.com/10.1007/BF00636177

29. Chang YC, Kwon-Chung KJ. Complementation of a capsule-deficient mutation of Cryptococcus neoformans restores its virulence. Mol Cell Biol [Internet]. 1994 Jul [cited 2022 Dec 15];14(7):4912–9. Available from: https://pubmed.ncbi.nlm.nih.gov/8007987/

30. O'Meara TR, Norton D, Price MS, Hay C, Clements MF, Nichols CB, et al. Interaction of Cryptococcus neoformans Rim101 and protein kinase a regulates capsule. PLoS Pathog [Internet]. 2010 Feb [cited 2022 Dec 15];6(2). Available from: https://pubmed.ncbi.nlm.nih.gov/20174553/

31. CONCEA. Normativas do CONSELHO NACIONAL DE CONTROLE DE EXPERIMENTAÇÃO ANIMAL (CONCEA) [Internet]. Brasília, Brasil; 2016. Available from: https://www.ceua.ufv.br/wp-content/uploads/2018/08/NORMATIVAS-DO-CONCEA-3ª-EDIÇÃO2.pdf

32. Jacobson ES, Ayers DJ, Harrell AC, Nicholas CC. Genetic and phenotypic characterization of capsule mutants of Cryptococcus neoformans. J Bacteriol [Internet]. 1982 Jun [cited 2019 Aug 11];150(3):1292–6. Available from: http://www.ncbi.nlm.nih.gov/pubmed/7042689

33. Lutz MB, Kukutsch N, Ogilvie AL., Rößner S, Koch F, Romani N, et al. An advanced culture method for generating large quantities of highly pure dendritic cells from mouse bone marrow. J Immunol Methods

[Internet]. 1999;223(1):77–92. Available from: http://www.sciencedirect.com/science/article/pii/S002217599800204X

34. Cock PJA, Fields CJ, Goto N, Heuer ML, Rice PM. The Sanger FASTQ file format for sequences with quality scores, and the Solexa/Illumina FASTQ variants. Nucleic Acids Res [Internet]. 2010 [cited 2020 Jul 14];38(6):1767–71. Available from: http://www.bioruby.org

35. Andrews S, Krueger F, Seconds-Pichon A, Biggins F, Wingett S. FastQC. A quality control tool for high throughput sequence data. Babraham Bioinformatics [Internet]. Babraham Bioinformatics; 2015 [cited 2019 Aug 17]. Available from: https://www.bioinformatics.babraham.ac.uk/projects/fastqc/

36. Martin M. Cutadapt removes adapter sequences from high-throughput sequencing reads. EMBnet.journal [Internet]. 2011 May 2 [cited 2019 Aug 17];17(1):10. Available from: http://journal.embnet.org/index.php/embnetjournal/article/view/200

37. Kim D, Pertea G, Trapnell C, Pimentel H, Kelley R, Salzberg SL. TopHat2: Accurate alignment of transcriptomes in the presence of insertions, deletions and gene fusions. Genome Biol [Internet]. 2013;14(4):R36. Available from: http://genomebiology.com/2013/14/4/R36

38. Anders S, Pyl PT, Huber W. HTSeq-A Python framework to work with high-throughput sequencing data. Bioinformatics [Internet]. 2015 Jan 15 [cited 2019 Aug 17];31(2):166–9. Available from: http://www.ncbi.nlm.nih.gov/pubmed/25260700

39. Robinson MD, McCarthy DJ, Smyth GK. edgeR: A Bioconductor package for differential expression analysis of digital gene expression data. Bioinformatics [Internet]. 2010 Jan 1 [cited 2019 Aug 17];26(1):139–40. Available from: https://academic.oup.com/bioinformatics/article-lookup/doi/10.1093/bioinformatics/btp616

40. Benjamini Y, Hochberg Y. Controlling the False Discovery Rate: A Practical and Powerful Approach to Multiple Testing. J R Stat Soc Ser B [Internet]. 1995 Jan 1 [cited 2020 Jul 17];57(1):289–300. Available from: https://rss.onlinelibrary.wiley.com/doi/full/10.1111/j.2517-6161.1995.tb02031.x

41. Ogata H, Goto S, Sato K, Fujibuchi W, Bono H, Kanehisa M. KEGG: Kyoto encyclopedia of genes and genomes. Nucleic Acids Res [Internet]. 1999 Jan 1 [cited 2022 Dec 15];27(1):29–34. Available from: https://pubmed.ncbi.nlm.nih.gov/9847135/

42. Yu G, Wang LG, Han Y, He QY. ClusterProfiler: An R package for comparing biological themes among gene clusters. Omi A J Integr Biol [Internet]. 2012 May 1 [cited 2020 Jul 17];16(5):284–7. Available from: /pmc/articles/PMC3339379/?report=abstract

43. Livak KJ, Schmittgen TD. Analysis of relative gene expression data using real-time quantitative PCR and the 2-ΔΔCT method. Methods. 2001;25(4):402–8.

44. Vlachos IS, Hatzigeorgiou AG. Functional analysis of miRNAs using the DIANA tools online suite. In: Methods in Molecular Biology [Internet]. Methods Mol Biol; 2017 [cited 2022 Dec 15]. p. 25–50. Available from: https://pubmed.ncbi.nlm.nih.gov/27924472/

45. Tian X, Xie G, Xiao H, Ding F, Bao W, Zhang M. CXCR4 knockdown prevents inflammatory cytokine expression in macrophages by suppressing activation of MAPK and NF-κB signaling pathways. Cell Biosci [Internet]. 2019 Jul 3 [cited 2022 Dec 15];9(1). Available from: /pmc/articles/PMC6607528/

46. Mei C, Meng F, Wang X, Yan S, Zheng Q, Zhang X, et al. CD30L is involved in the regulation of the inflammatory response through inducing homing and differentiation of monocytes via CCL2/CCR2 axis and NF-κB pathway in mice with colitis. Int Immunopharmacol [Internet]. 2022 Sep 1 [cited 2022 Dec 15];110. Available from: https://pubmed.ncbi.nlm.nih.gov/35834956/

47. Richter AM, Küster MM, Woods ML, Walesch SK, Gökyildirim MY, Krueger M, et al. RASSF10 is a TGFβ-target that regulates ASPP2 and e-cadherin expression and acts as tumor suppressor that is epigenetically downregulated in advanced cancer. Cancers (Basel) [Internet]. 2019 Dec 1 [cited 2022 Dec 15];11(12). Available from: /pmc/articles/PMC6966473/

48. Subbannayya Y, Pinto SM, Bösl K, Keshava Prasad TS, Kandasamy RK. Dynamics of dual specificity phosphatases and their interplay with protein kinases in immune signaling. Int J Mol Sci [Internet]. 2019 May 1 [cited 2022 Dec 15];20(9). Available from: /pmc/articles/PMC6539644/

49. Michaille JJ, Awad H, Fortman EC, Efanov AA, Tili E. miR-155 expression in antitumor immunity: The higher the better? Genes Chromosom Cancer [Internet]. 2019 Apr 1 [cited 2022 Dec 15];58(4):208–18.

Available from: https://pubmed.ncbi.nlm.nih.gov/30382602/

50. Li X, Wang S, Mu W, Barry J, Han A, Carpenter RL, et al. Reactive oxygen species reprogram macrophages to suppress antitumor immune response through the exosomal miR-155-5p/PD-L1 pathway. J Exp Clin Cancer Res [Internet]. 2022 Dec 1 [cited 2022 Dec 15];41(1). Available from: https://pubmed.ncbi.nlm.nih.gov/35086548/

51. Wei T-T, Cheng Z, Hu Z-D, Zhou L, Zhong R-Q. Upregulated miR-155 inhibits inflammatory response induced by C. albicans in human monocytes derived dendritic cells via targeting p65 and BCL-10. Ann Transl Med [Internet]. 2019 Dec [cited 2022 Dec 15];7(23):758–758. Available from: /pmc/articles/PMC6989962/

52. Tang B, Xiao B, Liu Z, Li N, Zhu ED, Li BS, et al. Identification of MyD88 as a novel target of miR-155, involved in negative regulation of Helicobacter pylori-induced inflammation. FEBS Lett [Internet]. 2010 Apr [cited 2022 Dec 15];584(8):1481–6. Available from: https://pubmed.ncbi.nlm.nih.gov/20219467/

53. Gottwein E, Mukherjee N, Sachse C, Frenzel C, Majoros WH, Chi JTA, et al. A viral microRNA functions as an orthologue of cellular miR-155. Nature [Internet]. 2007 Dec 12 [cited 2022 Dec 15];450(7172):1096–9. Available from: /pmc/articles/PMC2614920/

54. Zaragoza O, Rodrigues ML, De Jesus M, Frases S, Dadachova E, Casadevall A. Chapter 4 The Capsule of the Fungal Pathogen Cryptococcus neoformans [Internet]. 1st ed. Vol. 68, Advances in Applied Microbiology. Elsevier Inc.; 2009. 133–216 p. Available from: http://dx.doi.org/10.1016/S0065-2164(09)01204-0

55. Denham ST, Verma S, Reynolds RC, Worne CL, Daugherty JM, Lane TE, et al. Regulated release of cryptococcal polysaccharide drives virulence and suppresses immune cell infiltration into the central nervous system. Infect Immun [Internet]. 2018 Mar 1 [cited 2022 Dec 15];86(3). Available from: /pmc/articles/PMC5820953/

56. Yauch LE, Lam JS, Levitz SM. Direct inhibition of T-cell responses by the Cryptococcus capsular polysaccharide glucuronoxylomannan. PLoS Pathog [Internet]. 2006 Nov [cited 2022 Dec 15];2(11):1060–8. Available from: https://pubmed.ncbi.nlm.nih.gov/17096589/

57. Monari C, Bistoni F, Vecchiarelli A. Glucuronoxylomannan exhibits potent immunosuppressive properties. FEMS Yeast Res. 2006;6(4):537–42.

58. Monari C, Paganelli F, Bistoni F, Kozel TR, Vecchiarelli A. Capsular polysaccharide induction of apoptosis by intrinsic and extrinsic mechanisms. Cell Microbiol [Internet]. 2008 [cited 2022 Dec 15];10(10):2129–37. Available from: https://pubmed.ncbi.nlm.nih.gov/18647312/

59. Trizzino M, Zucco A, Deliard S, Wang F, Barbieri E, Veglia F, et al. EGR1 is a gatekeeper of inflammatory enhancers in human macrophages. Sci Adv [Internet]. 2021 Jan 13 [cited 2022 Dec 15];7(3). Available from: /pmc/articles/PMC7806227/

60. Bogdan C, Röllinghoff M, Diefenbach A. The role of nitric oxide in innate immunity. Immunol Rev [Internet]. 2000 [cited 2022 Dec 15];173:17–26. Available from: https://pubmed.ncbi.nlm.nih.gov/10719664/

61. Hardison SE, Ravi S, Wozniak KL, Young ML, Olszewski MA, Wormley FL. Pulmonary infection with an interferon-γ-producing cryptococcus neoformans strain results in classical macrophage activation and protection. Am J Pathol [Internet]. 2010 [cited 2022 Dec 15];176(2):774–85. Available from: https://pubmed.ncbi.nlm.nih.gov/20056835/

62. Scriven JE, Graham LM, Schutz C, Scriba TJ, Wilkinson KA, Wilkinson RJ, et al. A glucuronoxylomannan-associated immune signature, characterized by monocyte deactivation and an increased interleukin 10 level, is a predictor of death in cryptococcal meningitis. J Infect Dis [Internet]. 2016 Jun 1 [cited 2022 Dec 15];213(11):1725–34. Available from: https://pubmed.ncbi.nlm.nih.gov/26768248/

63. Xu J, Eastman AJ, Flaczyk A, Neal LM, Zhao G, Carolan J, et al. Disruption of early tumor necrosis factor alpha signaling prevents classical activation of dendritic cells in lung-associated lymph nodes and development of protective immunity against cryptococcal infection. MBio [Internet]. 2016 Jul 1 [cited 2022 Dec 15];7(4). Available from: https://pubmed.ncbi.nlm.nih.gov/27406560/

64. Howrylak JA, Nakahira K. Inflammasomes: Key Mediators of Lung Immunity. Annu Rev Physiol [Internet]. 2017 Feb 10 [cited 2022 Dec 15];79:471–94. Available from: https://pubmed.ncbi.nlm.nih.gov/28192059/

65. Briardi B, Malireddi RKS, Kannegantii TD. Role of inflammasomes/pyroptosis and PANoptosis during

fungal infection. PLoS Pathog [Internet]. 2021 Mar 1 [cited 2022 Dec 15];17(3). Available from: /pmc/articles/PMC7971547/

66. Guo C, Chen M, Fa Z, Lu A, Fang W, Sun B, et al. Acapsular Cryptococcus neoformans activates the NLRP3 inflammasome. Microbes Infect [Internet]. 2014 Oct [cited 2019 Sep 12];16(10):845–54. Available from: https://linkinghub.elsevier.com/retrieve/pii/S1286457914001282

67. Bürgel PH, Marina CL, Saavedra PHV, Albuquerque P, De Oliveira SAM, Veloso Janior PH de H, et al. Cryptococcus neoformans Secretes Small Molecules That Inhibit IL-1 β Inflammasome-Dependent Secretion. Mediators Inflamm [Internet]. 2020 [cited 2022 Dec 15];2020. Available from: https://pubmed.ncbi.nlm.nih.gov/33380899/

68. Neal LM, Xing E, Xu J, Kolbe JL, Osterholzer JJ, Segal BM, et al. Cd4+ T cells orchestrate lethal immune pathology despite fungal clearance during cryptococcus neoformans meningoencephalitis. MBio [Internet]. 2017 Nov 1 [cited 2022 Dec 15];8(6). Available from: /pmc/articles/PMC5698549/

69. Kawasaki T, Ikegawa M, Kawai T. Antigen Presentation in the Lung. Front Immunol [Internet]. 2022 May 9 [cited 2022 Dec 15];13. Available from: /pmc/articles/PMC9124800/

70. Carenza C, Calcaterra F, Oriolo F, Di Vito C, Ubezio M, Porta MG Della, et al. Costimulatory molecules and immune checkpoints are differentially expressed on different subsets of dendritic cells. Front Immunol [Internet]. 2019 [cited 2022 Dec 15];10(JUN):1325. Available from: /pmc/articles/PMC6579930/

71. Gibson JF, Johnston SA. Immunity to Cryptococcus neoformans and C. gattii during cryptococcosis. Fungal Genet Biol [Internet]. 2015 May 1 [cited 2022 Dec 15];78:76–86. Available from: /pmc/articles/PMC4503824/

72. Jarvis JN, Casazza JP, Stone HH, Meintjes G, Lawn SD, Levitz SM, et al. The phenotype of the cryptococcus-specific CD4+ memory T-cell response is associated with disease severity and outcome in HIV-associated cryptococcal meningitis. J Infect Dis [Internet]. 2013 Jun 15 [cited 2022 Dec 15];207(12):1817–28. Available from: https://pubmed.ncbi.nlm.nih.gov/23493728/

73. Wozniak KL, Young ML, Wormley FL. Protective immunity against experimental pulmonary cryptococcosis in T cell-depleted mice. Clin Vaccine Immunol [Internet]. 2011 May [cited 2022 Dec 15];18(5):717–23. Available from: https://pubmed.ncbi.nlm.nih.gov/21450975/

74. Williamson PR, Jarvis JN, Panackal AA, Fisher MC, Molloy SF, Loyse A, et al. Cryptococcal meningitis: Epidemiology, immunology, diagnosis and therapy. Nat Rev Neurol [Internet]. 2016 Dec 28 [cited 2022 Dec 15];13(1):13–24. Available from: https://pubmed.ncbi.nlm.nih.gov/27886201/

75. Van Der Velden AWM, Copass MK, Starnbach MN. Salmonella inhibit T cell proliferation by a direct, contact-dependent immunosuppressive effect. Proc Natl Acad Sci U S A [Internet]. 2005 Dec 6 [cited 2022 Dec 15];102(49):17769–74. Available from: https://pubmed.ncbi.nlm.nih.gov/16306269/

76. Croston TL, Lemons AR, Beezhold DH, Green BJ. MicroRNA regulation of host immune responses following fungal exposure. Front Immunol. 2018;9(FEB).

77. Drury RE, O'Connor D, Pollard AJ. The clinical application of MicroRNAs in infectious disease. Front Immunol [Internet]. 2017 Sep 25 [cited 2022 Dec 15];8(SEP). Available from: https://pubmed.ncbi.nlm.nih.gov/28993774/

78. Das Gupta M, Fliesser M, Springer J, Breitschopf T, Schlossnagel H, Schmitt AL, et al. Aspergillus fumigatus induces microRNA-132 in human monocytes and dendritic cells. Int J Med Microbiol [Internet]. 2014 [cited 2022 Dec 15];304(5–6):592–6. Available from: https://pubmed.ncbi.nlm.nih.gov/24841251/

79. Agustinho DP, de Oliveira MA, Tavares AH, Derengowski L, Stolz V, Guilhelmelli F, et al. Dectin-1 is required for miR155 upregulation in murine macrophages in response to Candida albicans. Virulence. 2017;8(1):41–52.

80. Monk CE, Hutvagner G, Arthur JSC. Regulation of miRNA transcription in macrophages in response to candida albicans. PLoS One. 2010;5(10).

81. Chen H, Jin Y, Chen H, Liao I, Yan W, Chen J. MicroRNA-mediated inflammatory responses induced by Cryptococcus neoformans are dependent on the NF-κB pathway in human monocytes. Int J Mol Med [Internet]. 2017 Jun [cited 2018 May 30];39(6):1525–32. Available from: http://www.ncbi.nlm.nih.gov/pubmed/28440395

82. Antonakos N. Modes of action and diagnostic value of miRNAs in sepsis. Front Immunol [Internet]. 2022

Aug 5 [cited 2022 Dec 15];13. Available from: /pmc/articles/PMC9389448/

83. Kumar R, Halder P, Sahu SK, Kumar M, Kumari M, Jana K, et al. Identification of a novel role of ESAT-6-dependent miR-155 induction during infection of macrophages with mycobacterium tuberculosis. Cell Microbiol [Internet]. 2012 Oct [cited 2022 Dec 15];14(10):1620–31. Available from: https://pubmed.ncbi.nlm.nih.gov/22712528/

84. Ceppi M, Pereira PM, Dunand-Sauthier I, Barras E, Reith W, Santos MA, et al. MicroRNA-155 modulates the interleukin-1 signaling pathway in activated human monocyte-derived dendritic cells. Proc Natl Acad Sci [Internet]. 2009 Feb 24 [cited 2018 May 30];106(8):2735–40. Available from: http://www.pnas.org/lookup/doi/10.1073/pnas.0811073106

85. Schulte LN, Westermann AJ, Vogel J. Differential activation and functional specialization of miR-146 and miR-155 in innate immune sensing. Nucleic Acids Res [Internet]. 2013 Jan 7 [cited 2019 Aug 29];41(1):542–53. Available from: http://academic.oup.com/nar/article/41/1/542/1149200/Differential-activation-and-functional

86. Banerjee S, Thompson WE, Chowdhury I. Emerging roles of microRNAs in the regulation of Toll-like receptor (TLR)-signaling. Front Biosci - Landmark [Internet]. 2021 Jan 1 [cited 2022 Dec 15];26(4):771–96. Available from: https://pubmed.ncbi.nlm.nih.gov/33049693/

87. Ghafouri-Fard S, Abak A, Shoorei H, Talebi SF, Mohaqiq M, Sarabi P, et al. Interaction between non-coding RNAs and Toll-like receptors. Biomed Pharmacother [Internet]. 2021 Aug 1 [cited 2022 Dec 15];140. Available from: https://pubmed.ncbi.nlm.nih.gov/34087695/

88. Bayraktar R, Bertilaccio MTS, Calin GA. The interaction between two worlds: MicroRNAs and Toll-like receptors. Front Immunol [Internet]. 2019 [cited 2022 Dec 15];10(MAY):1053. Available from: /pmc/articles/PMC6527596/

6. Figures and legends

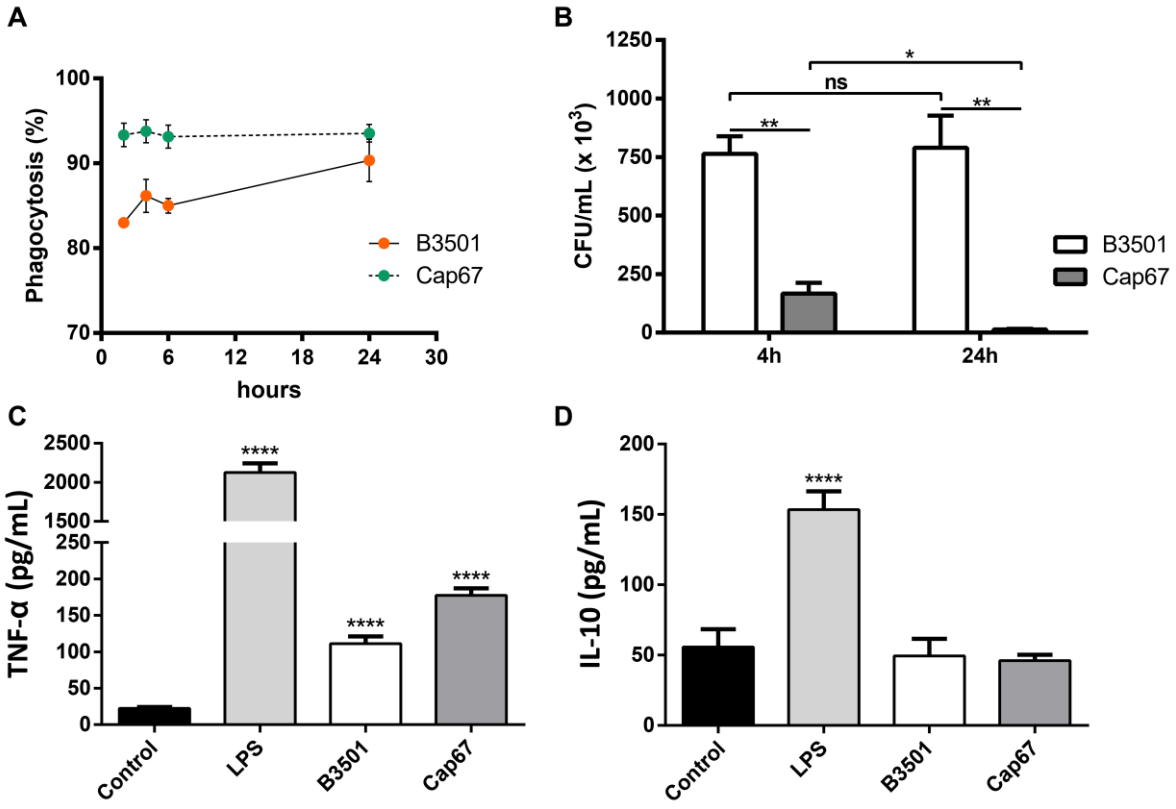

Figure 1. Kinetic of infection of macrophages by two strains of *C. neoformans*.
A) Percentage of phagocytosis in different times of interaction. **B)** CFU counts of B3501 and Cap67 strains after 4 h and 24 h post infection. **C-D)** Cytokines release from macrophages infected by B3501 and Cap67 strains in 24 h post infection. Data are presented as mean ± SEM. Statistical significancy was calculated by t-Student test (**B**) and one-way ANOVA with posttest Dunnett's multiple comparisons (**C-D**). * Adjusted *p*-value < 0.05.

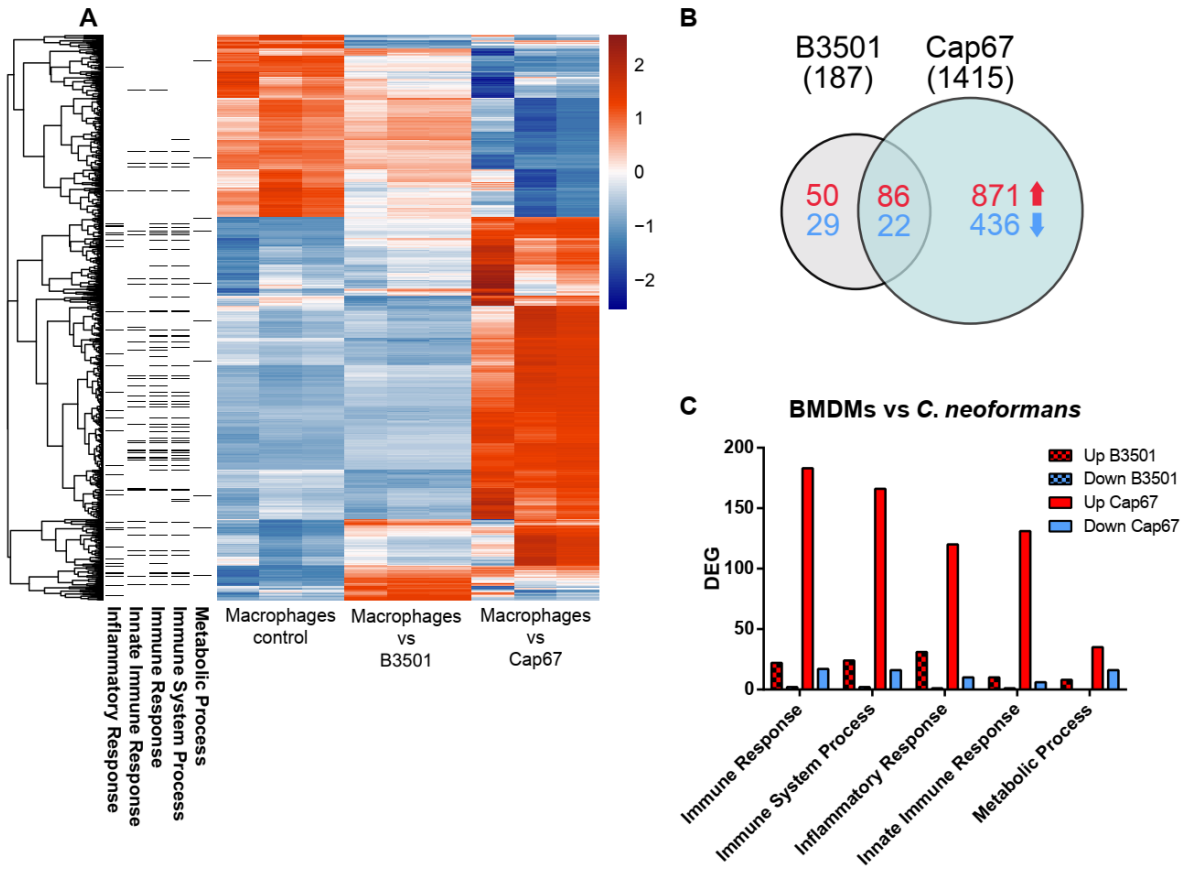

Figure 2. Differential gene expression of bone marrow-derived macrophages upon 4 h of interaction with two strains of *C. neoformans*.

A) Global heatmap showing all genes differentially modulated, comparing control samples (BMDMs noninfected), and infected macrophages by B3501 and Cap67 strains. **B)** Venn diagram of positively (red) and negatively (blue) regulated genes of macrophages infected by B3501 and Cap67 strains. All genes with adjusted *p*-value < 0.05, and fold change ≥ ±2 was considered as differentially expressed genes (DEGs). **C)** Number of DEGs correlated to different Gene Ontology (GO) terms in macrophages infected by B3501 and Cap67 strains of *C. neoformans*.

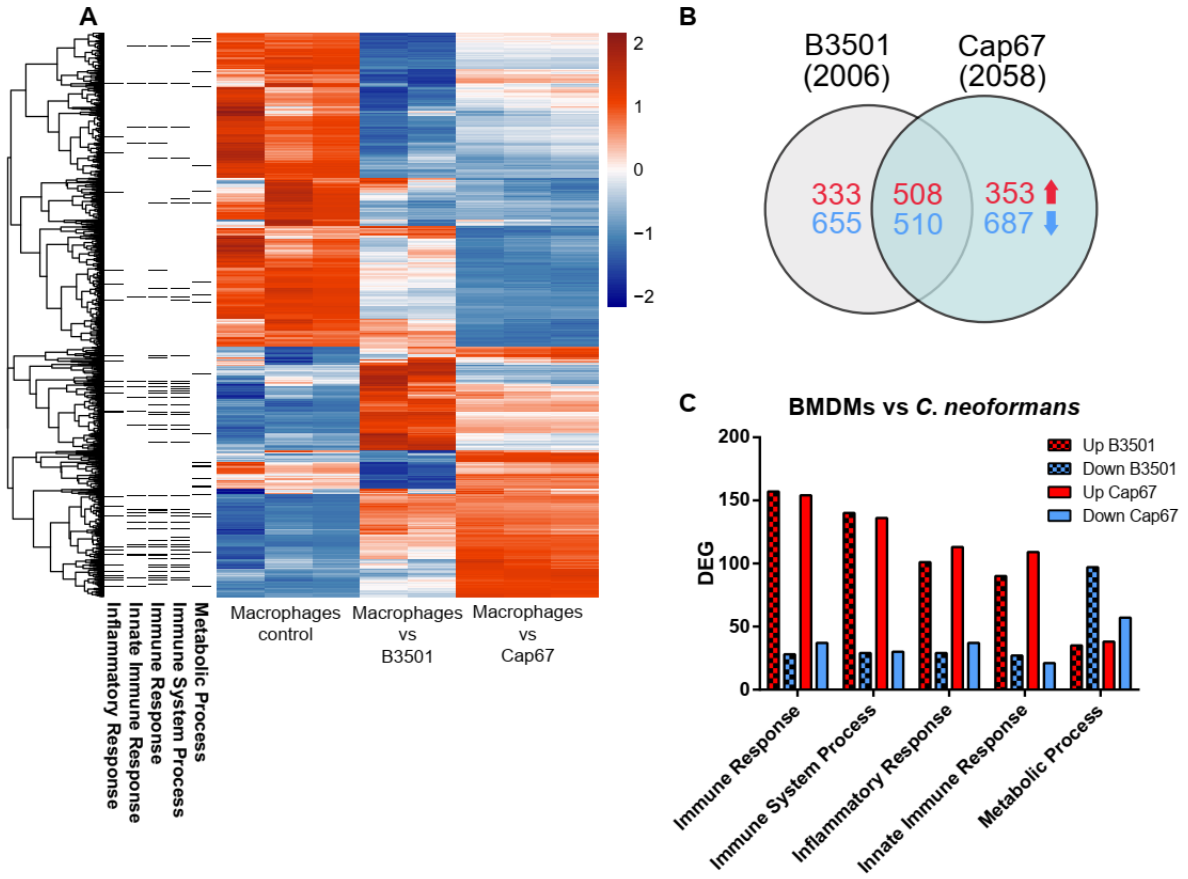

Figure 3. Differential gene expression of bone marrow-derived macrophages upon 24 h of interaction with two strains of *C. neoformans*.

A) Global heatmap showing all genes differentially modulated, comparing control samples (BMDMs noninfected), and infected macrophages by B3501 and Cap67 strains. **B)** Venn diagram of positively (red) and negatively (blue) regulated genes of macrophages infected by B3501 and Cap67 strains. All genes with adjusted *p*-value < 0.05, and fold change ≥ ±2 was considered as differentially expressed genes (DEGs). **C)** Number of DEGs correlated to different Gene Ontology (GO) terms in macrophages infected by B3501 and Cap67 strains of *C. neoformans*.

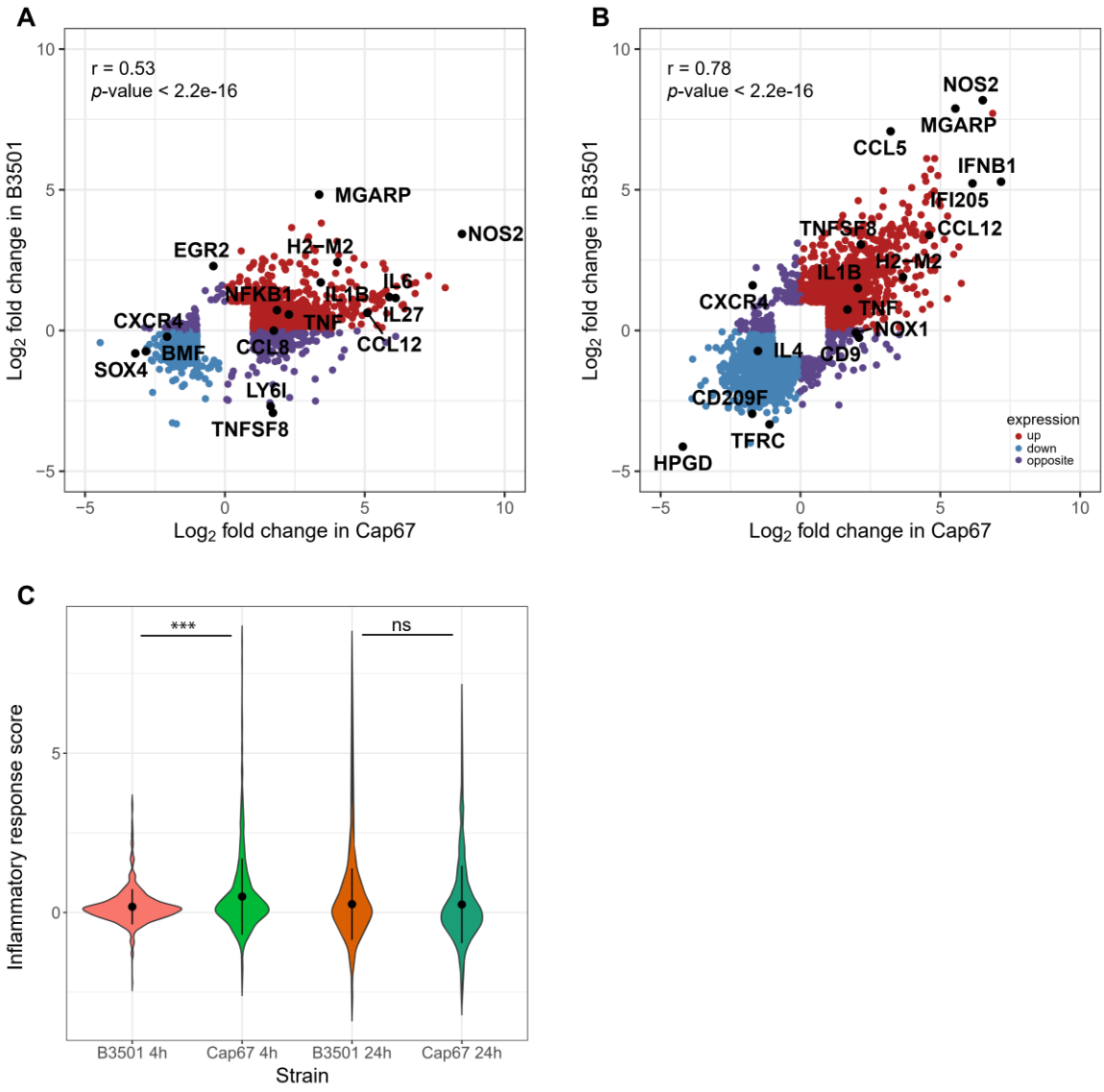

Figure 4. Distribution of gene modulation in macrophages infected by *C. neoformans*. **A - B)** Scatter plot displaying all genes differentially modulated in 4 h (**A**) and 24 h (**B**) post infection. The axis represents the log_2 values of the fold change observed for each transcript in B3501 (*y*-axis) and Cap67 (*x*-axis) infection. Genes with positive regulation (>0) were indicated in red, negative regulation (<0) in blue, and genes with opposite regulation between the two strains were indicated in purple. Significance was calculated by Pearson's correlation. **C**) Violin plot of inflammatory response score for each sample and time frame. Middle points and lines indicate mean and SD values. Significance was calculated using two-sided Wilcoxon test; *** Adjusted *p*-value < 0.01.

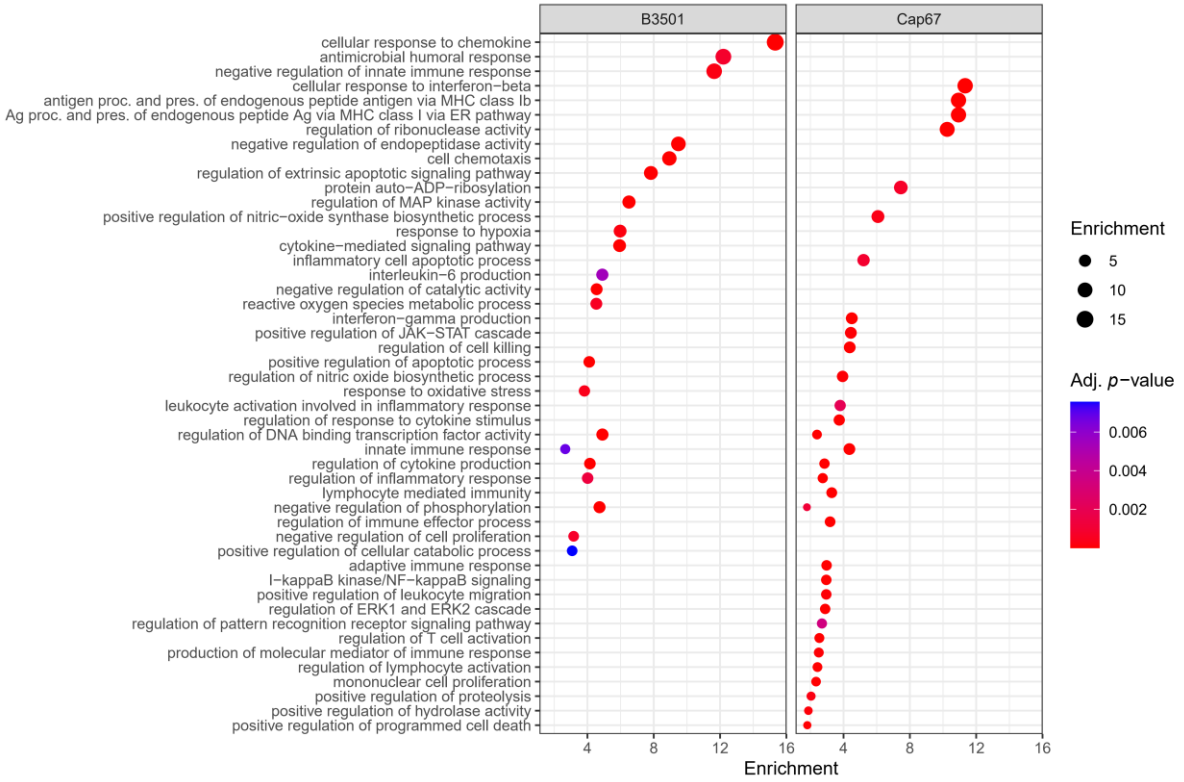

Figure 5. Gene ontology enrichment of differentially expressed genes in macrophages after 4 hours of *C. neoformans* infection.

Enriched ontological terms from biological processes category (adjusted *p*-value < 0.01) associated with upregulated DEG in macrophages infected by B3501 and Cap67 strains at 4 hpi. Dot size represents the enrichment (gene modulated ratio/gene background ratio) for each GO term.

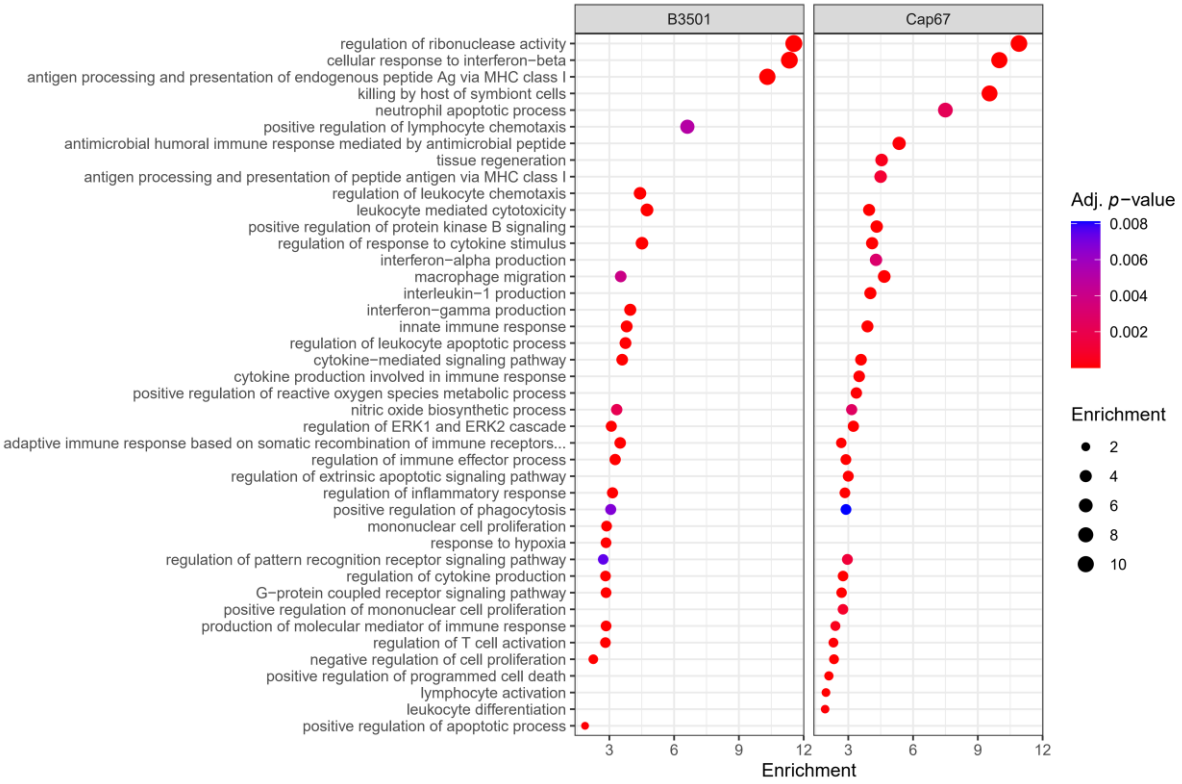

Figure 6. Gene ontology enrichment of differentially expressed genes in macrophages after 24 hours of *C. neoformans* infection.

Enriched ontological terms from biological processes category (adjusted *p*-value < 0.01) associated with upregulated DEG in macrophages infected by B3501 and Cap67 strains at 24 hpi. Dot size represents the enrichment (gene modulated ratio/gene background ratio) for each GO term.

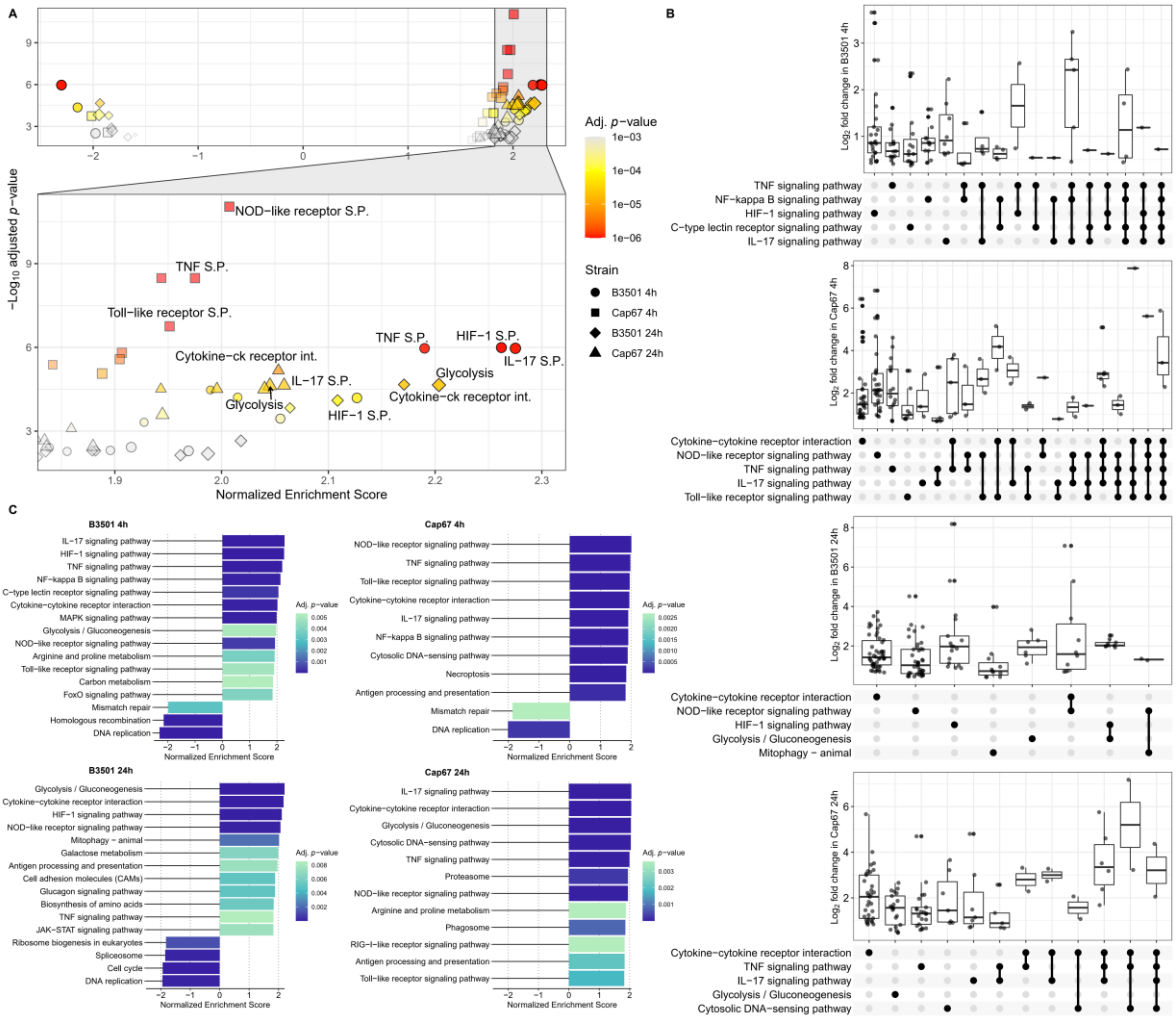

Figure 7. KEGG pathway enrichment from gene expression in macrophages after *C. neoformans* infection.

A) Enriched pathways from KEGG database (adjusted *p*-value < 0.01) associated with up- and down-regulated genes in macrophages infected by B3501 and Cap67 strains at 4 and 24 hours post infection. **B)** UpSet plot visualizing the fold change distribution of core enrichment genes in top 5 pathways among strain infections. A line linking multiple filled circles represents genes are shared among more than one group comparison. **C)** Bar chart displaying the normalized enrichment scores of top pathways from GSEA. Exact *p*-values are provided in the supplemental information (Table S3).

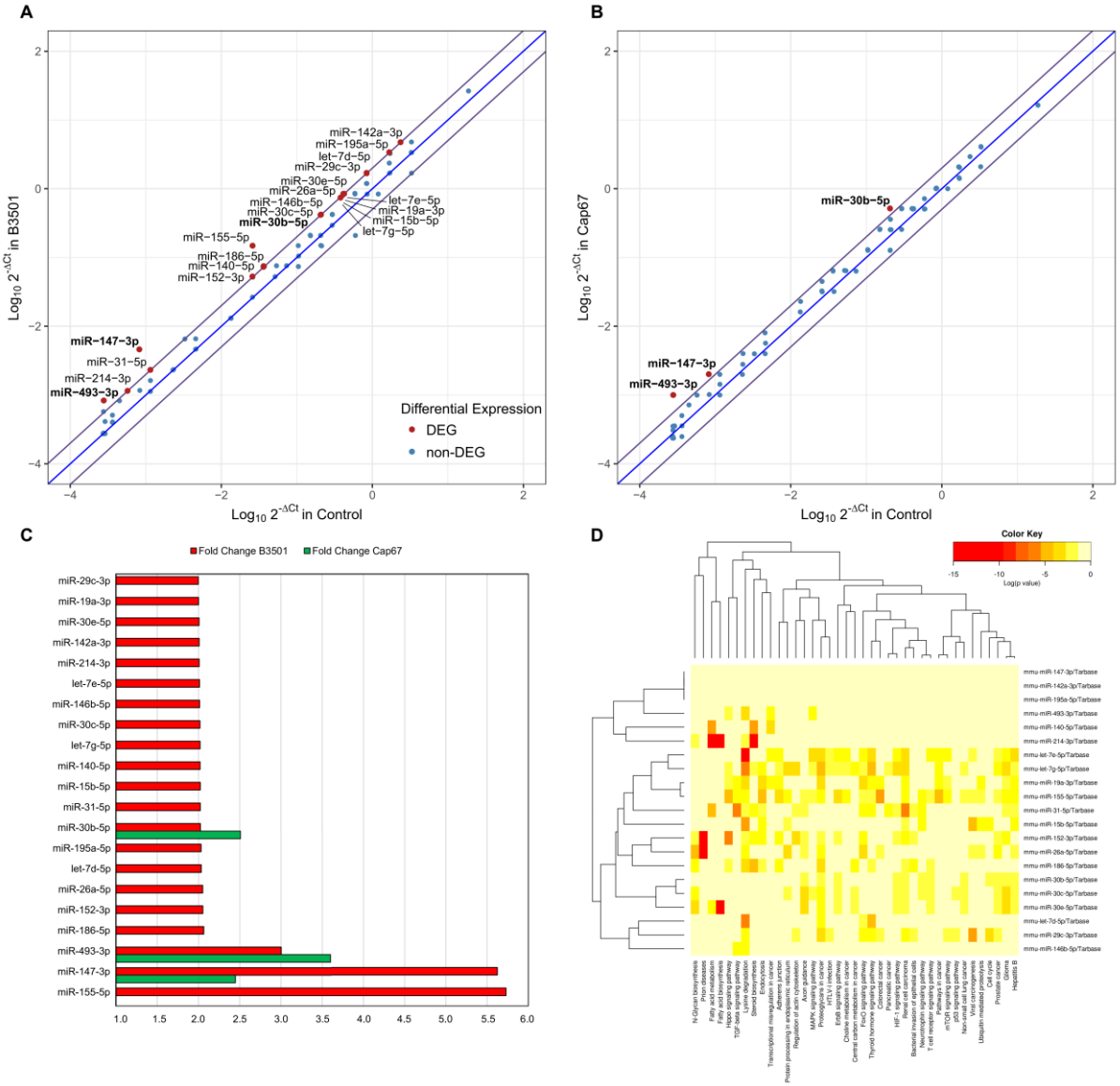

Figure 8. Differential miRNA expression in macrophages upon *C. neoformans* infection. **A)** Scatter plot showing miRNA expression changes comparing infected macrophages by B3501 strain vs. control (noninfected) samples. **B)** Scatter plot showing miRNA expression changes comparing infected BMDMs by Cap67 strain vs. control (noninfected) samples. The axis represents the $\log_{10}$ values of the fold changes ($2^{-\Delta Ct}$) observed for each miRNA on infected samples (*y*-axis) and control samples (*x*-axis). The differentially expressed miRNAs (DEGs: *p*-value < 0.05, and fold change ≥ ±2) are highlighted (red dots). In bold are highlighted significant miRNAs for two strains. The blue line indicates fold changes ($2^{-\Delta Ct}$) of 1. The purple lines indicate the cutoff of the fold-change in gene expression threshold (fold change ≥ ±2). **C)** Fold change of differentially modulated miRNAs in macrophages infected by *C. neoformans* strains. **D)** Enriched pathways from KEGG database (adjusted *p*-value < 0.05) associated with all differentially expressed-miRNA targets from Tarbase database. Neighbourhood lines indicate the shared target mRNAs found in a defined pathway.

7. Supplemental information

Table S1. Primers sequences of selected genes for RNA-seq validation.

Gene	Sequence forward	Sequence reverse
TNF	5'-GTACCTTGTCTACTCCCAGGTTCTCT-3'	5'-GTGGGTGAGGAGCACGTAGTC-3'
Myd88	5'-ACTGGCCTGAGCAACTAGGA-3'	5'-CGTGCCACTACCTGTAGCAA-3'
IL-10	5'-GCTCTTACTGACTGGCATGAG-3'	5'- CGCAGCTCTAGGAGCATGTG-3'
Cxcl10	5'-CCAAGTGCTGCCGTCATTTTC-3'	5'-GGCTCGCAGGGATGATTTCAA-3'
Ikbke	5'-CCAGCAGCCCTCTAACTCTG-3'	5'-ACGAACTTTGGGACATCCAG-3'
Stat1	5'-TCACAGTGGTTCGAGCTTCAG-3'	5'- GCAAACGAGACATCATAGGCA-3'
IL-1β	5'-GTGTGTGACGTTCCCATTAGACA-3'	5'-CAGCACGAGGCTTTTTTGTTG-3'
Dectin-1	5'-TAATCTCTGCCCCCAAAACC-3'	5'-AACTGCTTCGACCCAGACCT-3'
Socs1	5'-ACTTCTGGCTGGAGACCTCA-3'	5'-CCCAGACACAAGCTGCTACA-3'
Socs3	5'-ATTCACCCAGGTGGCTACAG-3'	5'-GCCAATGTCTTCCCAGTGTT-3'
Rps9	5'-CGCCAGAAGCTGGGTTTGT-3'	5'-CGAGACGCGACTTCTCGAA-3'

Table S2. Comparison of the modulation of selected genes in macrophages infected by B3501 and Cap67 *C. neoformans* strains.

Gene	Experimental condition (Fold change*)			
	Infection at 4 h		Infection at 24 h	
	B3501	Cap67	B3501	Cap67
Cxcr4	-1.17	**-4.19**	**3.04**	**-3.27**
Tnfsf8	**-7.61**	**3.29**	**8.32**	**4.47**
Med12l	**-5.93**	**3.05**	**2.29**	1.18
Vnn3	-1.00	2.25	**2.07**	**-2.50**
Rassf10			**2.09**	**-2.62**
Dcbld2	1.26	**2.94**	**-2.51**	**4.70**
Dusp18	1.24	-1.74	**-2.25**	**2.21**
Rcn1	1.20	**2.65**	**-2.01**	**2.01**
Rnu3b1	1.43	**2.21**	**-3.06**	**2.56**
Tlr2	1.65	**4.66**	**-2.51**	-1.53
Tlr3	1.10	**8.27**	**2.34**	**3.69**
Tlr7	1.11	**2.07**	1.07	-1.18
Myd88	1.23	**4.02**	-1.12	1.28
Nlrp3	1.71	**4.44**	1.17	1.41
Aim2	1.12	**5.22**	1.39	1.35
Gsdmd	-1.02	**2.20**	1.17	1.17
Ccl3	1.53	**8.45**	1.39	1.92
Tnf	1.48	**4.88**	1.67	**3.21**
Il6	2.28	**58.77**		
Casp1	1.33	**3.71**	1.44	1.88
Casp4	1.46	**6.22**	1.37	**2.24**
Casp8	-1.08	**2.01**	1.07	1.16
NF-κB1	1.65	**3.63**	-1.56	-1.06
NF-κB2	1.64	**3.14**	**-2.04**	-1.34
Il1β	**3.26**	**10.74**	**2.84**	**4.15**
Il18	1.54	**6.61**	**2.08**	**2.11**
Ccl2	1.60	**6.37**	**4.91**	**9.06**
Nos2	**10.78**	**355.56**	**290.56**	**91.70**
Arg1	**2.58**	**2.00**	**69.08**	**22.85**
Ikbke	1.09	**2.64**	-1.10	1.03
Bach1	1.19	**2.45**	1.50	1.03
Egr2	**4.89**	-1.33	-1.83	1.89
Ccl3	1.53	**8.45**	1.39	1.92
Ccl12	1.55	**34.08**	**10.49**	**24.35**
Cd40	1.61	**35.51**	1.72	**3.55**
Cd86	1.98	**2.21**	-1.01	1.89

* Genes in bold lettering had their transcript levels significantly modulated (FC ≥ ± 2.0 and adjusted *p*-value < 0.05 as described in Materials and Methods). Positive and negative values represent genes with expression induced and repressed, respectively.

Table S3. Enriched KEGG pathways in macrophages infected by B3501 and Cap67 *C. neoformans* strains.

ID	Description	setSize	NES	p.adjust	core_enrichment	time	Strai
mmu04066	HIF-1 signaling pathway	88	2,26211E+14	101897379,2	Egln3/Slc2a1/Egln1/Pfkfb3/Pdk1/Pfkl/Hmox1/H	4h	B3501 4h
mmu04657	IL-17 signaling pathway	67	2,27524E+14	108283364,7	Mmp13/Cxcl2/Ptgs2/Cxcl1/Il1b/Tnfaip3/Cxcl3/(	4h	B3501 4h
mmu04668	TNF signaling pathway	100	2,19015E+13	108283364,7	Cxcl2/Ptgs2/Cxcl1/Il1b/Tnfaip3/Cxcl3/Jag1/Csf1	4h	B3501 4h
mmu03030	DNA replication	35	-2,30241E+13	108283364,7	Mcm5/Pole/Prim2/Rfc1/Rfc3/Prim1/Rpa2/Mcm	4h	B3501 4h
mmu04010	MAPK signaling pathway	204	1,98949E+14	3350025104	Gadd45b/Pdgfb/Met/Hspa1a/Il1b/Dusp5/Dusp	4h	B3501 4h
mmu03440	Homologous recombination	39	-2,14906E+14	4347251303	Blm/Rad52/Xrcc2/Rad51d/Abraxas1/Eme1/Rad	4h	B3501 4h
mmu04060	Cytokine-cytokine receptor interaction	126	2,01508E+14	6203212577	Cxcl2/Il1rn/Acvrl1/Cxcl1/Il1b/Cxcl3/Ccl4/Ccl7/P	4h	B3501 4h
mmu04064	NF-kappa B signaling pathway	79	2,12678E+14	6479574167	Cxcl2/Gadd45b/Ptgs2/Il1b/Tnfaip3/Ccl4/Malt1/	4h	B3501 4h
mmu04625	C-type lectin receptor signaling pathway	89	2,05507E+14	3,56653E+14	Ptgs2/Egr2/Il1b/Clec7a/Egr3/Malt1/Jun/Clec4e/	4h	B3501 4h
mmu04621	NOD-like receptor signaling pathway	142	1,9274E+14	4,8281E+14	Cxcl2/Cxcl1/Ripk2/Il1b/Tnfaip3/Cxcl3/Gabarapl	4h	B3501 4h
mmu04151	PI3K-Akt signaling pathway	216	1,77262E+13	2,77668E+14	Pdgfb/Gys1/Met/Csf1/Vegfa/Eif4ebp1/Mcl1/M	4h	B3501 4h
mmu03430	Mismatch repair	22	-1,97839E+14	3,10765E+13	Rpa1/Pold2/Pms2/Rfc5/Pold3/Mlh1/Rfc2/Msh2	4h	B3501 4h
mmu00330	Arginine and proline metabolism	35	1,91535E+13	3,75614E+14	P4ha2/P4ha1/Arg1/Smox/Nos2/Odc1	4h	B3501 4h
mmu04068	FoxO signaling pathway	108	1,83877E+14	3,92721E+14	Plk2/Bnip3/Gadd45b/Gadd45g/Gabarapl1/Map	4h	B3501 4h
mmu04062	Chemokine signaling pathway	139	1,79039E+14	4,39398E+14	Cxcl2/Cxcl1/Cxcl3/Ccl4/Ccl7/Ppbp/Map2k1/Ccr	4h	B3501 4h
mmu04620	Toll-like receptor signaling pathway	79	1,89579E+14	4,91014E+14	Il1b/Ccl4/Map2k1/Jun/Traf6/Cd86/Pik3cb/Traf	4h	B3501 4h
mmu04510	Focal adhesion	146	1,73759E+14	5,03359E+14	Pdgfb/Met/Vcl/Vegfa/Map2k1/Jun/Itga5/Pik3cb	4h	B3501 4h
mmu00010	Glycolysis / Gluconeogenesis	44	1,96901E+14	5,12466E+14	Pgm1/Pfkp/Pfkl/Tpi1/Pgam1/Hk1/Ldha/Pgk1/G	4h	B3501 4h
mmu01200	Carbon metabolism	95	1,85526E+14	5,35789E+14	Pfkp/Pfkl/Tpi1/Pgam1/Hk1/Pgk1/Gpi1/Eno1/Es	4h	B3501 4h
mmu04621	NOD-like receptor signaling pathway	142	2,00727E+14	909,8966441	Ccl5/Ccl12/Ccl2/Ripk2/Casp1/Il1b/Tnf/Casp4/Il	4h	Cap67 4h
mmu04668	TNF signaling pathway	100	1,97508E+13	329894,745	Ccl5/Ccl12/Ccl2/Il1b/Socs3/Tnf/Mlkl/Csf1/Il6/Pt	4h	Cap67 4h
mmu04060	Cytokine-cytokine receptor interaction	126	1,94361E+14	329894,745	Ccl5/Cd40/Ccl7/Ccl4/Ccl12/Il27/Ccl3/Tnfsf15/Cc	4h	Cap67 4h
mmu04620	Toll-like receptor signaling pathway	79	1,9513E+14	17566759,33	Ccl5/Cd40/Ccl4/Ccl3/Tlr3/Il1b/Tnf/Il6/Irf7/Myd	4h	Cap67 4h
mmu04657	IL-17 signaling pathway	67	1,90661E+14	15658670,16	Mmp13/Ccl7/Ccl12/Ccl2/Il1b/Tnf/Il6/Ptgs2/Cxc	4h	Cap67 4h
mmu04064	NF-kappa B signaling pathway	79	1,90456E+14	266231048,4	Cd40/Ccl4/Il1b/Tnf/Ptgs2/Cxcl2/Traf1/Myd88/T	4h	Cap67 4h
mmu04217	Necroptosis	126	1,84184E+14	418363833,3	Tlr3/Casp1/Il1b/Tnf/Mlkl/Tnfsf10/Jak2/Il1a/Fas	4h	Cap67 4h
mmu04062	Chemokine signaling pathway	139	1,79779E+14	777521849,6	Ccl5/Ccl7/Ccl4/Ccl12/Ccl3/Ccl2/Cxcl2/Jak2/Gnb	4h	Cap67 4h
mmu04623	Cytosolic DNA-sensing pathway	44	1,88808E+14	864847126,4	Ccl5/Ccl4/Casp1/Il1b/Il6/Aim2/Il18/Irf7/Nfkb1/	4h	Cap67 4h
mmu04612	Antigen processing and presentation	56	1,81827E+14	1,05716E+14	H2-T10/Tnf/H2-T22/H2-Q4/Tap1/Tap2/H2-Q10/	4h	Cap67 4h
mmu04145	Phagosome	127	1,75316E+14	1,05716E+14	H2-T10/H2-T22/H2-Q4/Tap1/Tap2/H2-Q10/Tlr2	4h	Cap67 4h
mmu04514	Cell adhesion molecules (CAMs)	79	1,81254E+14	1,16119E+14	Cd40/H2-T10/H2-T22/Cd274/H2-Q4/Sdc4/H2-Q	4h	Cap67 4h
mmu03030	DNA replication	35	-2,01567E+14	1,80244E+14	Rpa1/Pola2/Rfc1/Pold2/Rpa2/Fen1/Prim1/Mcm	4h	Cap67 4h
mmu04630	JAK-STAT signaling pathway	92	1,71018E+13	4,97799E+14	Socs3/Socs1/Cdkn1a/Il6/Il15/Jak2/Socs7/Il10/Il	4h	Cap67 4h
mmu03430	Mismatch repair	22	-1,86186E+14	2,68334E+14	Rpa1/Rfc1/Pold2/Rpa2/Mlh3/Lig1/Rfc4/Rpa3/M	4h	Cap67 4h
mmu04622	RIG-I-like receptor signaling pathway	46	1,6829E+14	4,7371E+14	Tnf/Tank/Irf7/Azi2/Ifih1/Nfkb1/Cxcl10/Nfkbib/I	4h	Cap67 4h
mmu04625	C-type lectin receptor signaling pathway	89	1,65635E+14	6,23478E+14	Casp1/Il1b/Tnf/Il6/Ptgs2/Il10/Clec4e/Nlrp3/Src	4h	Cap67 4h
mmu04210	Apoptosis	118	1,60915E+14	9,30252E+14	Tnf/Tnfsf10/Gadd45g/Traf1/Fas/Parp3/Map2k1	4h	Cap67 4h
mmu04110	Cell cycle	117	-1,93575E+14	2157927060	Stag1/Hdac2/Cdc25a/Pkmyt1/Rad21/Cdc25c/Tg	24h	B3501 24h
mmu04060	Cytokine-cytokine receptor interaction	126	2,17095E+14	2157927060	Ccr1/Ccr5/Ccl12/Il7r/Ccl5/Il1rn/Ccl2/Gdf15/Il1a	24h	B3501 24h
mmu00010	Glycolysis / Gluconeogenesis	43	2,20363E+14	2226413337	Pgam1/Tpi1/Pgm1/Pfkl/Pfkp/Ldha/Gapdh/Pgk1	24h	B3501 24h
mmu04066	HIF-1 signaling pathway	87	2,10869E+14	7983755366	Egln3/Slc2a1/Egln1/Nos2/Serpine1/Pfkl/Eif4ebp	24h	B3501 24h
mmu03030	DNA replication	35	-1,94427E+14	1,46005E+14	Pold1/Rfc3/Pole4/Rnaseh2a/Prim2/Pole2/Rnas	24h	B3501 24h
mmu04621	NOD-like receptor signaling pathway	143	2,06407E+13	1,47179E+14	Ifi204/Ccl12/Irf7/Ccl5/Mefv/Oas3/Ccl2/Stat2/Ir	24h	B3501 24h
mmu03040	Spliceosome	127	-1,85179E+13	1,65204E+14	Ppie/Snu13/Snrpa1/Lsm5/Snrpa/Lsm4/Cdc5l/C	24h	B3501 24h
mmu03008	Ribosome biogenesis in eukaryotes	73	-1,82571E+13	1,25428E+14	Csnk2a1/Bms1/Pwp2/Rexo5/Drosha/Nol6/Spat	24h	B3501 24h
mmu03440	Homologous recombination	39	-1,81797E+13	2,06513E+14	Rad50/Mre11a/Brca1/Rad54b/Palb2/Brca2/Bar	24h	B3501 24h
mmu04137	Mitophagy - animal	61	2,01815E+14	2,22926E+14	Bnip3/Bnip3l/Jun/Bcl2l1/Src/Ubb/Atf4/Tbc1d15	24h	B3501 24h
mmu03013	RNA transport	142	-1,59984E+14	3,98507E+14	Strap/Sumo3/Rbm8a/Nup93/Eif2s1/Pom121/Fr	24h	B3501 24h
mmu04514	Cell adhesion molecules (CAMs)	77	1,88198E+14	5,0886E+14	Cd274/Mpzl1/H2-Q7/H2-Ab1/H2-T24/Sdc3/H2-	24h	B3501 24h
mmu04922	Glucagon signaling pathway	77	1,87895E+14	5,0886E+14	Gys1/Slc2a1/Pgam1/Pfkl/Ldha/Creb3l1/Pkm/Cr	24h	B3501 24h
mmu01230	Biosynthesis of amino acids	56	1,83515E+14	5,50275E+14	Arg1/Pgam1/Tpi1/Pfkl/Pfkp/Gapdh/Pgk1/Eno1/	24h	B3501 24h
mmu03015	mRNA surveillance pathway	76	-1,66944E+14	5,78075E+14	Ppp2r2d/Ppp2ca/Ppp1cb/Pabpc1/Cpsf2/Smg5/	24h	B3501 24h
mmu00052	Galactose metabolism	23	1,98729E+14	6,43975E+14	Pgm1/Pfkl/Pfkp/Hk2/Gla/Ugp2/Galk1/Hk1	24h	B3501 24h
mmu04612	Antigen processing and presentation	58	1,96151E+14	7,3348E+14	H2-Q7/H2-Ab1/H2-T24/H2-Q6/Hspa1a/B2m/H2	24h	B3501 24h
mmu04630	JAK-STAT signaling pathway	95	1,82333E+14	7,45412E+13	Il7r/Socs3/Pdgfb/Stat2/Irf9/Il15/Stat1/Bcl2l1/Il	24h	B3501 24h
mmu04668	TNF signaling pathway	101	1,82796E+14	8,52515E+14	Ccl12/Socs3/Ccl5/Ccl2/Gm5431/Il15/Jun/Creb3	24h	B3501 24h
mmu04060	Cytokine-cytokine receptor interaction	126	2,05325E+14	67673621,79	Ccr1/Il1rn/Ccl12/Ccl2/Il7r/Ccl4/Ccl7/Cxcl3/Cxcl	24h	Cap67 24h
mmu04657	IL-17 signaling pathway	66	2,05856E+14	2305333478	Mmp13/Ccl12/Ccl2/Ccl7/Cxcl3/Cxcl10/Hsp90aa	24h	Cap67 24h
mmu00010	Glycolysis / Gluconeogenesis	43	2,04527E+14	2363738789	Pgam1/Ldha/Tpi1/Pfkp/Pgk1/Eno1/Pgm1/Pfkl/(	24h	Cap67 24h
mmu04668	TNF signaling pathway	101	1,99563E+14	310613246,4	Ccl12/Ccl2/Cxcl3/Ifi47/Cxcl10/Csf1/Edn1/Pik3cb	24h	Cap67 24h
mmu04621	NOD-like receptor signaling pathway	143	1,94317E+14	310613246,4	Ccl12/Ifi204/Ccl2/Cxcl3/Irf7/Oas3/Oas1a/Oas1g	24h	Cap67 24h
mmu04623	Cytosolic DNA-sensing pathway	44	2,04027E+13	310613246,4	Zbp1/Ccl4/Cxcl10/Ddx58/Irf7/Adar/Ifnb1/Il1b/(	24h	Cap67 24h
mmu03050	Proteasome	43	1,94459E+14	2,59812E+14	Psmd8/Psmb6/Psme2/Psma4/Psmd11/Psmb3/I	24h	Cap67 24h
mmu04145	Phagosome	127	1,85927E+14	8,14682E+14	Tubb6/Atp6v0d2/Itga5/Tuba4a/Msr1/Fcgr1/H2	24h	Cap67 24h
mmu04620	Toll-like receptor signaling pathway	79	1,82586E+14	1,80285E+14	Ccl4/Cxcl10/Irf7/Ctsk/Pik3cb/Stat1/Tnf/Map2k1	24h	Cap67 24h
mmu04066	HIF-1 signaling pathway	87	1,81738E+14	1,89971E+14	Egln3/Slc2a1/Ldha/Pgk1/Eno1/Nos2/Pdk1/Edn1	24h	Cap67 24h
mmu04612	Antigen processing and presentation	58	1,83418E+14	2,15621E+14	Hspa1a/Hspa1b/Hsp90aa1/Tnf/H2-T24/Tap1/H2	24h	Cap67 24h
mmu00330	Arginine and proline metabolism	35	1,87958E+14	3,60069E+14	P4ha1/P4ha2/Arg1/Nos2/Smox/Aldh1b1/Odc1/	24h	Cap67 24h
mmu04622	RIG-I-like receptor signaling pathway	47	1,83598E+14	3,60069E+14	Dhx58/Cxcl10/Ddx58/Ifih1/Irf7/Isg15/Tnf/Ifnb1	24h	Cap67 24h
mmu01200	Carbon metabolism	93	1,68966E+13	7,27191E+14	Pgam1/Tpi1/Pfkp/Pgk1/Eno1/Pfkl/Gapdh/Aldo	24h	Cap67 24h

Table S4. Comparison of the modulation of miRNAs in macrophages infected by B3501 and Cap67 *C. neoformans* strains.

miRNA	Experimental condition			
	Infection by B3501		Infection by Cap67	
	Fold change*	*p*-value	Fold change*	*p*-value
let-7d-5p	**2.03**	1.20E-02	1.21	1.45E-01
let-7e-5p	**2.01**	9.44E-03	1.23	9.64E-02
let-7g-5p	**2.02**	1.24E-02	1.22	9.51E-02
miR-140-5p	**2.02**	1.19E-02	1.78	3.09E-03
miR-142a-3p	**2.01**	1.23E-02	1.24	3.48E-01
miR-146b-5p	**2.01**	1.23E-02	1.72	1.02E-01
miR-147-3p	**5.63**	2.01E-03	**2.45**	1.26E-02
miR-152-3p	**2.05**	9.03E-03	1.26	5.15E-02
miR-155-5p	**5.73**	1.51E-03	1.73	8.94E-02
miR-15b-5p	**2.02**	1.13E-02	1.23	7.22E-02
miR-186-5p	**2.06**	9.67E-03	1.75	3.32E-03
miR-195a-5p	**2.03**	1.02E-02	1.24	7.75E-02
miR-19a-3p	**2.00**	9.69E-03	1.20	1.13E-01
miR-214-3p	**2.01**	8.79E-03	1.73	1.46E-03
miR-26a-5p	**2.05**	1.03E-02	1.23	8.01E-02
miR-29c-3p	**2.00**	1.18E-02	1.20	1.40E-01
miR-30b-5p	**2.02**	1.04E-02	**2.51**	8.53E-05
miR-30c-5p	**2.02**	9.57E-03	1.22	7.44E-02
miR-30e-5p	**2.01**	9.95E-03	1.22	9.04E-02
miR-31-5p	**2.02**	9.86E-03	1.74	2.39E-03
miR-493-3p	**3.00**	9.84E-03	**3.60**	1.10E-03

* miRNAs in bold lettering had their transcript levels significantly modulated (FC $\geq \pm 2.0$ and *p*-value < 0.05 as described in Materials and Methods).

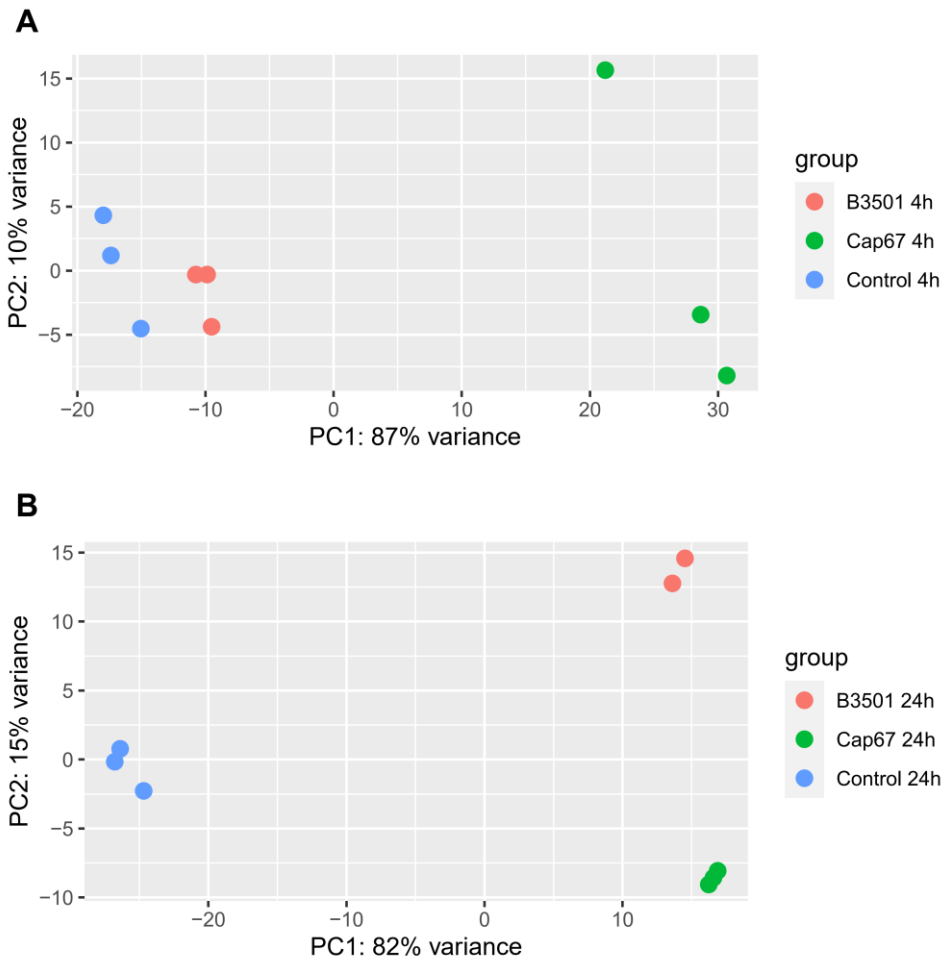

Figure S1. Gene expression variation between macrophages infected by *C. neoformans* strains and control noninfected.

Principal component analysis of transcriptomic profile of macrophages infected by B3501 and Cap67 strains at 4 (**A**) and at 24 (**B**) hours-post infection.

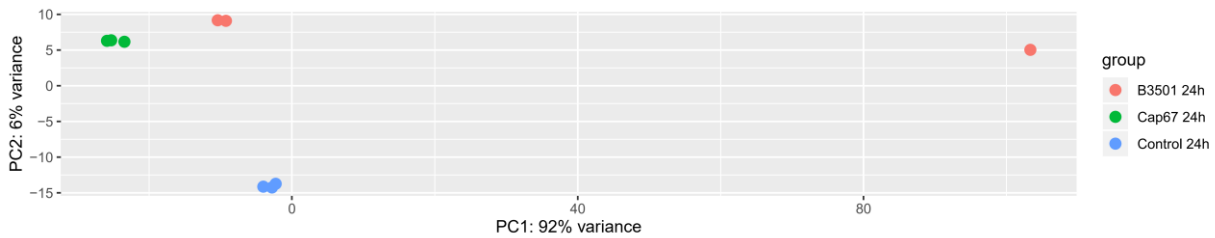

Figure S2. Gene expression variation between macrophages infected by *C. neoformans* strains and control noninfected at 24 hours-post infection.

Principal component analysis of transcriptomic profile of macrophages infected by B3501 and Cap67 strains, displaying all replicates for B3501 group.

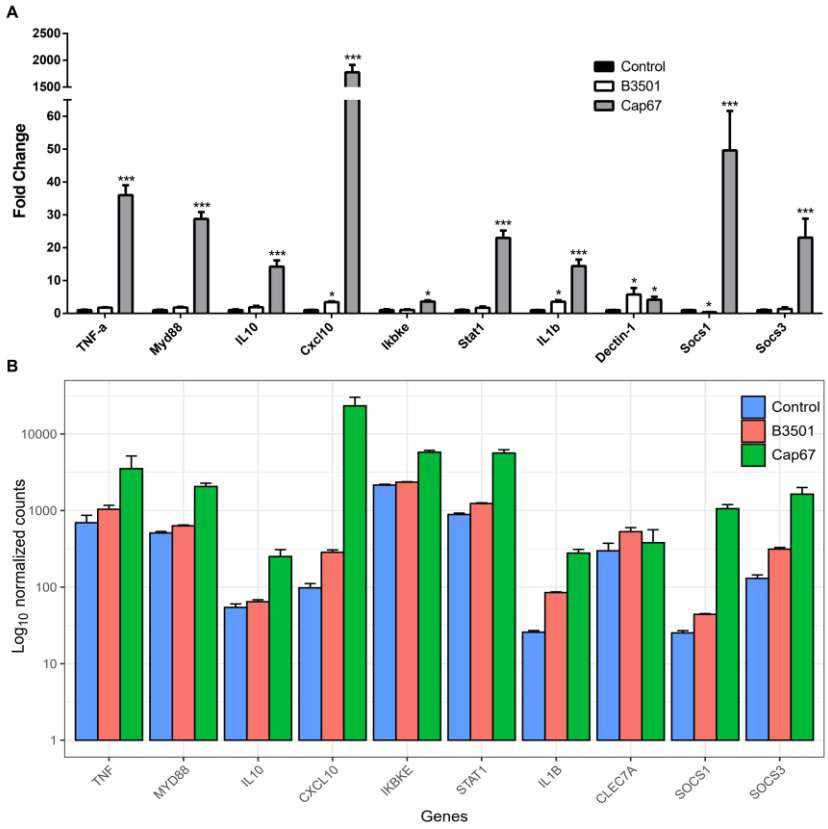

Figure S3. Validation of the results obtained in RNA-seq from macrophages infected by *C. neoformans* using RT-qPCR.

Murine bone-marrow derived macrophages were infected by B3501 and Cap67 strains of *C. neoformans* and the same total RNA used in the RNA-seq (**B**) was employed in RT-qPCR (**A**) assays. The primers sequences are described in Table S1 and all assay conditions are as described in the Materials and Methods section.

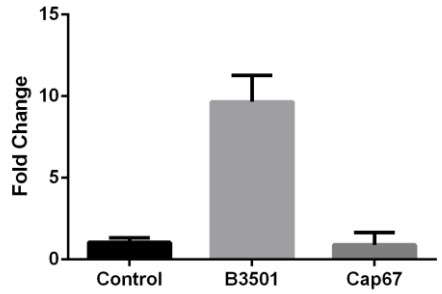

Figure S4. Validation of miR-155 expression in macrophages infected by *C. neoformans* strains.

Confirmation of the results obtained by the PCR-Array experiment for miR-155. miR-155 accumulation levels of macrophages infected with strains B3501 and Cap67 at 4 hpi. For cDNA synthesis of miRNAs, 10 ηg of RNA from the small RNA fraction were used per sample. For miRNA expression analysis, a specific Taqman kit for mir-155 was used according to the manufacturer's specification (Life Technologies). Small nuclear RNA (snRNA) U6 was used as an endogenous control.

8. Additional information

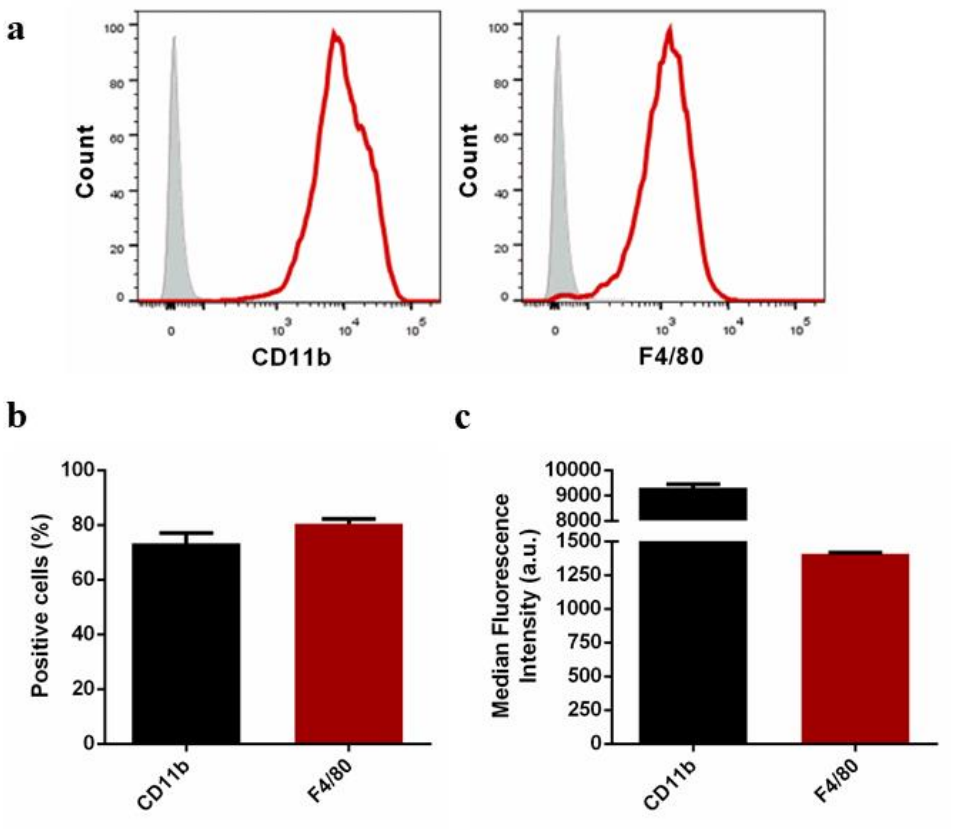

Figure A1. Analysis of the expression of surface markers CD11b and F4/80 in Bone marrow-derived macrophages.

a. Histograms showing expression markers CD11b and F4/80. **b.** Percentage of positive cells for each marker after culture with GM-CSF. **c**. Fluorescence intensity of each marker. u.a.: arbitrary units. Results are presented as means ± SD.

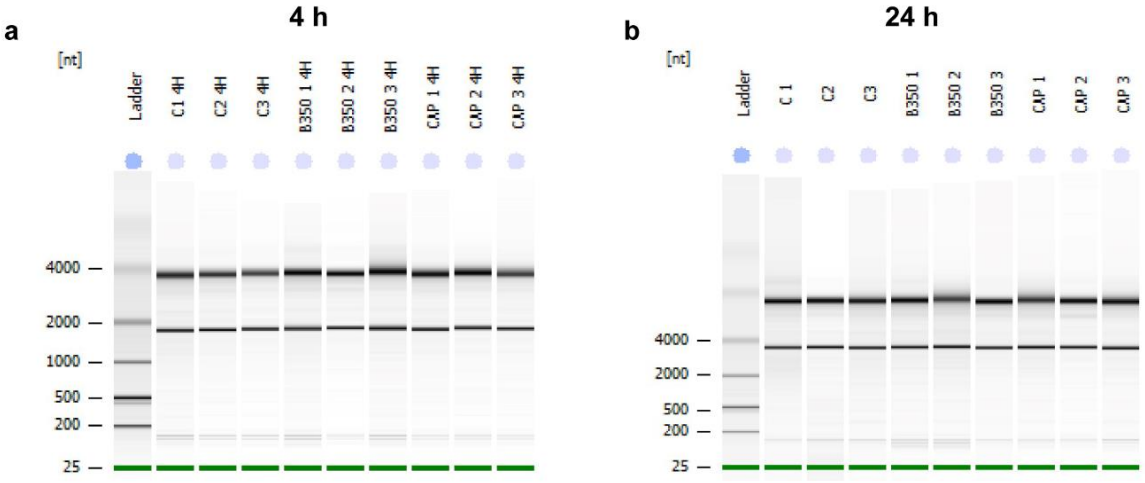

Figure A2. Gel image of microcapillary electrophoresis from Bioanalyzer.
Microcapillary electrophoresis for evaluating the quality of total RNA in control samples (C) and macrophages infected by *C. neoformans* B3501 (B350) and Cap67 (CAP) strains in 4 hpi (**a**) and 24 hpi (**b**).

Table A1. General results from high-throughput sequencing, filtering and mapping steps.

Sample	RIN	Total base pair	reads	Mapping reads (%)
Control 1 - 4 h	9.0	5.596.481.710	27.705.355	94.52
Control 2 - 4 h	9.1	4.686.462.620	23.200.310	90.31
Control 3 - 4 h	9.3	5.273.550.976	26.106.688	92.39
B3501 1 - 4 h	9.2	5.365.859.926	26.563.663	93.42
B3501 2 - 4 h	9.5	4.288.727.650	21.231.325	95.31
B3501 3 - 4 h	9.5	4.732.082.098	23.426.149	95.70
Cap67 1 - 4 h	9.4	5.669.630.152	28.067.476	90.06
Cap67 2 - 4 h	9.3	4.206.443.758	20.823.979	87.97
Cap67 3 - 4 h	9.4	5.135.309.246	25.422.323	92.05
Control 1 - 24 h	9.0	5.566.625.706	27.557.553	87.50
Control 2 - 24 h	9.8	4.641.297.036	22.976.718	94.96
Control 3 - 24 h	9.5	5.403.955.712	26.752.256	91.13
B3501 1 - 24 h	9.5	5.790.090.630	28.663.815	89.37
B3501 2 - 24 h	9.1	5.623.060.870	27.836.935	93.67
B3501 3 - 24 h	9.5	3.408.994.420	16.876.210	44.45
Cap67 1 - 24 h	9.3	5.398.288.602	26.724.201	93.24
Cap67 2 - 24 h	9.6	4.512.243.882	22.337.841	92.60
Cap67 3 - 24 h	9.5	4.864.007.894	24.079.247	94.82

Considerações finais e perspectivas

Nesse trabalho, analisamos o perfil transcritômico de fagócitos (células dendríticas e macrófagos) em resposta aos modelos de infecção por *P. brasiliensis* e *C. neoformans* a fim de contribuir com um melhor entendimento das bases moleculares da interação patógeno-hospedeiro.

Em termos gerais, o transcritoma de DCs após interação com *P. brasiliensis* revelou que a linhagem susceptível apresenta uma resposta inflamatória mais intensa e exacerbada. Dados relevantes das análises transcritômicas revelaram a diminuição nos níveis de transcritos relacionados a vários processos como acidificação do lisossomo, atividade catalítica e autofagia. Tais processos podem afetar o processamento e, em consequência, a apresentação de antígenos pelas DCs, provocando uma ativação ineficiente da resposta imune na linhagem de camundongos susceptível. Esses resultados corroboram a importância do *background* genético do hospedeiro no desfecho da infecção por *P. brasiliensis*, ressaltando a possível importância dos processos referidos acima.

Por outro lado, o transcritoma de macrófagos após infecção por *C. neoformans* revelou um atraso na ativação de uma resposta imune adequada no modelo de infecção pela linhagem capsular. Este fenômeno poderia favorecer as condições de adaptação do fungo no ambiente dentro do hospedeiro, possibilitando a ativação de atributos de virulência do fungo, que são necessários para a sua sobrevivência e disseminação. Além disso, foi demonstrada a modulação da expressão de 21 miRNAs em macrófagos infectados pela linhagem capsular. Em contraste, somente três miRNAs foram modulados positivamente na infecção pela linhagem acapsular. Considerando os níveis de indução, destacamos o aumento no acúmulo de miR-155. Subsequentes análises bioinformáticas dos genes alvos desse miRNA direcionam a possível relação do miR-155 na alteração da resposta inflamatória dos macrófagos.

Uma avaliação mais aprofundada dos processos e vias alteradas/afetadas, principalmente o processamento e apresentação de antígenos, poderia ser realizada *in vivo* ou com diferentes tipos celulares, para avançar a compreensão dos mecanismos moleculares da susceptibilidade e resistência às infecções fúngicas.

Os resultados justificam o aprofundamento dos estudos visando: i) identificação da função desses miRNAs e os respectivos alvos mediante ensaios de perda da função; ii) identificação dos mecanismos/vias de ativação da transcrição dos miRNAs usando camundongos *knock-out* para genes que codificam PRRs; iii) participação de miRNAs nas

diferentes vias de fagocitose de fungos patogênicos; iv) comparação da indução miRNAs e outros tipos de ncRNAs em resposta a isolados fúngicos com diferentes níveis de virulência.

Os resultados transcritômicos geram uma grande quantidade de informação, permitindo que novos estudos abordem com maior especificidade achados de interesse identificados com a análise abrangente dos dados. Os trabalhos aqui apresentados representam o ponto de partida para novas abordagens em projetos futuros de nosso grupo de pesquisa, dando continuidade às linhas de investigação.

Baseado nos resultados das análises iniciais do transcritoma, abordamos um projeto de pesquisa intitulado "*Papel das vias de internalização de Cryptococcus neoformans no acúmulo de miRNAs e regulação da resposta imune inata contra o fungo*". Esse projeto financiado pela FAP-DF encontra-se em andamento e está permitindo a continuação da linha de estudos dos miRNAs e contribuindo no desenvolvimento de outros projetos de doutorado e mestrado.

ANEXO - Produção científica durante o doutorado

Produção cientifica relacionada com o tema da tese.

Silva WMC, **Hurtado FA**, Simi K, Barros PHA, Sokolowskei D, Silva-Pereira I, et al. Transcriptome Analysis Using RNA-seq and scRNA-seq. In: Transcriptomics in Health and Disease. Springer, Cham; 2022. p. 73–107. Available from: https://link.springer.com/chapter/10.1007/978-3-030-87821-4_3

De-Souza-Silva CM†, **Hurtado FA**†, Tavares AH, de Oliveira GP, Raiol T, Nishibe C, et al. Transcriptional remodeling patterns in murine dendritic cells infected with *Paracoccidioides brasiliensis*: More is not necessarily better. J Fungi. 2020 Nov 24;6(4):1–22. † These authors have contributed equally to the work and share first authorship. Available from: https://www.mdpi.com/2309-608X/6/4/311

Produção cientifica em colaboração.

Oliveira RK de M, **Hurtado FA**, Gomes PH, Puglia LL, Ferreira FF, Ranjan K, et al. Base excision repair AP-endonucleases-like genes modulate DNA damage response and virulence of the human pathogen *Cryptococcus neoformans*. J Fungi. 2021 Feb 1;7(2):1–22. Available from: https://pubmed.ncbi.nlm.nih.gov/33673204/

Albuquerque P, Nicola AM, Magnabosco DAG, da Silveira Derengowski L, Crisóstomo LS, Xavier LCG, Frazão SO, Guilhelmelli F, de Oliveira MA, Dias JDN, **Hurtado FA**, et al. A hidden battle in the dirt: Soil amoebae interactions with *Paracoccidioides* spp. Reynolds TB, editor. PLoS Negl Trop Dis. 2019 Oct 7;13(10):e0007742. Available from: https://dx.plos.org/10.1371/journal.pntd.0007742

Veloso Júnior PH de H, Simon KS, de Castro RJA, Coelho LC, **Erazo FAH**, de Souza ACB, et al. Peptides ToAP3 and ToAP4 decrease release of inflammatory cytokines through TLR-4 blocking. Biomed Pharmacother. 2019 Oct 1;118. Available from: https://doi.org/10.1016/j.biopha.2019.109152